SNP2010, Nuclear Physics Institute, Řež

September 2010

Řež/Prague,
Czech Republic

Electromagnetic Strangeness Production

Reinhard Schumacher

Carnegie Mellon

Outline /Overview

- DAY 1
  - History of Strangeness Electromagnetic Physics
    - Strangeness
    - Earliest experiments
  - Physics issues
    - N* searches
    - Reaction mechanisms
    - Amplitudes
    - Spin observables
  - Photoproduction of elementary hyperons

- DAY 2
  - Electroproduction of elementary hyperons
  - Electroproduction of hypernuclei
  - Structure of the $\Lambda(1405)$
  - Y* (S=-1) production
  - Cascade (S=-2) production

The First Strange Particle Ever Seen

No. 4077 December 20, 1947 NATURE 855

EVIDENCE FOR THE EXISTENCE OF NEW UNSTABLE ELEMENTARY PARTICLES

By Dr. G. D. ROCHESTER
AND
Dr. C. C. BUTLER
Physical Laboratories, University, Manchester

AMONG some fifty counter-controlled cloud-chamber photographs of penetrating showers which we have obtained during the past year as part of an investigation of the nature of penetrating particles occurring in cosmic ray showers under lead, there are two photographs containing forked tracks of a very striking character. These photographs have been selected from five thousand photographs taken in an effective time of operation of 1,500 hours. On the basis of the analysis given below we believe that one of the forked tracks, shown in Fig. 1 (tracks a and b), represents the spontaneous transformation in the gas of the chamber of a new type of uncharged elementary particle into lighter charged particles, and that the other, shown in Fig. 2 (tracks a and b), represents similarly the transformation of a new type of charged particle into two light particles, one of which is charged and the other uncharged.

The experimental data for the two forks are given in Table 1; H is the value of the magnetic field, α the angle between
momentum and
the particles a
table, a plus
positive if mov
re-projection
shown that eac
over, both track
in a region of
background fog
good condensat

Though the
respects, they h
common: first,

TABLE 1. EXPERIMENTAL DATA

Photo-graph	H (gauss)	α (deg.)	Track	(eV/c)	(eV/c)	Sign
1	3500	66·6	a b	[illegible] × 10⁸ [illegible] × 10⁸	[illegible] × 10⁸ [illegible] × 10⁸	+ −
2	7200	161·1	a b	[illegible] × 10⁸ [illegible] × 10⁸	[illegible] × 10⁸ [illegible] × 10⁸	+ +

case is there any sign of a track due to a third ionizing particle. Further, very few events at all similar to these forks have been observed in the 3-cm. lead plate, whereas if the forks were due to any type of collision process one would have expected several hundred times as many as in the gas. This argument indicates, therefore, that the tracks cannot be due to a collision process but must be due to some type of spontaneous process for which the probability depends on the distance travelled and not on the amount of matter traversed.

This conclusion can be supported by detailed arguments. For example, if either forked track were due to the deflexion of a charged particle by collision with a nucleus, the transfer of momentum would be so large as to produce an easily visible recoil track. Then, again, the attempt to account for Fig. 2 by a collision process meets with the difficulty that the incident particle is deflected through 19° in a single collision in the gas and only 2·4° in traversing 3 cm. of lead—a most unlikely event. One specific collision process, that of electron
on in the field
grounds: the
uld only be a
1° for Fig. 1,
ponent should
ch case a lead

forked tracks
s do represent
present a type
familiar in the
d an assumed
of the heavy
Occhialini and

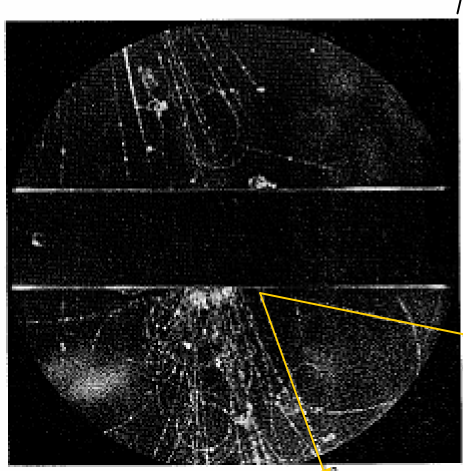

First cloud chamber photograph of a neutral V-particle. Obtained by G. D. Rochester and C. C. Butler at the University of Manchester, the V-particle was produced in a 3-inch thick lead plate and decayed into two particles identified by the arrows labeled 1 and 2 at the edge of the figure. (Reproduced through the courtesy of *Nature*.)

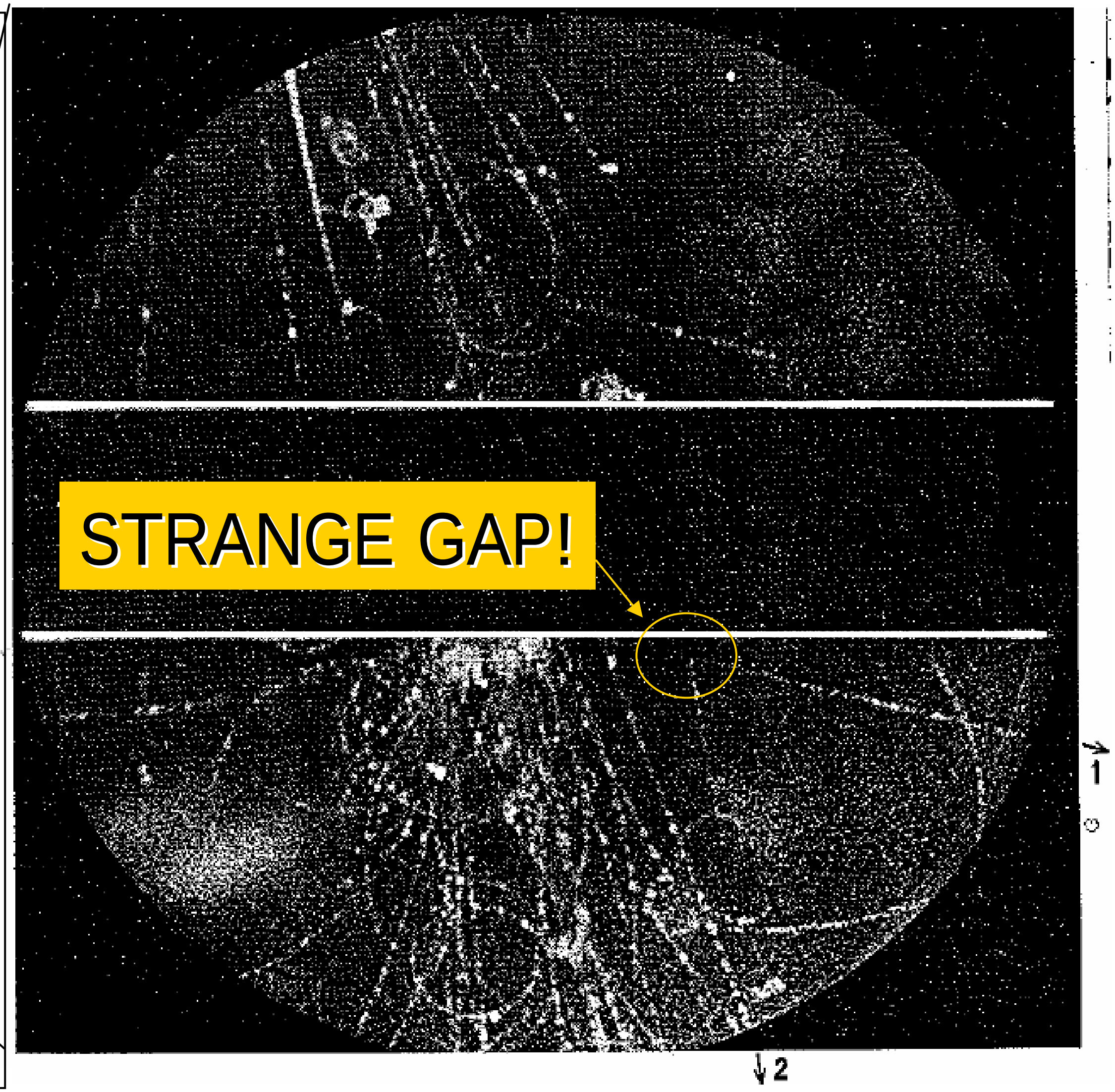

1^{st} K^+ Photoproduction Sighting

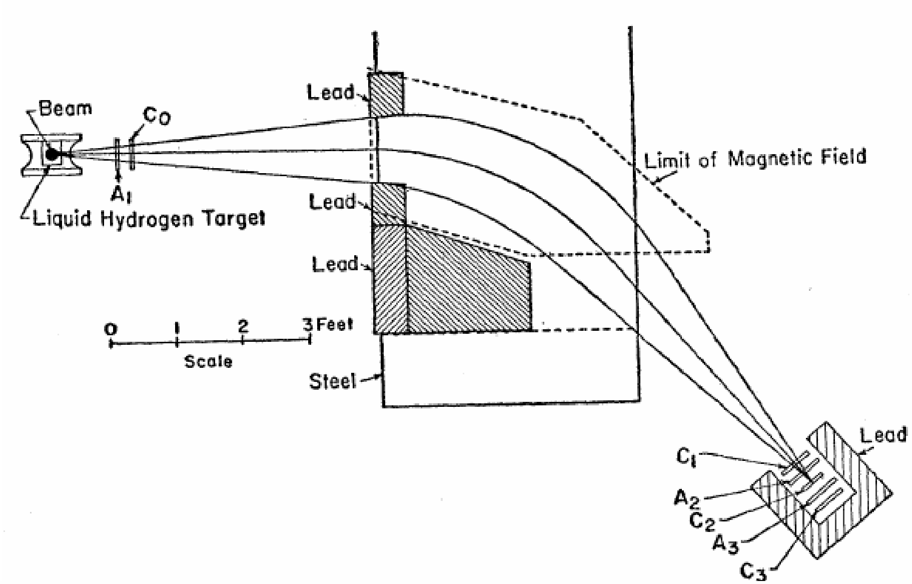

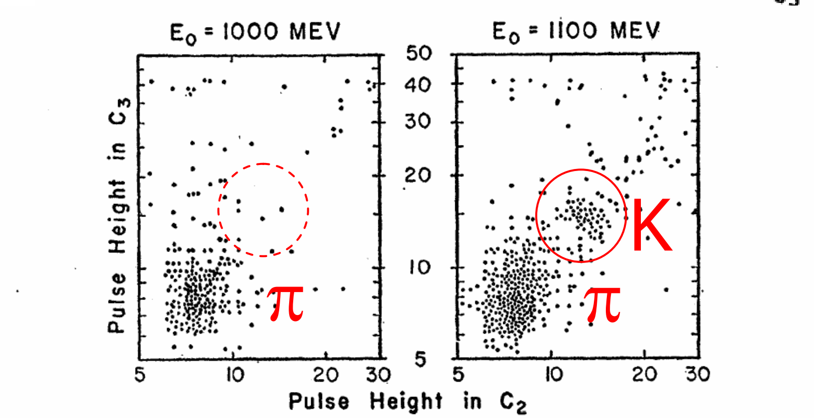

FIG. 2. Correlations in the pulse heights from counters C_2 and C_3 showing the pion peak and the cluster of points caused by K mesons. These data are for a momentum $p=520$ Mev/c and a lab angle 25°, corresponding to K mesons produced by 1060 Mev photons. The data on the left, taken with a sync $E_0=1000$ Mev, represent the background.

- CalTech; 1100MeV Bremsstrahlung beam
  - "Threshold" for 0° production of kaons $\gamma + p \rightarrow K^+ + \Lambda$ at E_γ = 911 MeV
  - Compared energy-loss dE/dx spectra in two counters…
  - Λ not directly reconstructed

P. L. Donoho & R. L. Walker Phys. Rev. **107** 1198 (1957)

An Early Bremsstrahlung Exp't

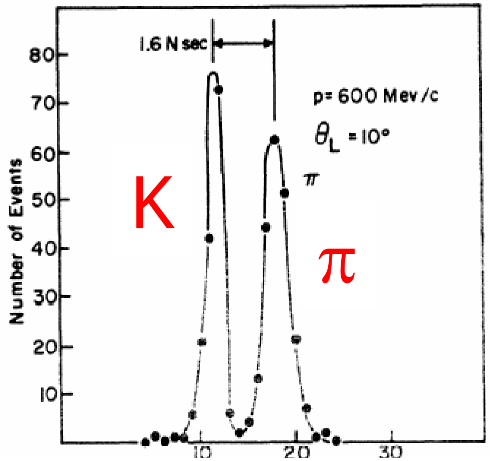

~TOF

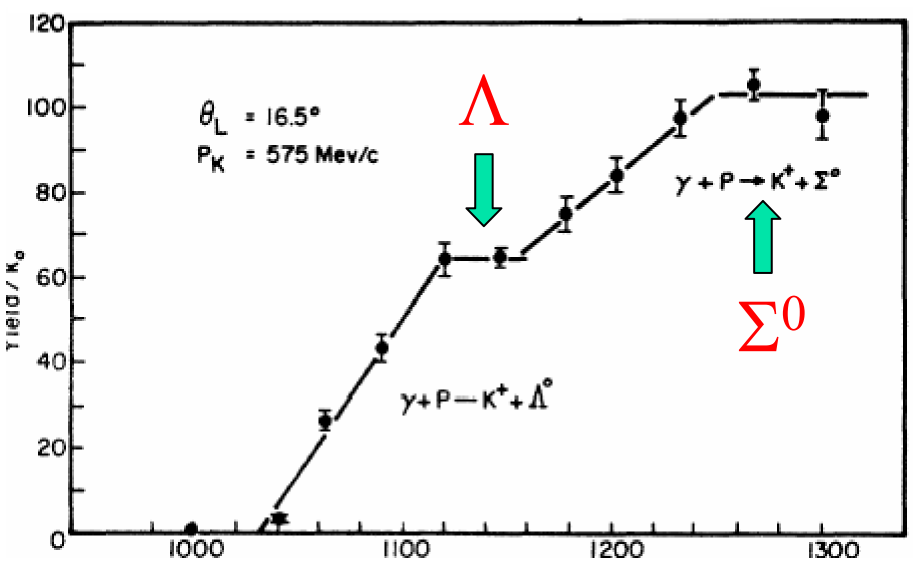

Synchrotron Energy (Photon Endpoint) MeV

- Cornell 1.4 GeV electron beam →Bremsstrahlung photons
- Magnetic spectrometer
  - Time-of-flight (TOF) K/π separation
  - Fixed angle & momentum
- "steps" due to Λ, Σ^0 formation

R. L. Anderson et al., Phys. Rev. Lett **9** 131 (1962)

The "Missing Mass" Technique

Incident Photon:
known 4-vector

$\overline{p}_{\gamma}$

Final State Meson:
measured 4-vector

$\overline{p}_{kaon}$

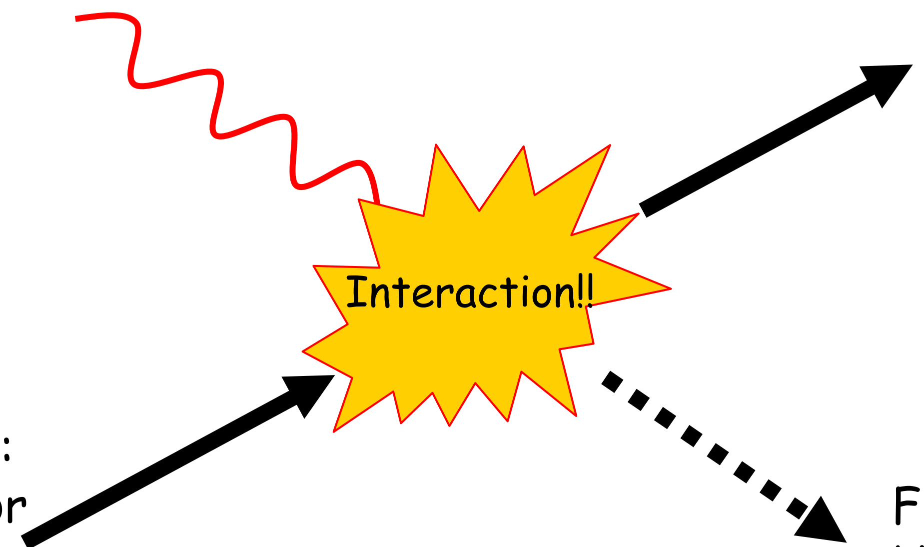

Target Proton:
known 4-vector

$\overline{p}_{proton}$

$\overline{p}_{hyperon}$

Final State Hyperon:
UN-measured 4-vector

From Special Relativity:

$$M_{hyperon}^{2} = \left(\overline{p}_{\gamma} + \overline{p}_{proton} - \overline{p}_{kaon}\right)^{2}$$

1st Hyperon Mass Spectrum

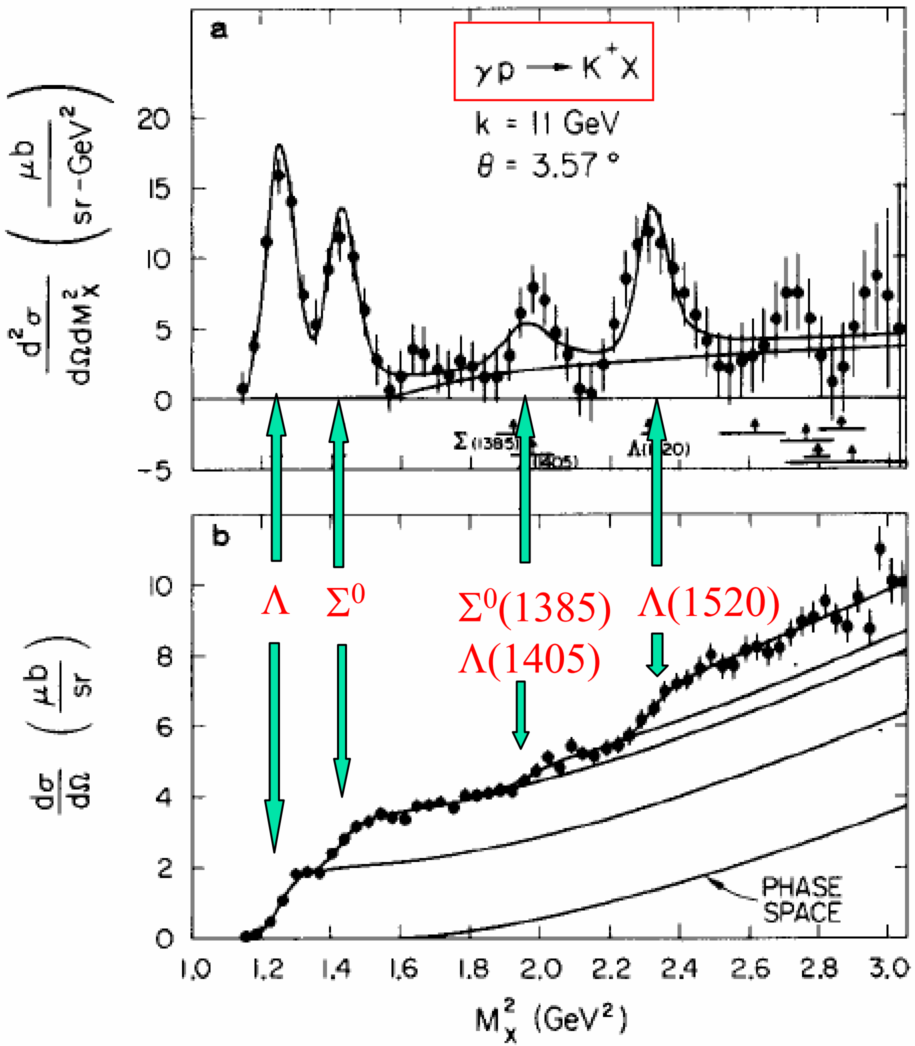

Fig. 1. One of the missing mass spectra obtained from hydrogen. The upper graph (a) is a derivative of the actual measured yields (b). The smooth curves repre-

- Used SLAC Bremsstrahlung photon beam: 11 GeV endpoint
- Far above the nucleon-resonance domain
- 20 GeV Spectrometer
  - *Angles below 5°*
- Obtain integrated cross sections at ~11 GeV for 4 hyperons

A. M. Boyarski et al.,
Phys. Lett. **34B**, 547 (1971)

How is Λ Polarization Measured?

In Λ rest frame:

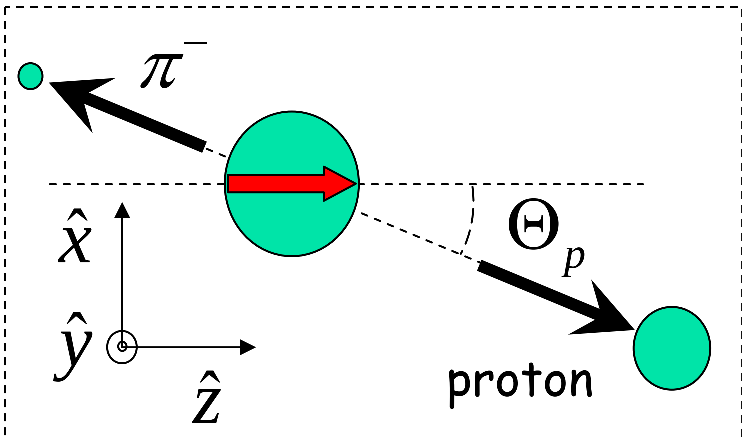

$$I(\Theta_p) = I_o\left(1 + \alpha P_\Lambda \cos(\Theta_p)\right)$$

- Pick any axis along which parity allows the Λ to be spin polarized
- $\frac{1}{2}^+ \to \frac{1}{2}^+ + 0^-$ S-wave
  - Parity forbidden
- $\frac{1}{2}^+ \to \frac{1}{2}^+ + 0^-$ P-wave
  - Parity allowed
- S-P interference gives cos θ term with α_Λ = .642

"Hyperon weak decay asymmetry"

1st Recoil Polarization Setup

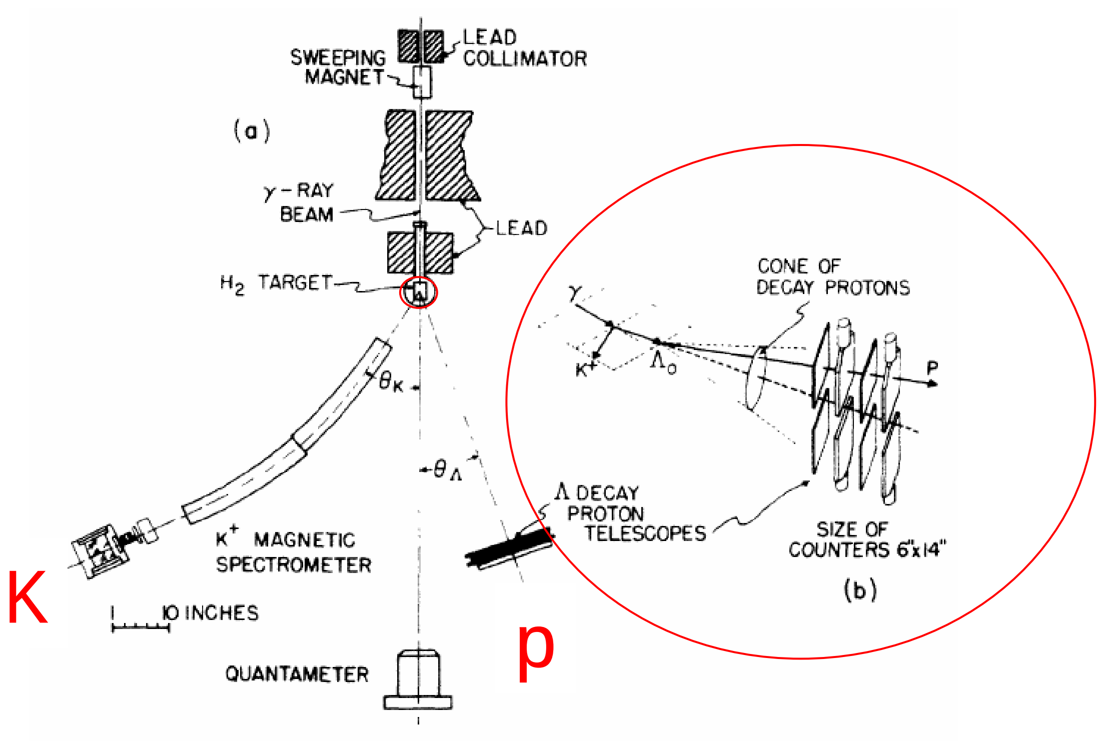

- Cornell 1120 MeV Bremsstrahlung beam
- Detect "up-down" asymmetry of protons from Λ decay.
- Measured result $P_{\Lambda} \sim +0.2$ near $\Theta_K = 90^o$ c.m.

H. Thom *et al.*, Phys. Rev. Lett. **11,** 433 (1963)

1st Electroproduction Sighting

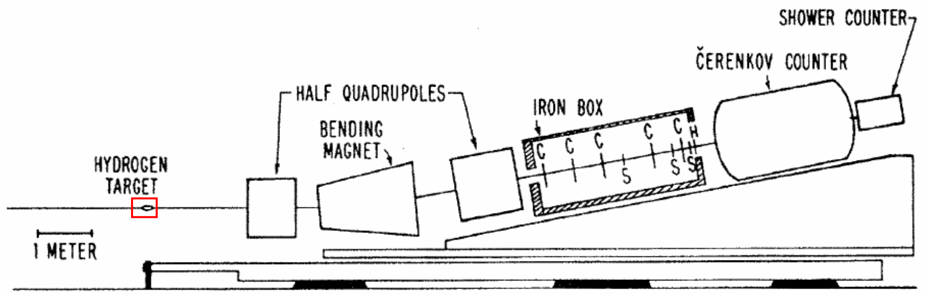

FIG. 1. Schematic diagram showing side view of one spectrometer. *C* denotes a wire spark-chamber module, *S* denotes a trigger counter, and *H* denotes a hodoscope.

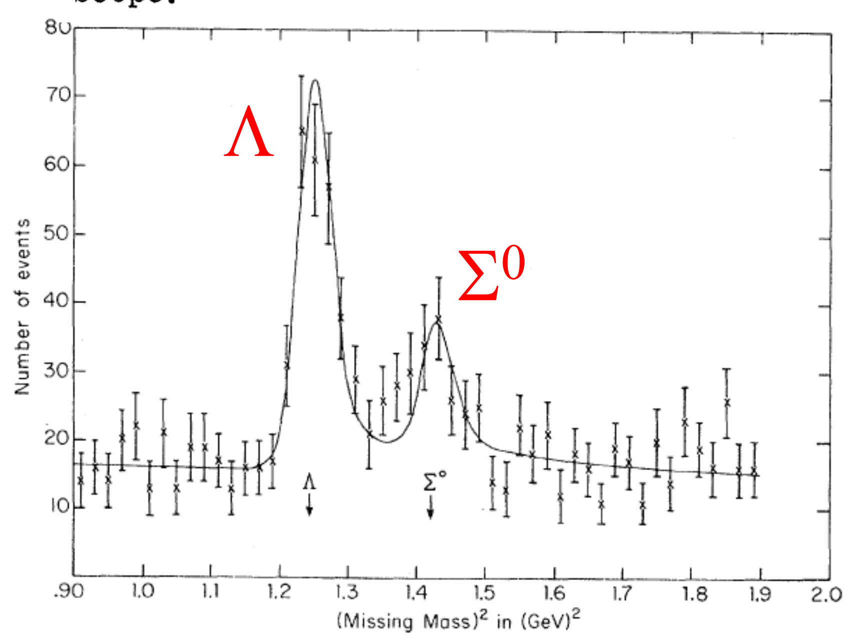

- Cambridge Electron Accelerator (CEA) (Massachusetts, USA)
- Two-arm spectrometer for $e^- + p \rightarrow e^- + K^+ + Y$
- Kinematics:
  - $0.18 < Q^2 < 1.2$ GeV^2
  - $1.85 < W < 2.60$ GeV
  - $0 < \Theta_K < 28^\circ$
  - $\varepsilon \sim 0.85$
- Found Σ^0/Λ ratio smaller than in photoproduction

C. N. Brown et al. Phys. Rev. Lett. **28** 1086 (1972).

Kaon Photoproduction

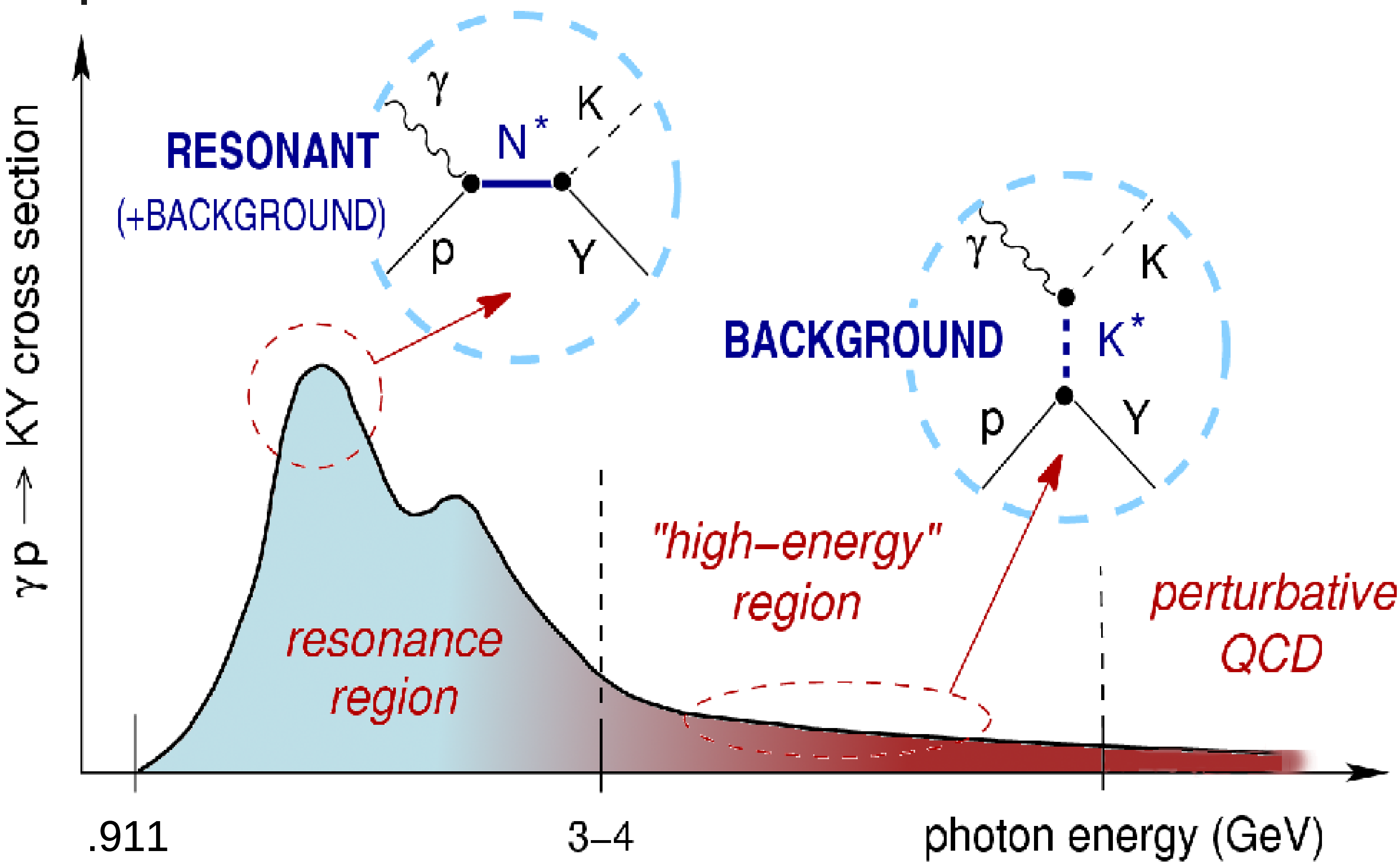

Contributing Processes

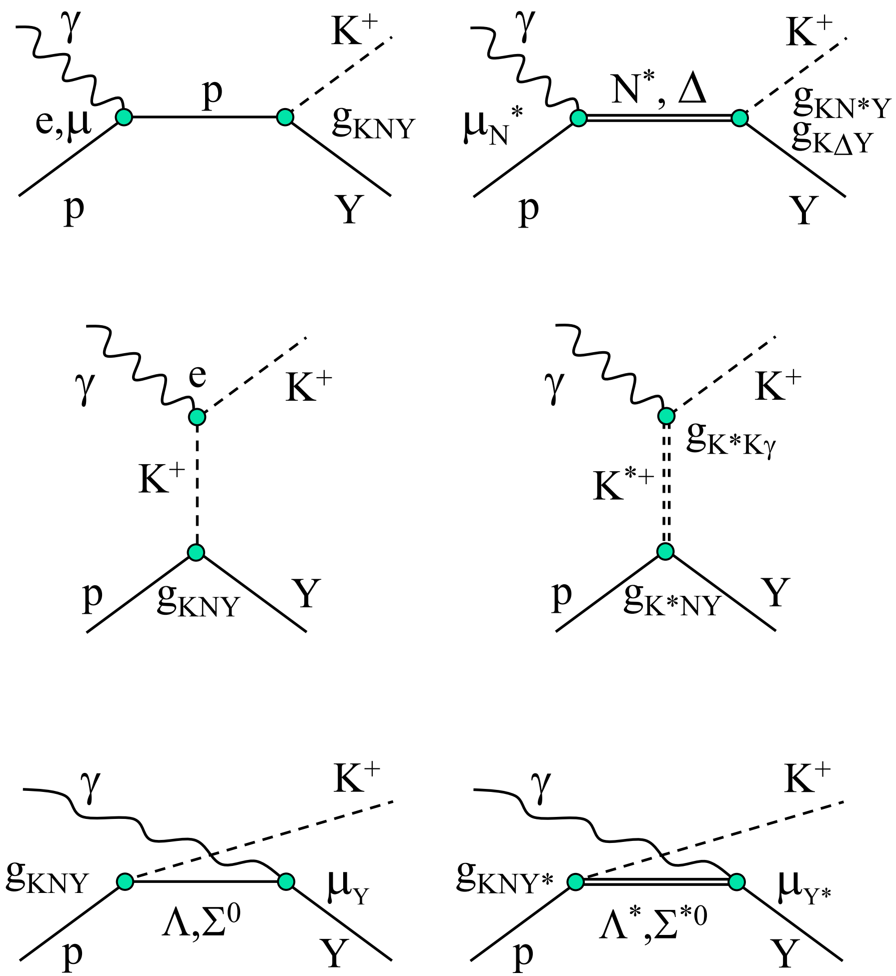

+ channel couplings...

Resonances in Quark Models

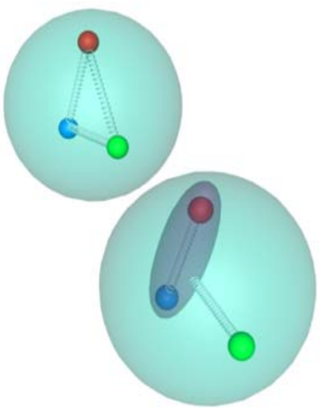

N^*	Status	$SU(6) \otimes O(3)$	Parity	Δ^*	Status	$SU(6) \otimes O(3)$
$P_{11}(938)$	****	$(56,0^+)$	$+$	$P_{33}(1232)$	****	$(56,0^+)$
$S_{11}(1535)$	****	$(70,1^-)$				
$S_{11}(1650)$	****	$(70,1^-)$		$S_{31}(1620)$	****	$(70,1^-)$
$D_{13}(1520)$	****	$(70,1^-)$	-	$D_{33}(1700)$	****	$(70,1^-)$
$D_{13}(1700)$	***	$(70,1^-)$				
$D_{15}(1675)$	****	$(70,1^-)$				
$P_{11}(1520)$	****	$(56,0^+)$		$P_{31}(1875)$	****	$(56,2^+)$
$P_{11}(1710)$	***	$(70,0^+)$	$+$	$P_{31}(1835)$		$(70,0^+)$
$P_{11}(1880)$		$(70,2^+)$				
$P_{11}(1975)$		$(20,1^+)$				
$P_{13}(1720)$	****	$(56,2^+)$		$P_{33}(1600)$	***	$(56,0^+)$
$P_{13}(1870)$	*	$(70,0^+)$		$P_{33}(1920)$	***	$(56,2^+)$
$P_{13}(1910)$		$(70,2^+)$	$+$	$P_{33}(1985)$		$(70,2^+)$
$P_{13}(1950)$		$(70,2^+)$				
$P_{13}(2030)$		$(20,1^+)$				
$F_{15}(1680)$	****	$(56,2^+)$		$F_{35}(1905)$	****	$(56,2^+)$
$F_{15}(2000)$	**	$(70,2^+)$	$+$	$F_{35}(2000)$	**	$(70,2^+)$
$F_{15}(1995)$		$(70,2^+)$				
$F_{17}(1990)$	**	$(70,2^+)$	$+$	$F_{37}(1950)$	****	$(56,2^+)$

$$L_{I\,J}\,(mass)$$

L = πN decay angular momentum state
I = isospin x 2
J = total spin of resonance x 2

Yellow = 4*

The "Missing Baryon" (N*) Problem

Center of mass energy of baryonic system

E_γ		W
2.3	⇔	2.28
1.5	⇔	1.92
0.7	⇔	1.48

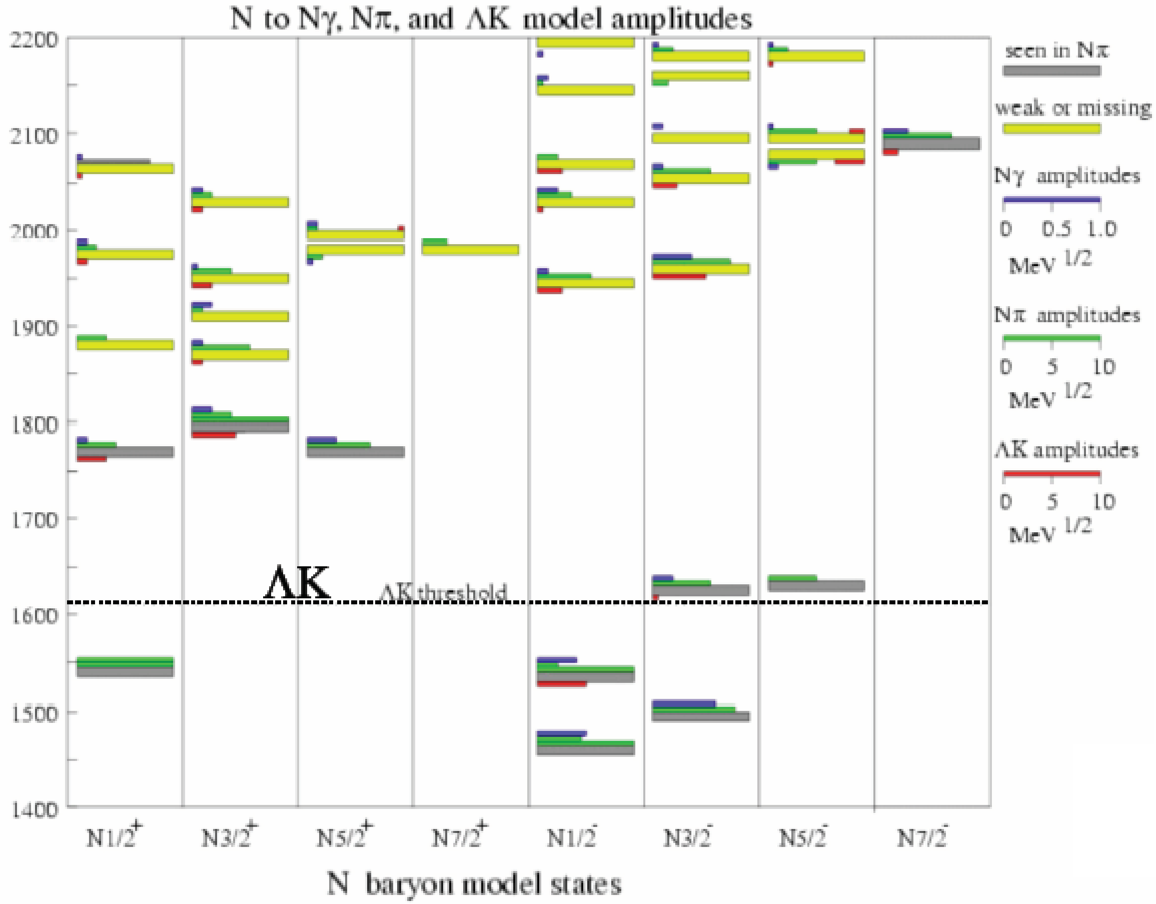

S. Capstick and W. Roberts, Phys. Rev. D **58**, 074011 (1998).

Meson Photoproduction Cross Sections

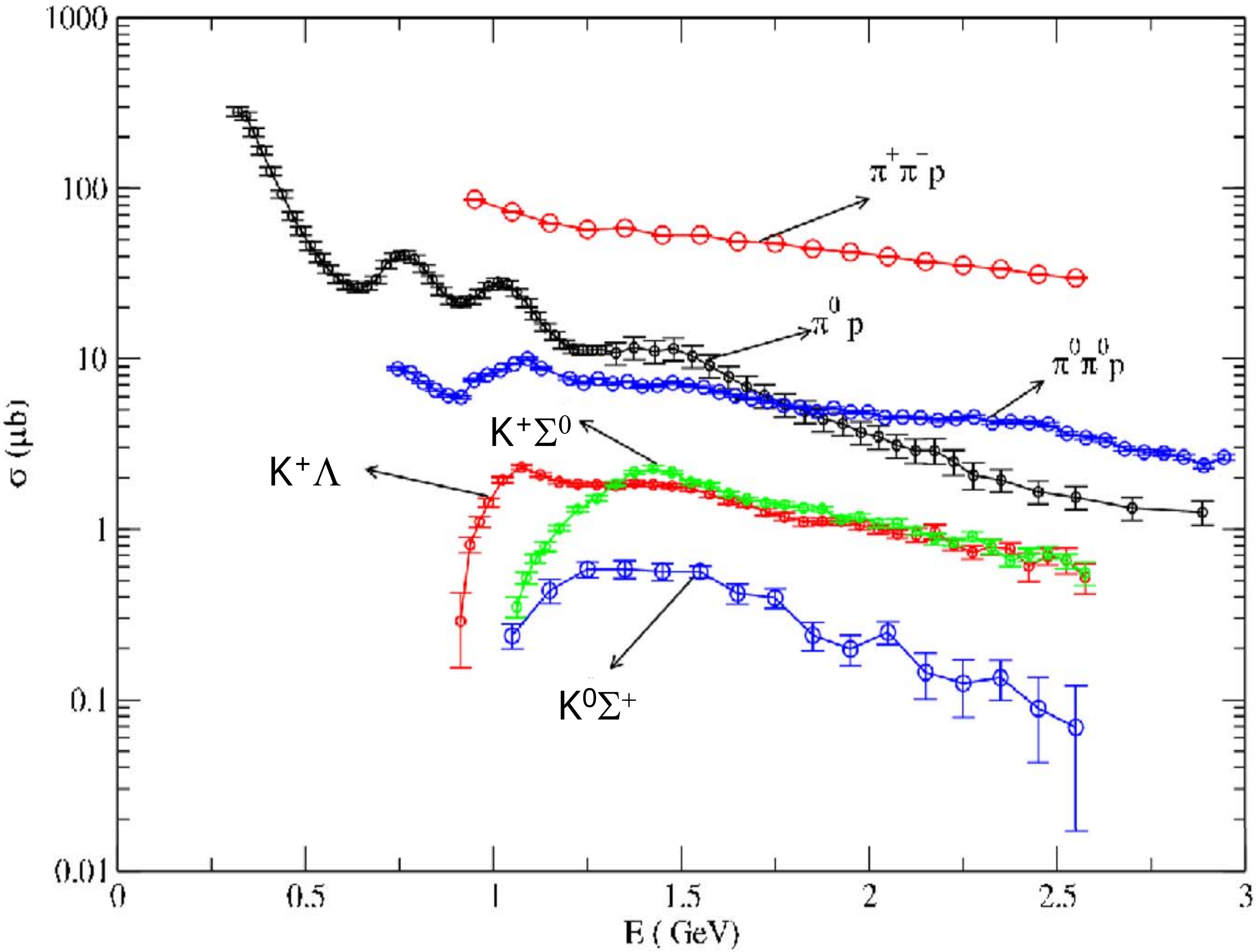

N* Physics via KY Channels

- $N^* \rightarrow KY$ decays are significant two-body decay channels in the mass range of the "missing" resonances (few μb near 1.6 to 2 GeV).
- Hyperons have PV weak decays, "self-analyzing", induced and transferred polarization are measured easily
- Full experimental decomposition of reaction amplitudes → models can divine the N* content of the reactions.

The Observables: 0^- mesons

- Photoproduction described by 4 complex amplitudes
- Bilinear combinations define 16 observables
- 8 measurements* needed to separate amplitudes at any given energy, W
  - differential cross section: $d\sigma/d\Omega$
  - 3 single polarization observables: P, T, Σ
  - <u>4 double polarization</u> observables…

* W-T. Chiang and F. Tabakin Phys Rev. C 55 2054 (1997)

4 Helicity Amplitudes

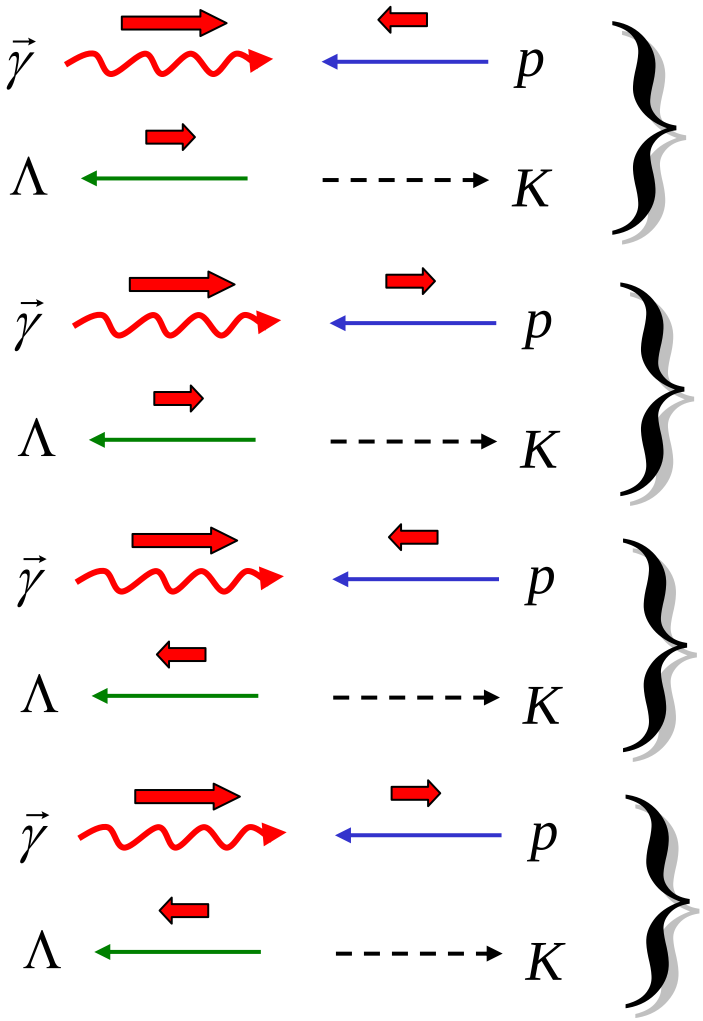

N — No overall helicity flip $= |\gamma - (p - \Lambda)|$

S_1 — Single helicity flip

S_2 — Single helicity flip

D — Double helicity flip

16 Pseudoscalar Meson Photoproduction Observables

Table 1
Observables

Usual symbol	Helicity representation	Experiment required a)

For γ + p→, K^+ Λ:

Single Polarization

R. Bradford *et al*. PRC **73** 035202 (2006), M. McCracken et al, PRC **81**, 025201 (2010).

C. Paterson *et al.* (Glasgow), to be published

J. McNabb *et al*. PRC **69** 042201 (2004), M. McCracken et al, PR C **81**, 025201 (2010).

Beam & Target

FroST (g9a) under analysis

FroST (g9b) data in 2010

Beam & Recoil

C. Paterson *et al.* (Glasgow), to be published

R. Bradford *et al*. Phys. Rev. C **75** 035205 (2007)

Target & Recoil

FroST (g9b) data in 2010

FroST (g9a) under analysis

I. S. Barker, A. Donnachie, J. K. Storrow, Nucl. Phys. B95 347 (1975).

Modern Facilities

- CLAS at Jefferson Lab
- Hall A and C Spectrometers at JLab
- LEPS at Spring-8
- GRAAL at Grenoble
- SAPHIR at Bonn
- KAOS at Mainz (near future)

In this talk I will feature JLab setups…

CEBAF accelerator at JLab

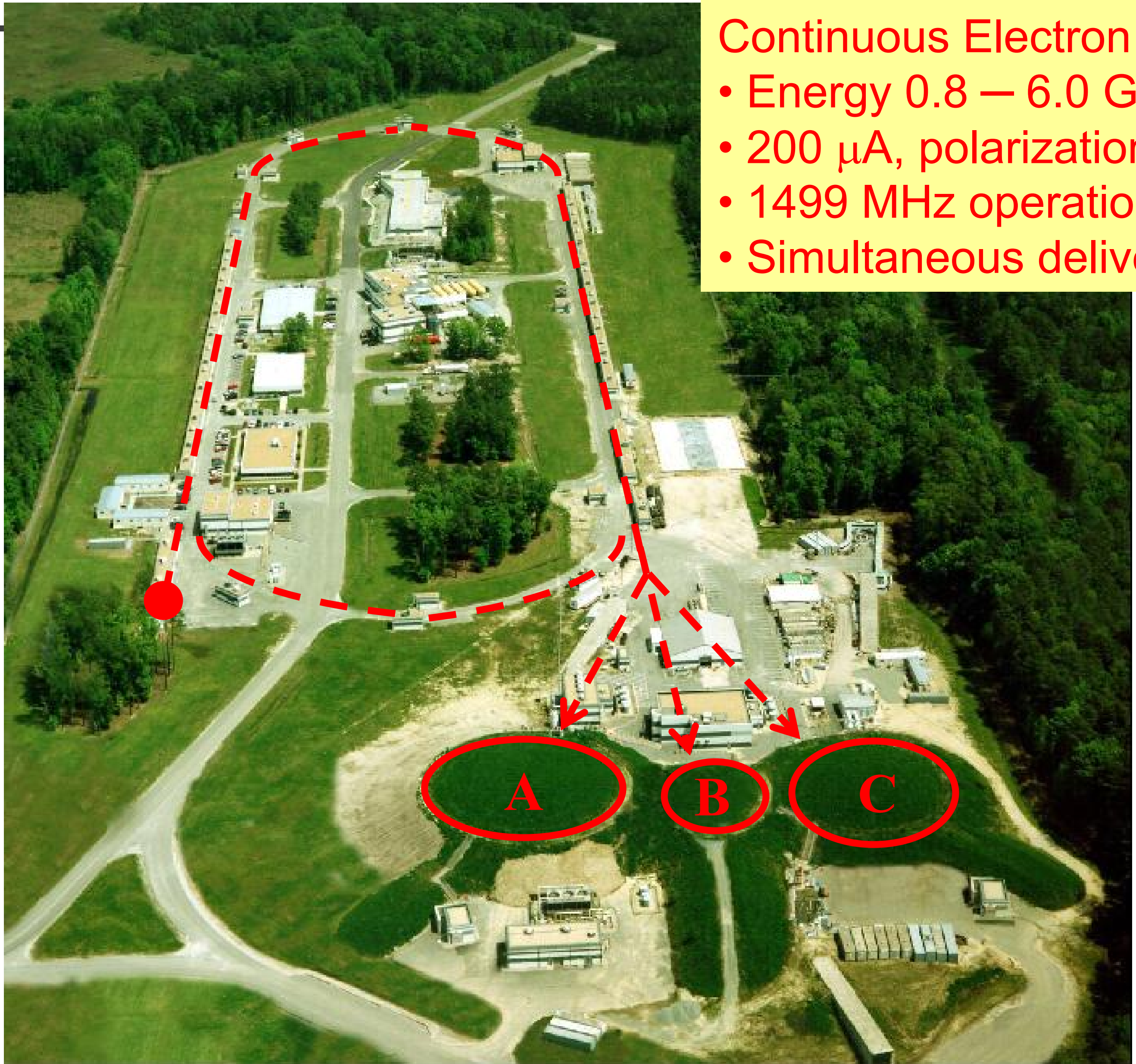

Continuous Electron Beam
- Energy 0.8 – 6.0 GeV
- 200 μA, polarization 75%
- 1499 MHz operation
- Simultaneous delivery 3 halls

What is CLAS?

- Most versatile detector system at Jefferson Lab
- Beams of up to 6 GeV real photon and electrons (→virtual photons) on hydrogen or light nuclear targets
- Detect multiple particles per "event"
- ~200 physicists from ~35 institutions from ~8 countries

The CLAS Detector in Hall B

CEBAF Large Acceptance Spectrometer

Torus magnet
6 superconducting coils

Electromagnetic calorimeters
Lead/scintillator, 1296 photomultipliers

Liquid H_2 target +
γ start counter; e minitorus

Drift chambers
argon/CO_2 gas, 35,000 cells

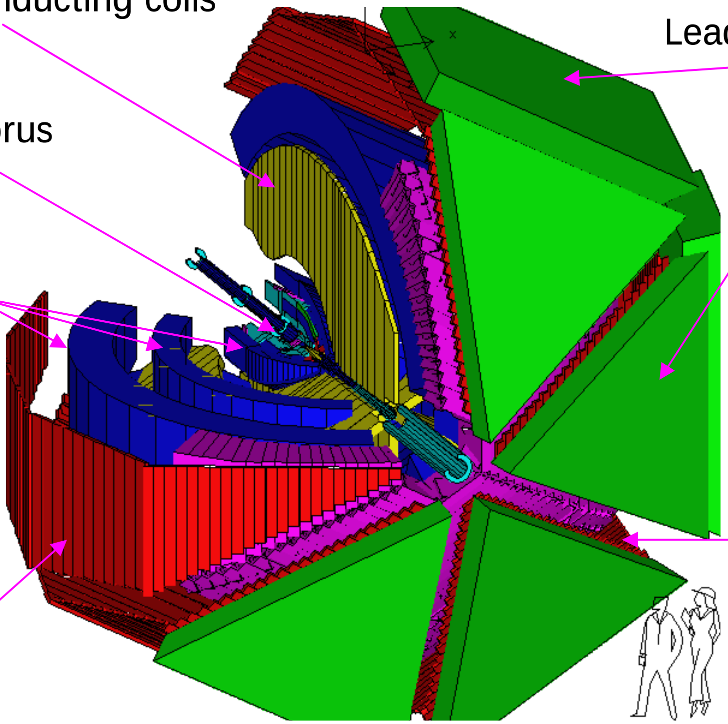

Gas Cherenkov counters
e/π separation, 256 PMTs

Time-of-flight counters
plastic scintillators, 684 photomultipliers

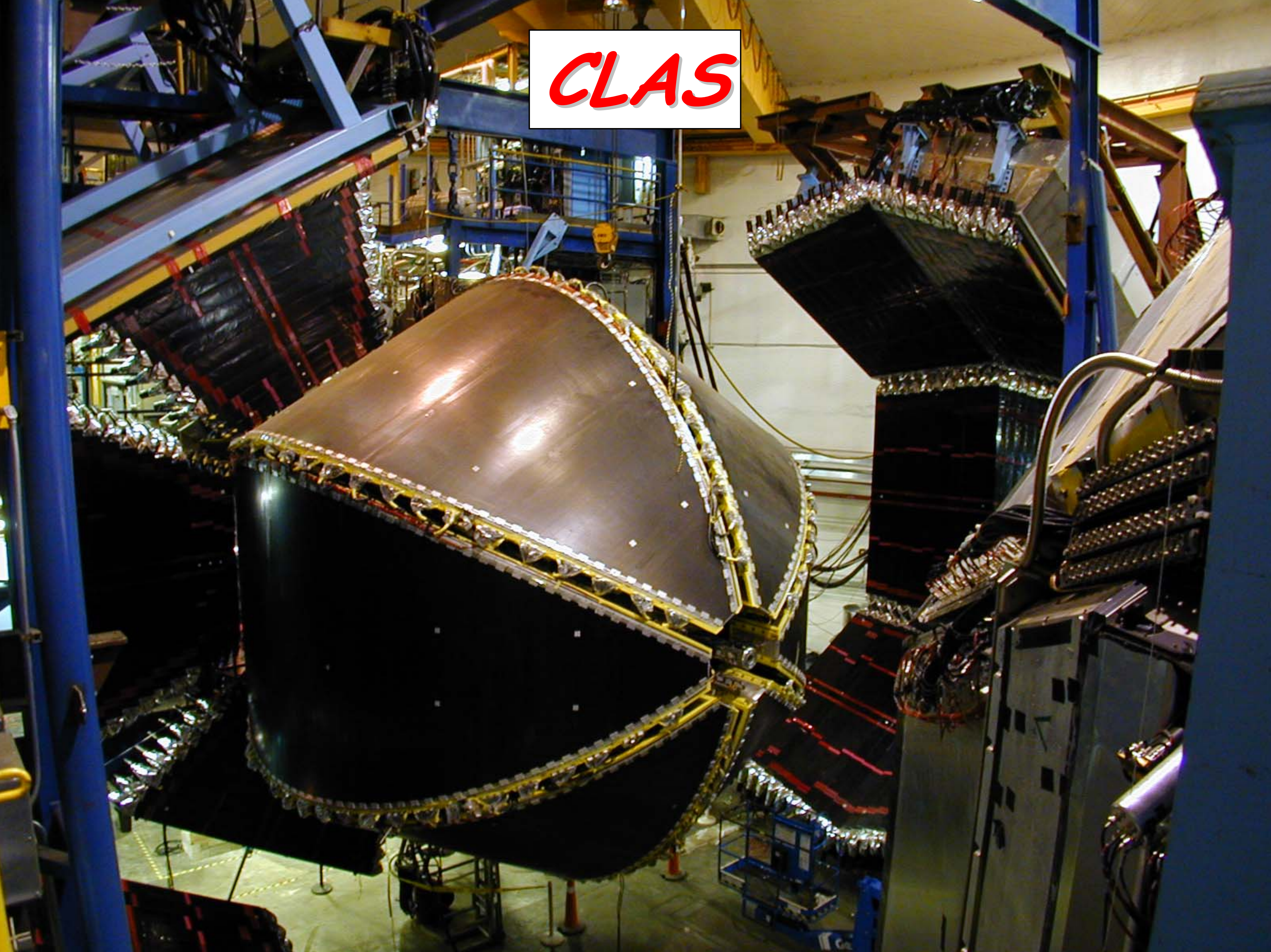
CLAS

"Region 1" Drift Chamber

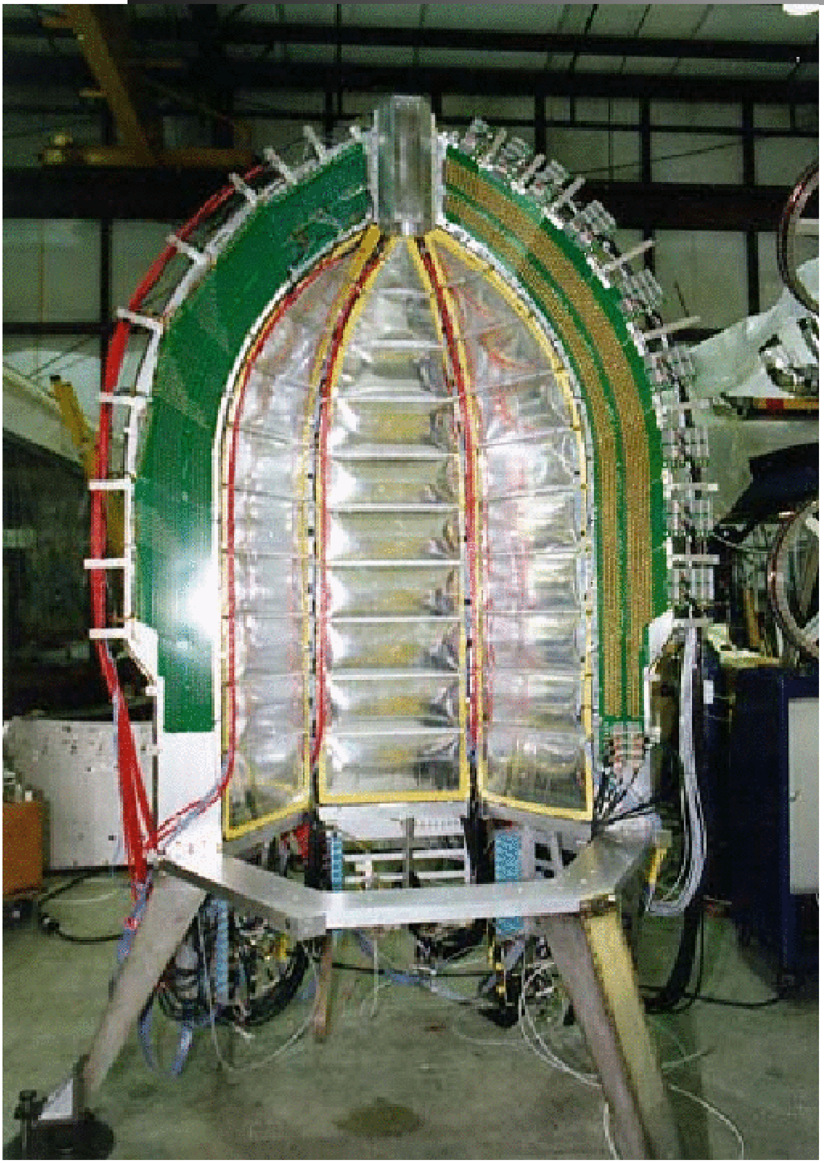

- Built at Carnegie Mellon and Pitt, then installed at JLab in Newport News
- 7776 "sense wires" and readout electronic channels
- View is of the ½ assembled structure, oriented sideways
- ~$750k, ~5 year project
- Has been in operation since 1998

The CLAS Photon Tagger

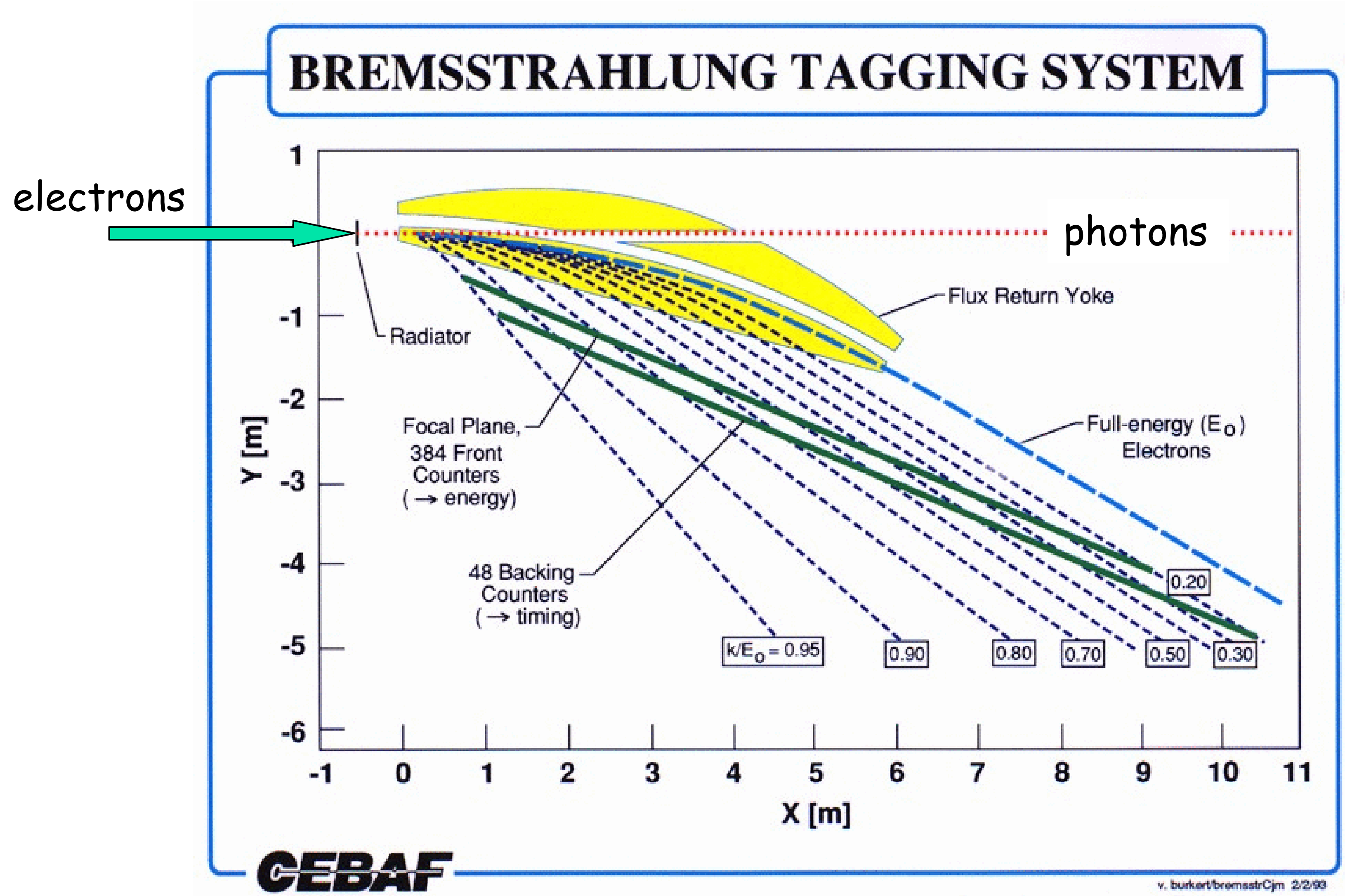

Tagged Polarized Photons in CLAS

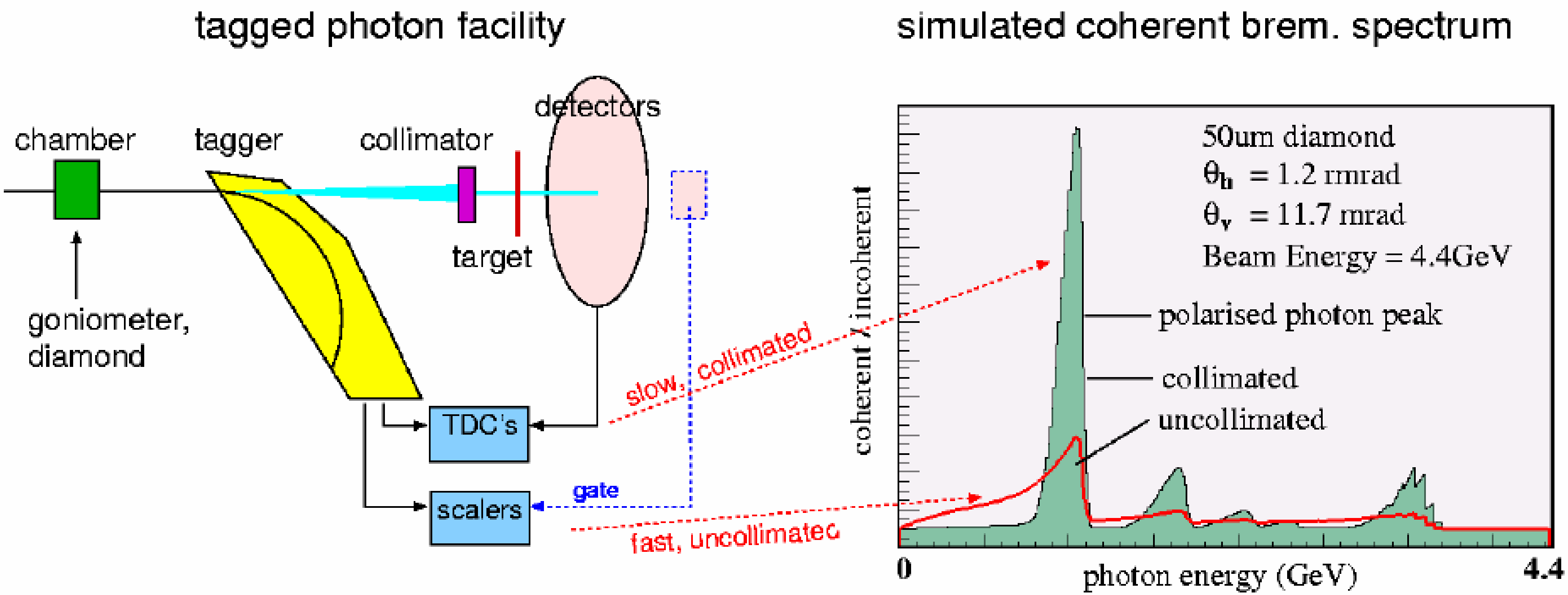

- $E_\gamma = E_0 - E'$
- **Circular Polarisation: polarised electron beam, amorphous radiator**
- **Linear polarisation: Crystal (diamond) radiator**

g9 FROST - FROzen Spin Target (Butanol = C_4H_9OH)

Meson photoproduction with linearly and circularly polarized photons on polarized target

- E02-112: $\gamma p \to KY$ ($K^+\Lambda$, $K^+\Sigma^0$, $K^0\Sigma^+$)
- E03-105/E04-102: $\gamma p \to \pi^0 p$, $\pi^+ n$
- E05-012: $\gamma p \to \eta p$
- E06-013: $\gamma p \to \pi^+\pi^- p$

Frozen Spin Mode

- Microwaves OFF
- Polarizing magnet OFF
- Holding magnet ON
- Temperature ≤0.05 K
- Photon beam ON

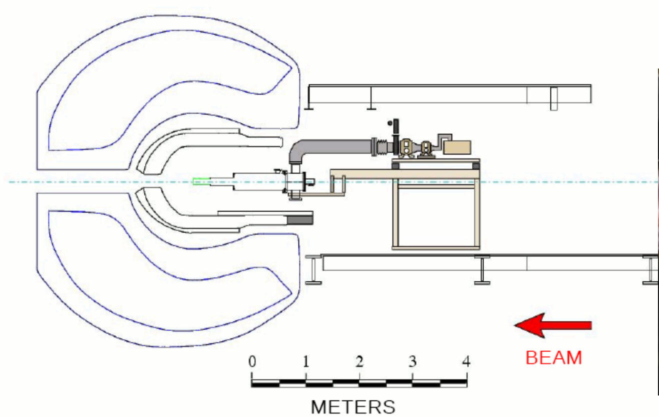

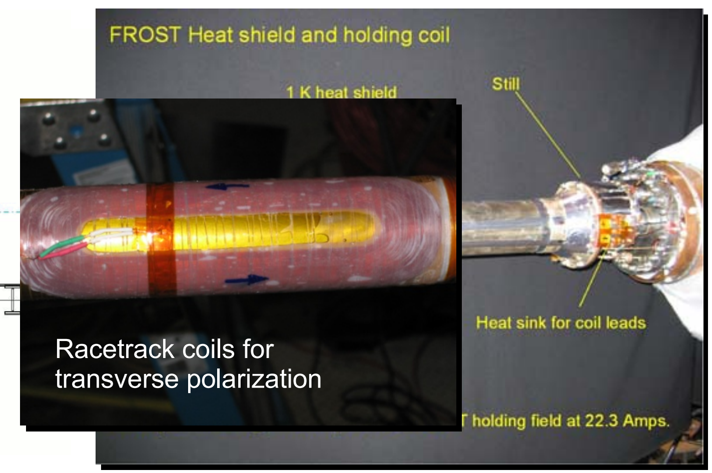

g9a running conditions

- November 3, 2007– February 12, 2008
- Longitudinally polarized target
- Circularly and linearly polarized photon beam 0.5-2.4 GeV
- Trigger: at least one charged particle in CLAS
- Target Pol > 80%, Relaxation time > 1600hrs – **better that design goals**

g9b

- March – July 2010
- Transversely polarized target

CLAS Single Event: $\gamma + p \rightarrow K^+ + \Lambda \rightarrow K^+ + p + \pi^-$

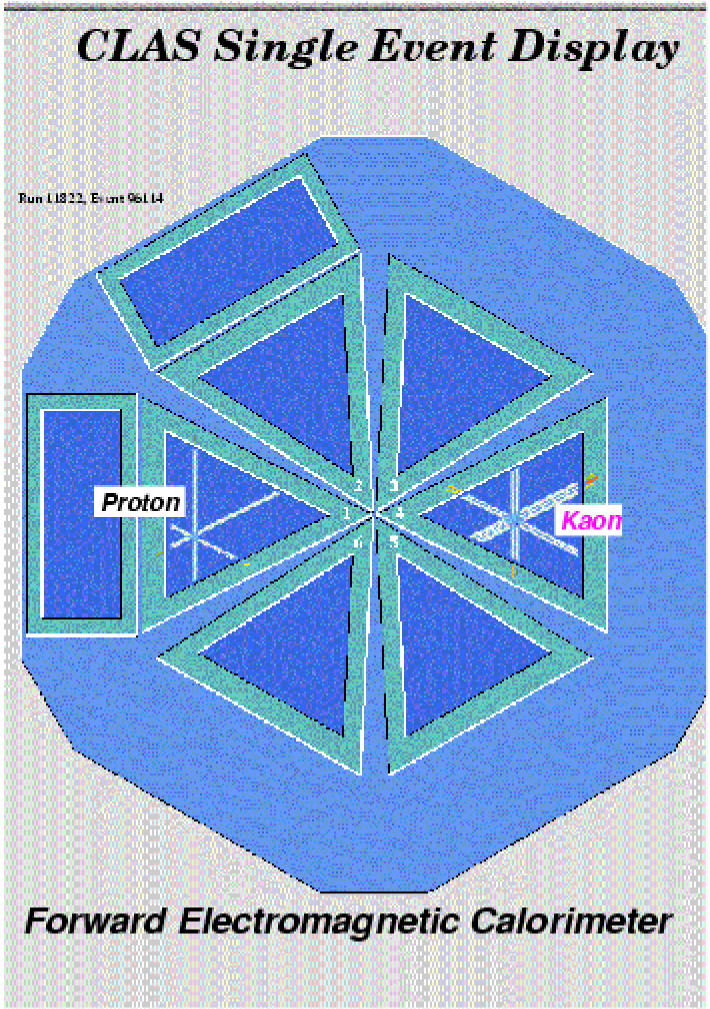

Beam Photon: 1.58 GeV

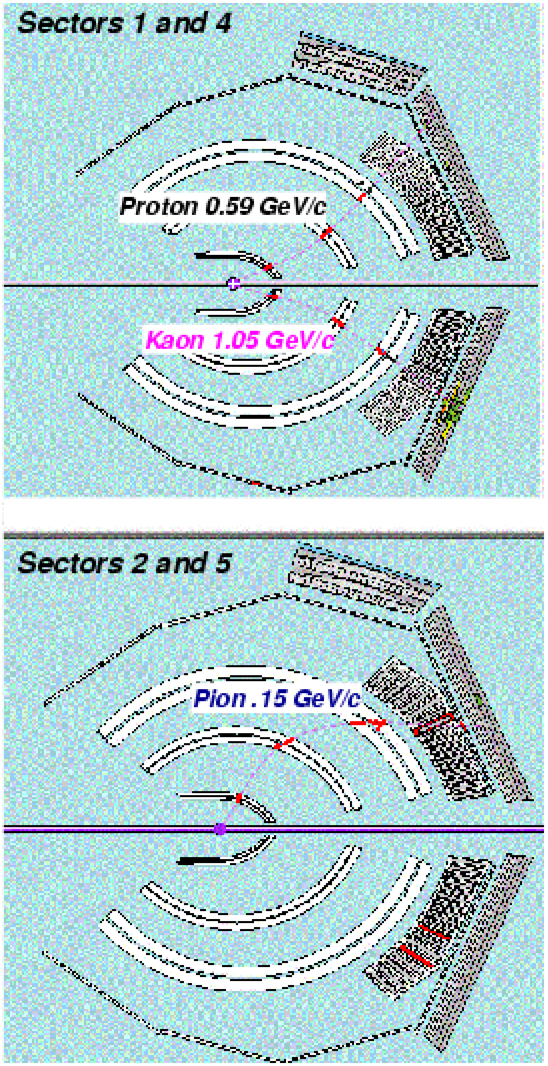

Analysis Steps to get Cross Sections

$$\frac{d\sigma}{d\Omega}\left(\theta_K^{c.m.}\right) = \frac{N_Y(E_\gamma,\theta_K^{c.m.})}{N_\gamma(E_\gamma)} \frac{T_c}{A(E_\gamma,\theta_K^{c.m.})}$$

We need:

1. Event sample
2. N_Y = hyperon yield
3. N_γ = photon normalization
4. A = acceptance & efficiency
5. T_c = target constants

Analysis Ingredients

1. If require K⁺ & p detection:
2. Yields from Missing Mass off $(\gamma, K^+)Y$:
   - Gaussian + polyomial fits
   - sideband subtractions
3. Standard CLAS photon normalization procedure GFLUX
   - based on counting/scaling accidental hits in photon tagger
4. Full GEANT/ GSIM/GPP- based simulations for acceptance

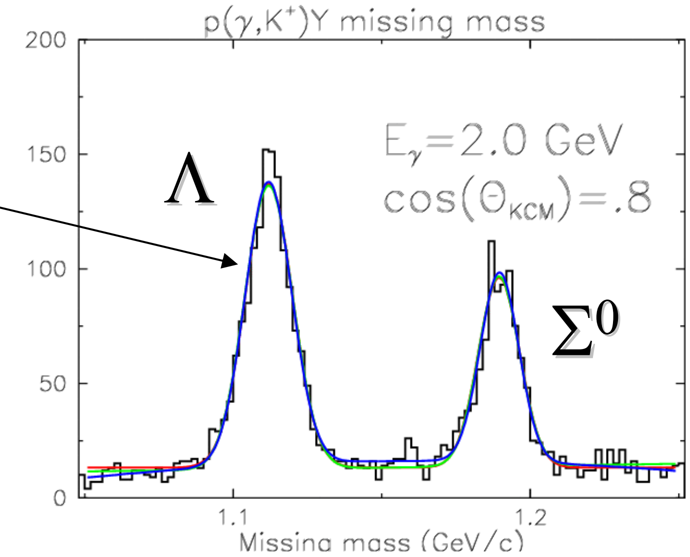

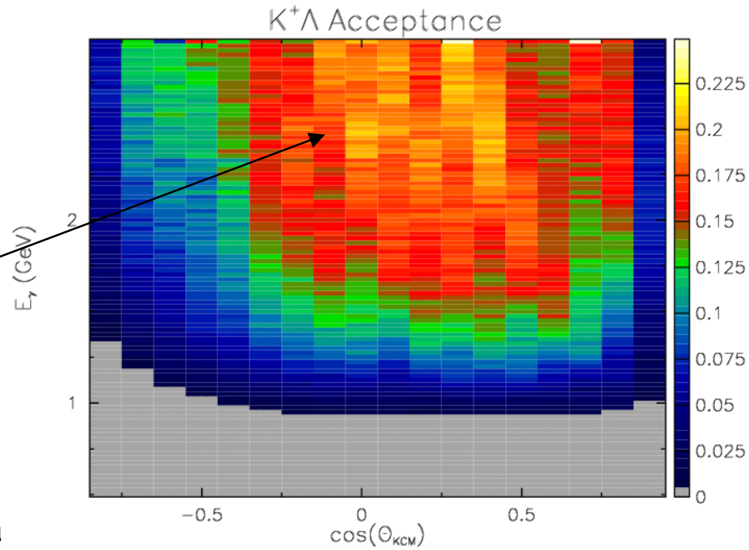

$\gamma p \rightarrow K^+\Lambda$ Cross Sections

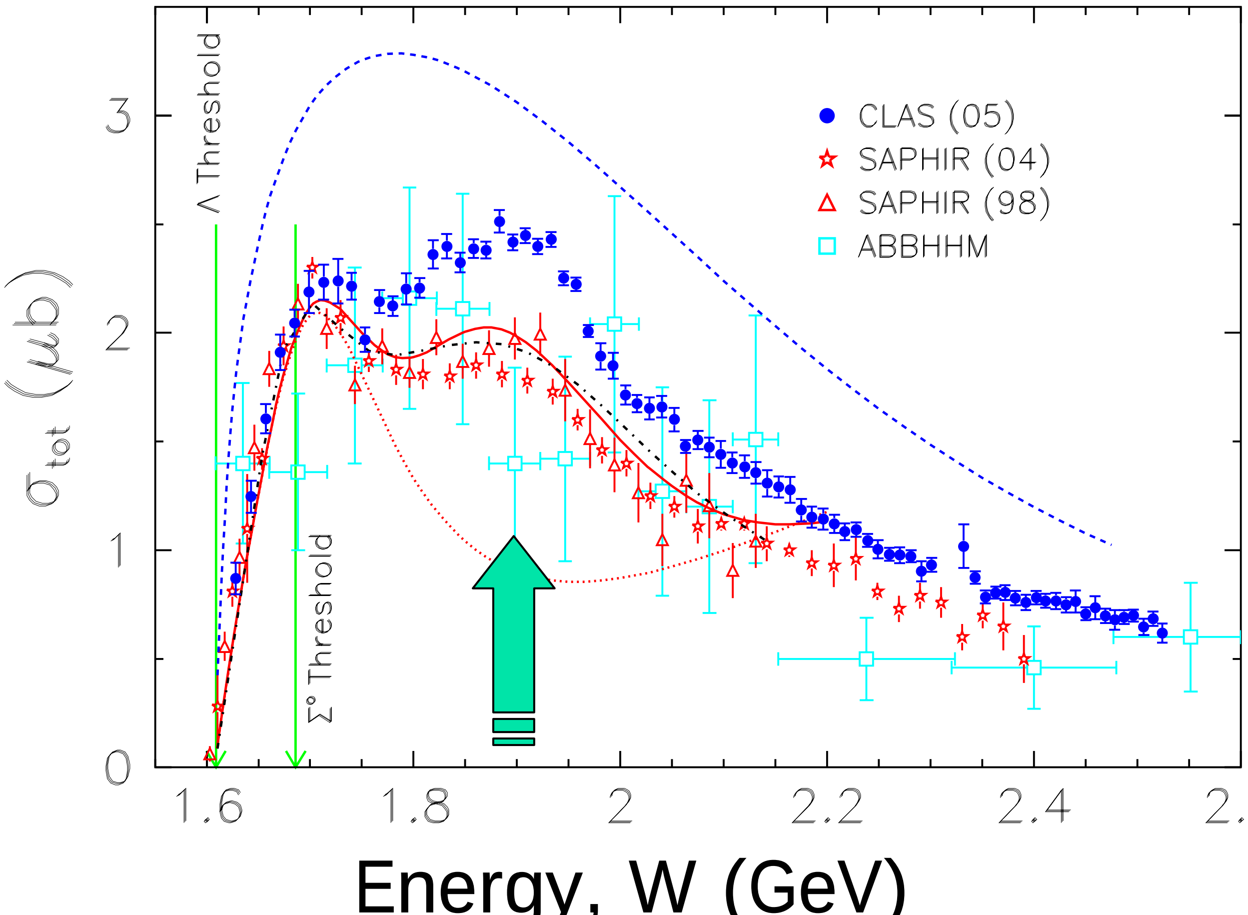

- Two-bump structure seen
- Resonance-like structure at 1.9 GeV:
  - D_{13} (Bennhold & Mart)[a]
  - P_{13} (Bonn-Gachina)[b]
  - P_{11} (Ghent "RPR" model)[c]
  - $\bar{K}KN$ bound state (Valencia model)[d]
  - Coupled-channel effects (Giessen)[e]

R. Bradford *et al*. Phys. Rev. C**73** 035202 (2006)
K. H. Glander *et al*. Eur. Phys. J. A**19** 251 (2004)

a) T, Mart, C. Bennhold, Phys Rev C **61**, 012201(R) (1999).
b) V. Nikanov et al, Phys Lett B **662**, 245 (2008).
c) T. Corthals, et al., PRC **73**, 045207 (2006).
d) A. MartinezTorres, et al., Eur. Phys J. A 41, **361** (2009).
e) R. Shyam, O.Scholten & H.Lenske, PRC **81**, 015204 (2010).

$\gamma p \rightarrow K^{+}\Lambda$ Cross Sections

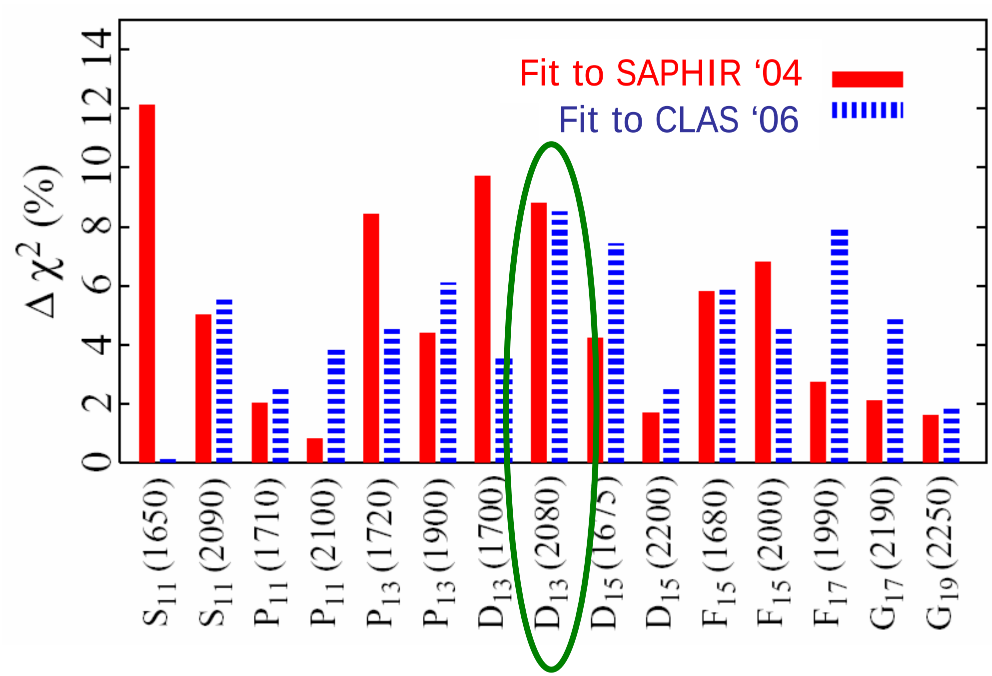

- Example of recent work:
- T. Mart *et al.* found:
  - Single channel effective Lagrangian analysis
  - Bump in total cross section traced to "missing" $D_{13}(2080)$
  - Two experiments yield inconsistent resonance parameters
  - Recent CLAS C_x C_z results change the story (see later)

T. Mart, arXiv[nucl-th]0808.0771 (Aug. 2008)

see also: P. Bydzovsky and T. Mart Phys Rev C 76 065202 (2007).

Compare CLAS'05, CLAS'09, SAPHIR

$\gamma p \rightarrow K^+ \Lambda$

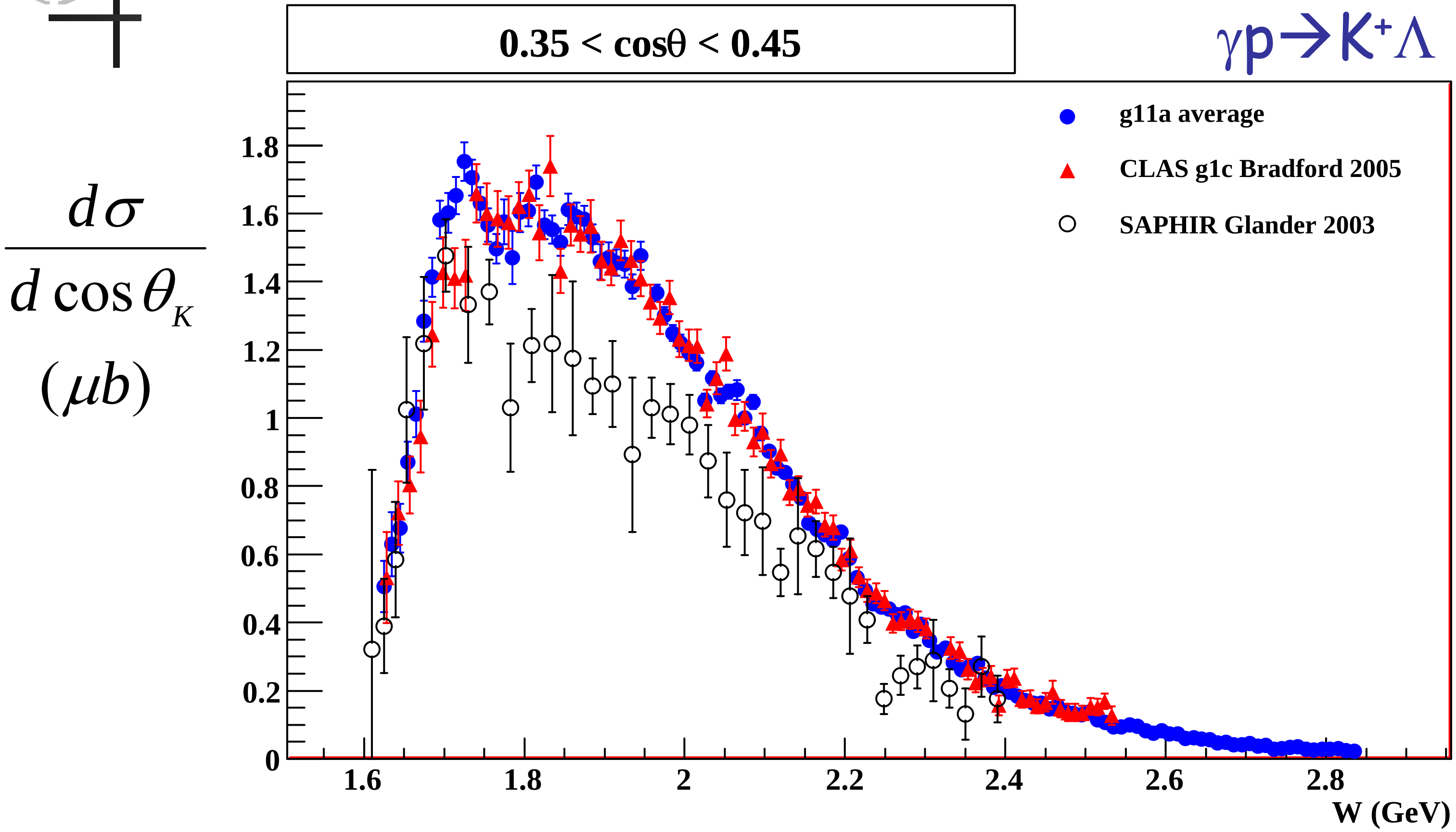

- CLAS 'g11' data: broader energy range, better statistics, good agreement with 'g1c' (Bradford *et al.*)
  - Different data set, different trigger, different analysis chain
  - M. McCracken et al. Phys. Rev. C **81**, 025201 (2010).
  - PWA analysis underway

Photoproduction of $K^+\Lambda$

R. Bradford et al., Phys.Rev.C73, 035202 (2006)

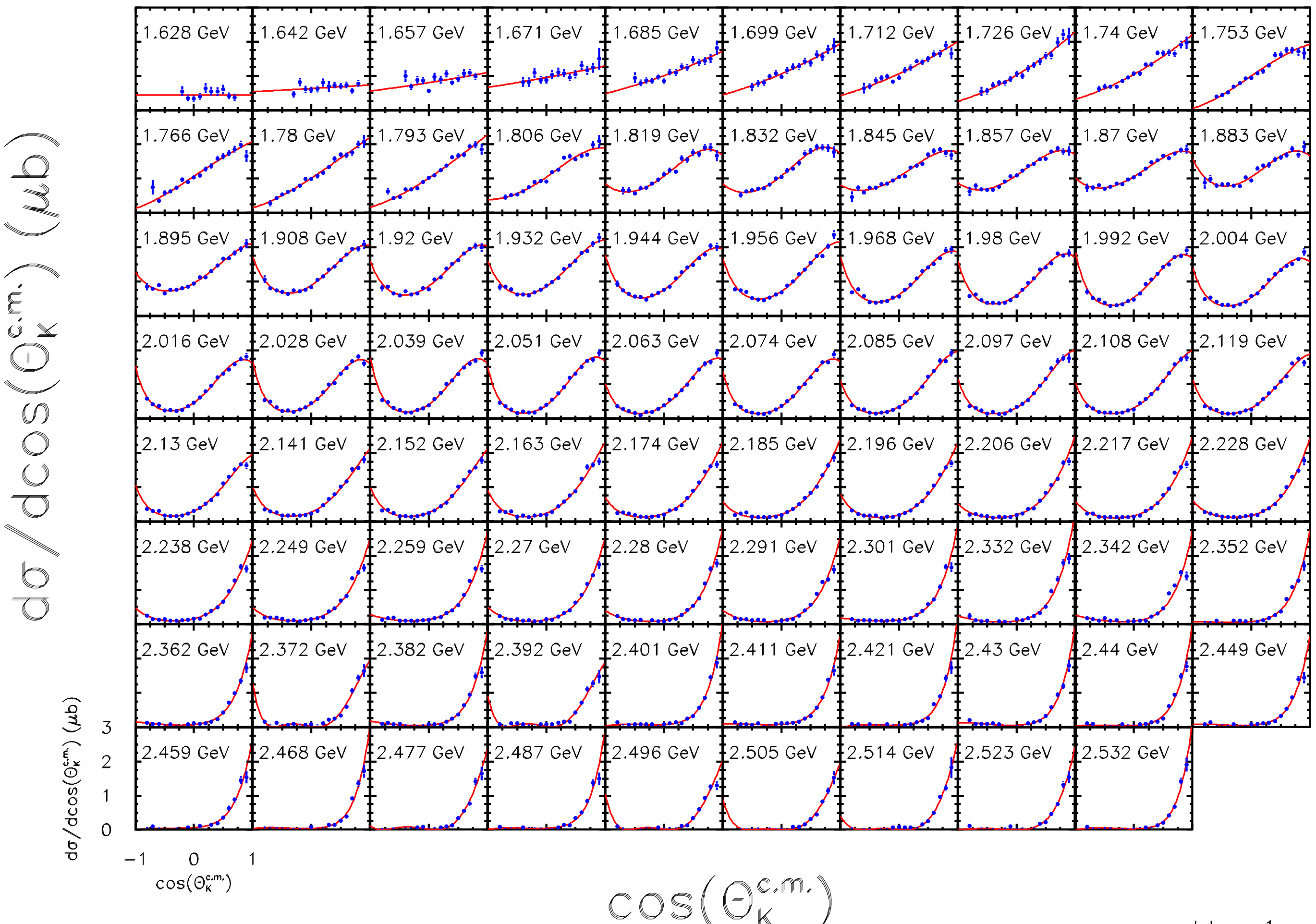

- Forward peaking indicates t-channel processes at high W
- Angular dependence at lower W consistent with s- and u-channel processes.

$\gamma p \rightarrow K^+\Lambda$ Cross Sections

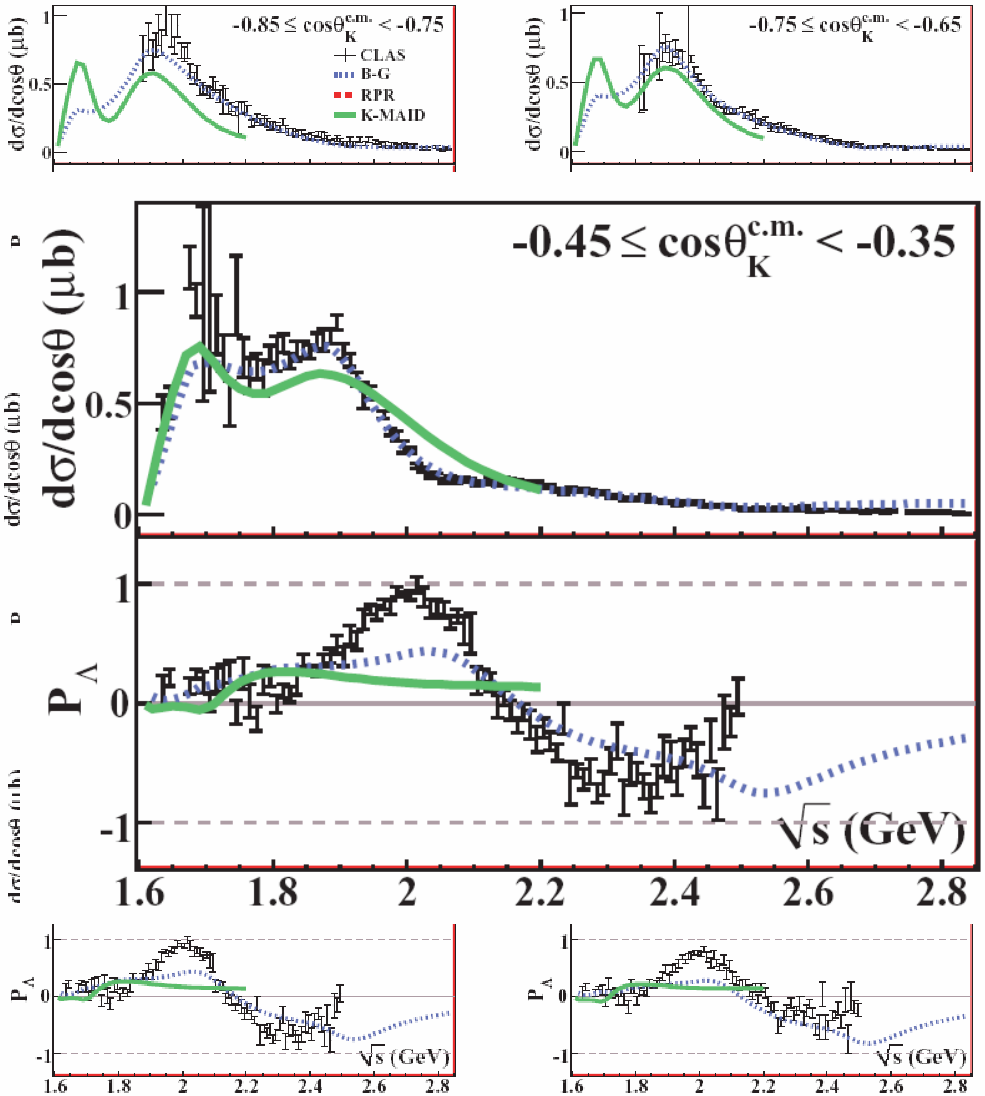

- Kaon-MAID model (green)
  - F.X.Lee et al., Nucl. Phys. **A695**, 237 (2001).
  - Single-channel BW resonance fits
  - No longer up-to-date
- Bonn-Gachina model (blue)
  - A.V. Sarantsev et al., Eur. Phys. J., A **25**, 441 (2005).
  - Multi-channel, unitary, BW resonance fit
  - Large suite of N* contributions
  - Was not predictive for recoil polarization

M. McCracken et al, (CLAS) Phys. Rev. C **81**, 025201 (2010).

$\gamma p \rightarrow K^+\Sigma^0$ Cross Sections

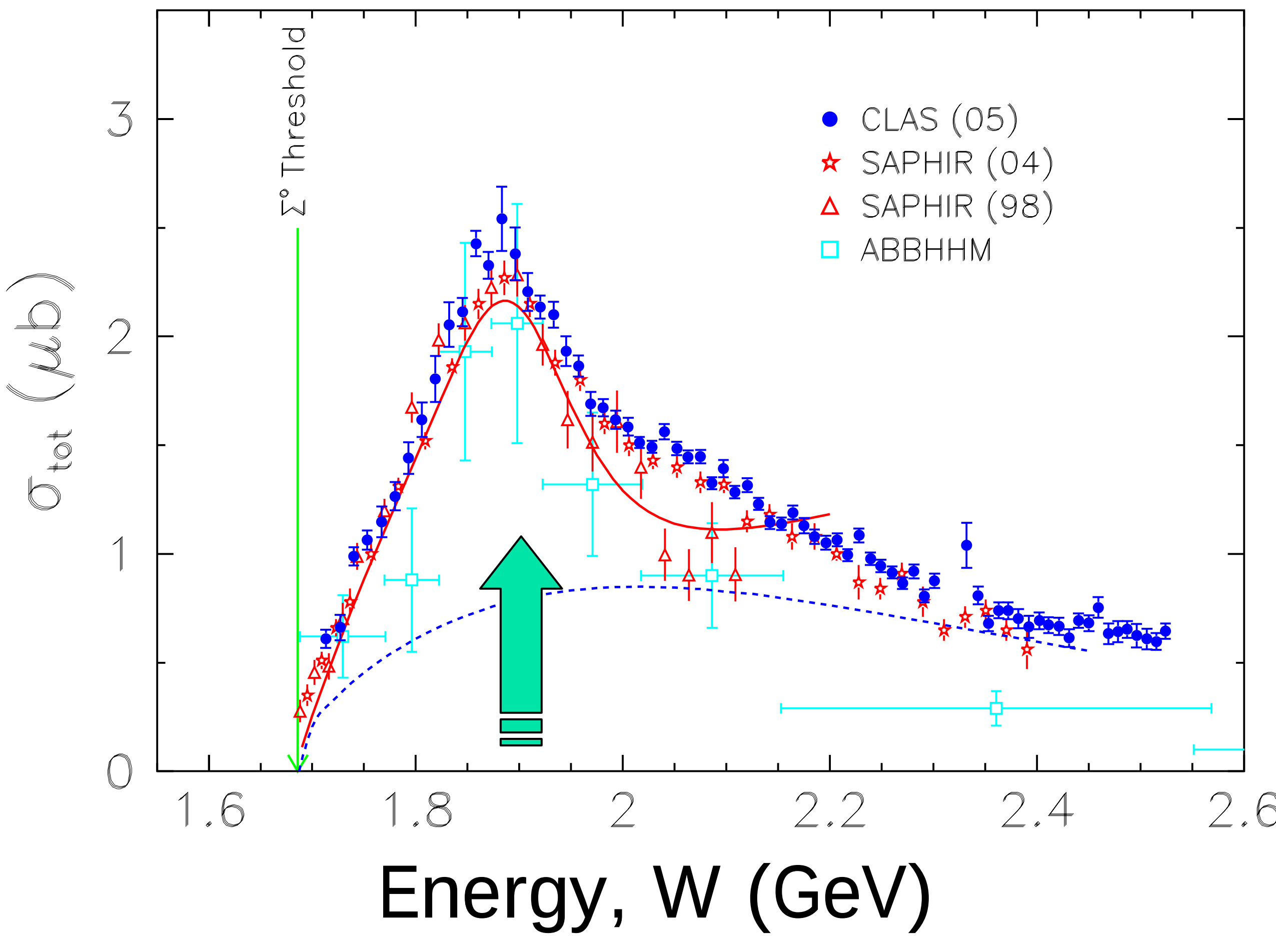

- Single-bump: resonance-like structure near 1.9 GeV
  - N* & Δ resonances: both isospins 1/2 and 3/2 contribute
- CLAS & SAPHIR: fair agreement

R. Bradford *et al.* Phys. Rev. C**73** 035202 (2006)
K.H. Glander *et al.* Eur. Phys. J. A**19** 251 (2004)

Photoproduction of $K^+\Sigma^0$

R. Bradford et al., Phys.Rev.C73, 035202 (2006)

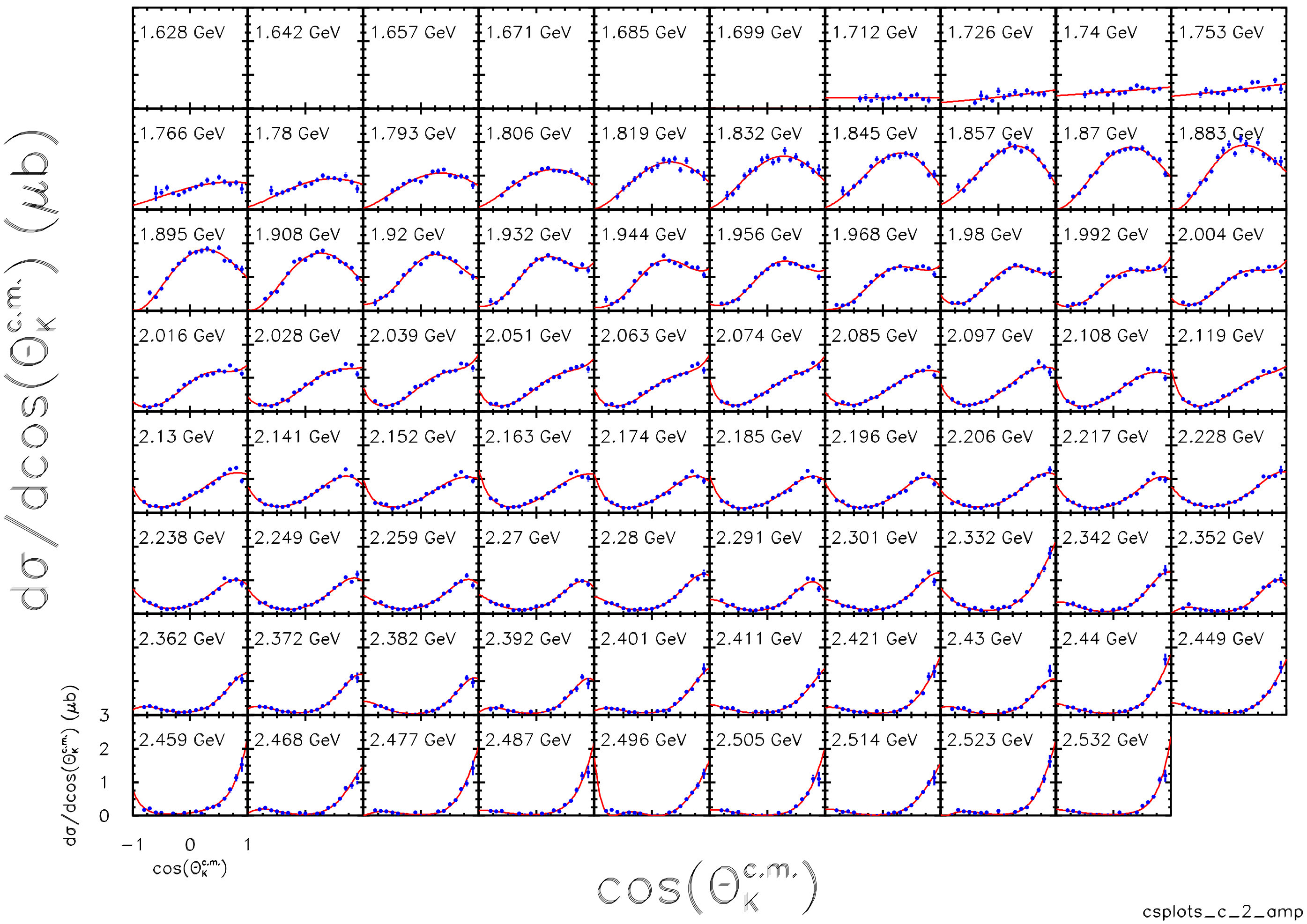

- Angular dependence indicates presence of s-channel resonances.

$\gamma p \rightarrow K^+\Sigma^0$ Cross Sections

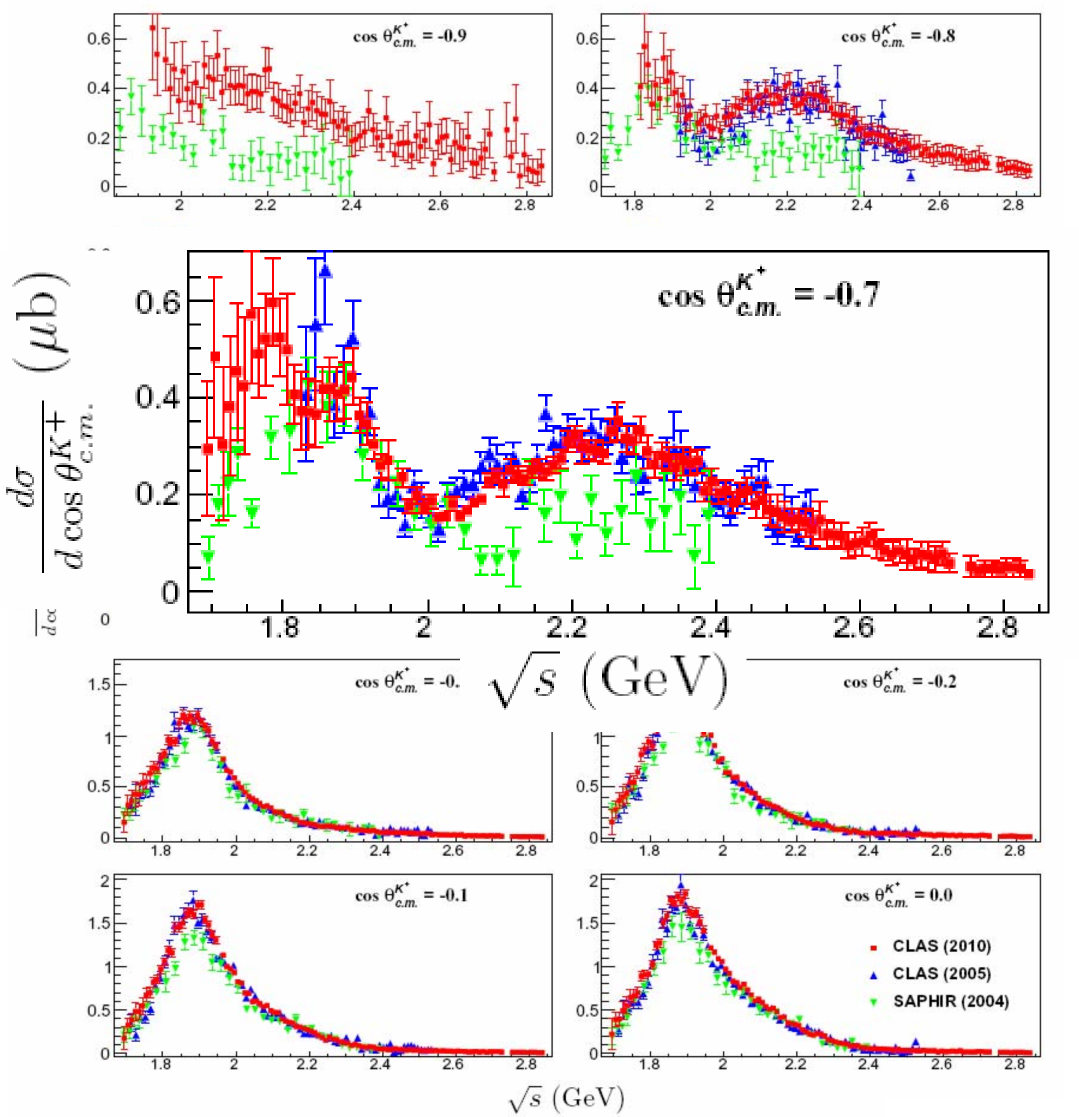

- New results from CLAS
- Unbinned maximum likelihood method
- Excellent agreement with previous CLAS publication (Bradford etal.)
- Resonance-like structure at 2.3 GeV at back angles
- PWA analysis underway

B. Dey *et al.* (CLAS) Phys Rev C **82** 025202 (2010)

Regge-scaling in t and u in $\gamma p \rightarrow K^+\Sigma^0$

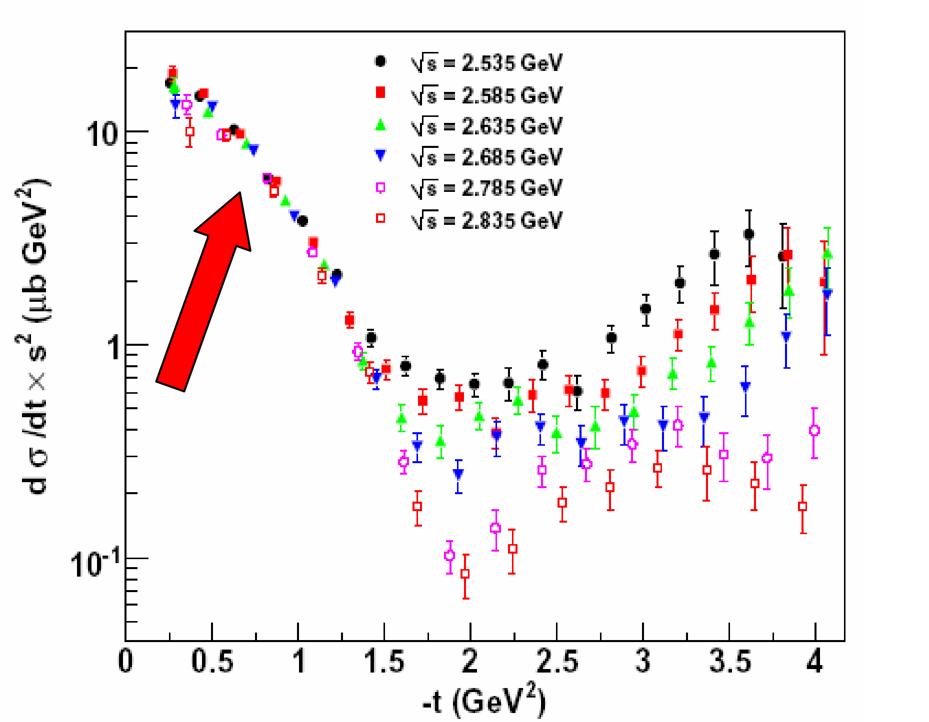

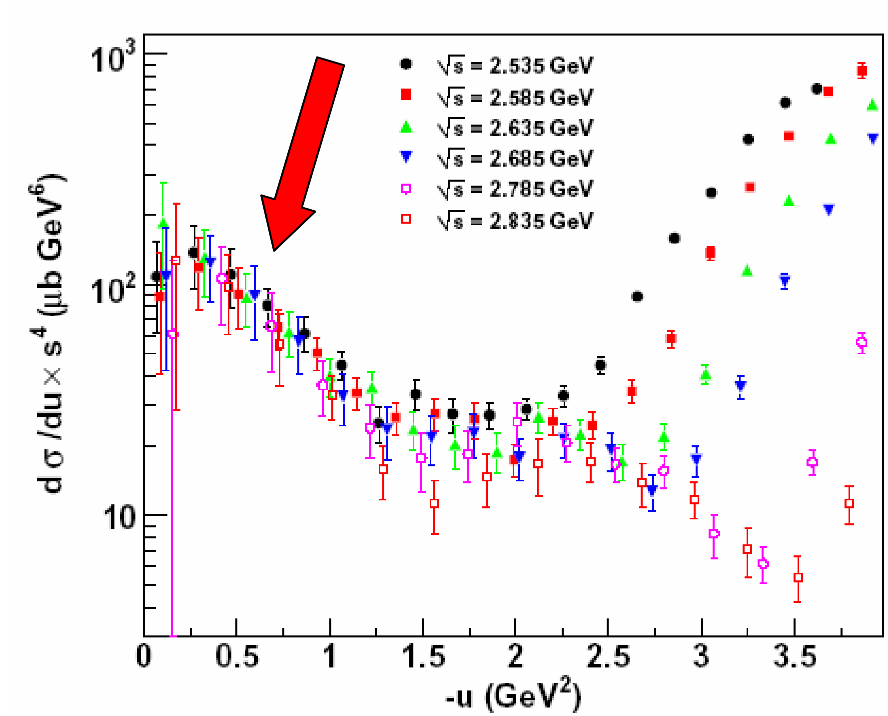

$$d\sigma / dt \sim s^{2\alpha_{eff}(t)-2}$$

$$\alpha_{eff} = \alpha_{K^+} + \alpha_{K*(892)} \approx 0, t \rightarrow 0$$

- Cross section scales as $\sim s^2$

$$d\sigma / du \sim s^{2\alpha_{eff}(u)-2}$$

$$\alpha_{eff} = \alpha_{\Lambda} + \alpha_{\Sigma} \approx -1.4, u \rightarrow 0$$

- Cross section scales as $\sim s^4$

B. Dey *et al.* (CLAS) to be submitted (2010)

$\gamma n \rightarrow K^+\Sigma^-$ on bound neutrons

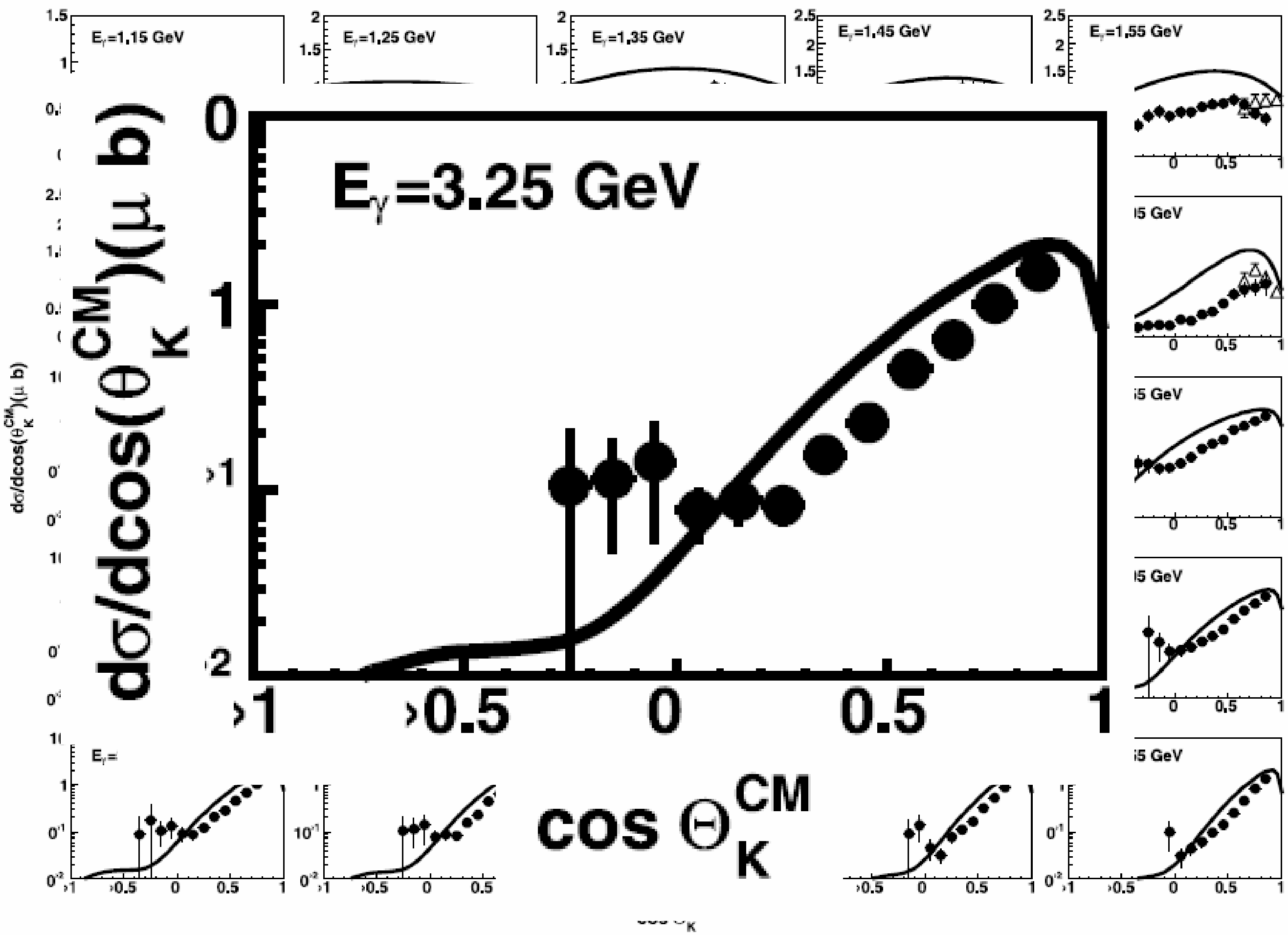

- First "complete" look at Y production off neutron
- Deuteron target, proton spectator, FSI ~ 10%
- Modeled with K^+ and K*(892) in Regge trajectories (no resonances)
  - Ghent model, Ryckebusch *et al.*
- Hint of back-angle rise → u-channel contribution

S. Anefalos Pereira *et al.*, (CLAS) PhysLett B **688**, 289 (2010)

Define the Spin Observables

(for target polarization zero)

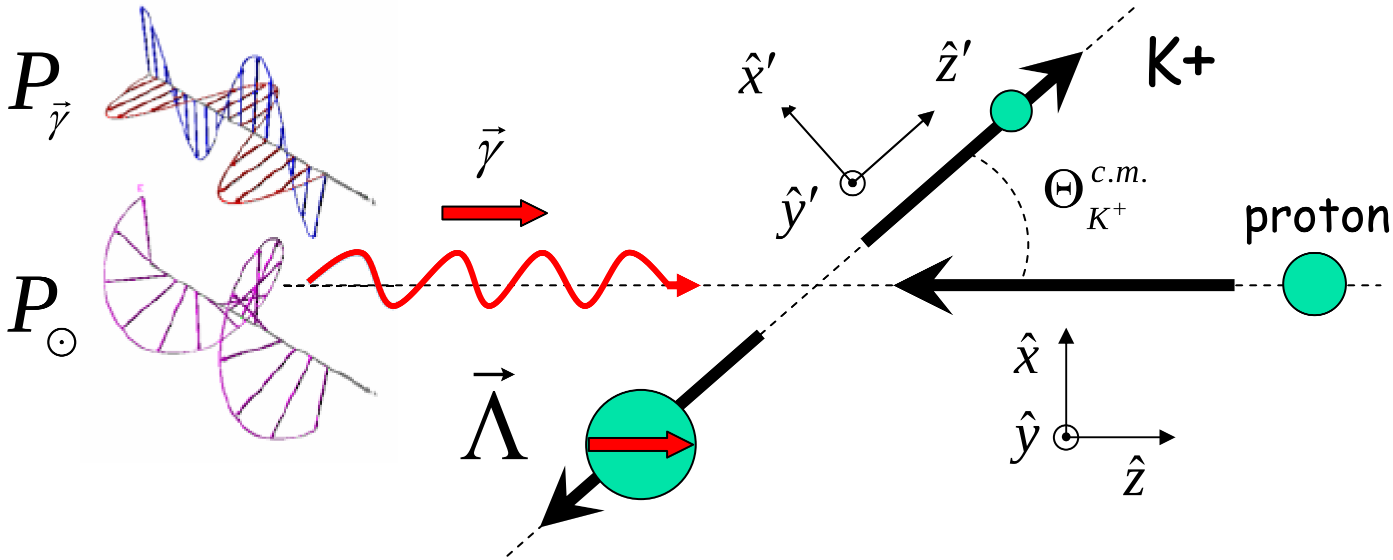

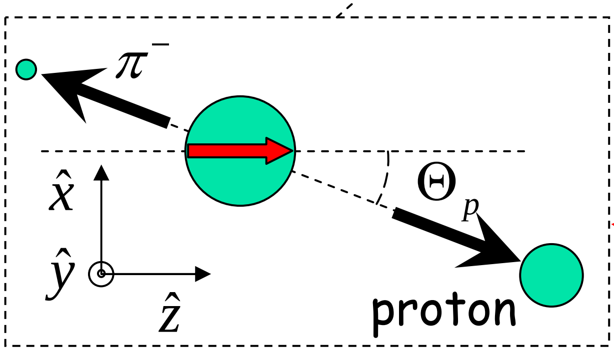

$$\frac{d\sigma}{d\Omega} = \sigma_0 \left\{ \begin{array}{l} 1 - P_{\vec{\gamma}} \Sigma \cos 2\phi \\ \quad - \alpha \cos\theta_{x'} \sin 2\phi P_{\vec{\gamma}} O_{x'} - \alpha \cos\theta_{x'} P_{\odot} C_{x'} \\ \quad - \alpha \cos\theta_{z'} \sin 2\phi P_{\vec{\gamma}} O_{z'} - \alpha \cos\theta_{z'} P_{\odot} C_{z'} \\ \quad + \alpha \cos\theta_{y'} P - \alpha \cos\theta_{y'} P_{\vec{\gamma}} T \cos 2\phi \end{array} \right\}$$

$\gamma p \rightarrow K^+\Lambda$ Hyperon Recoil Polarization

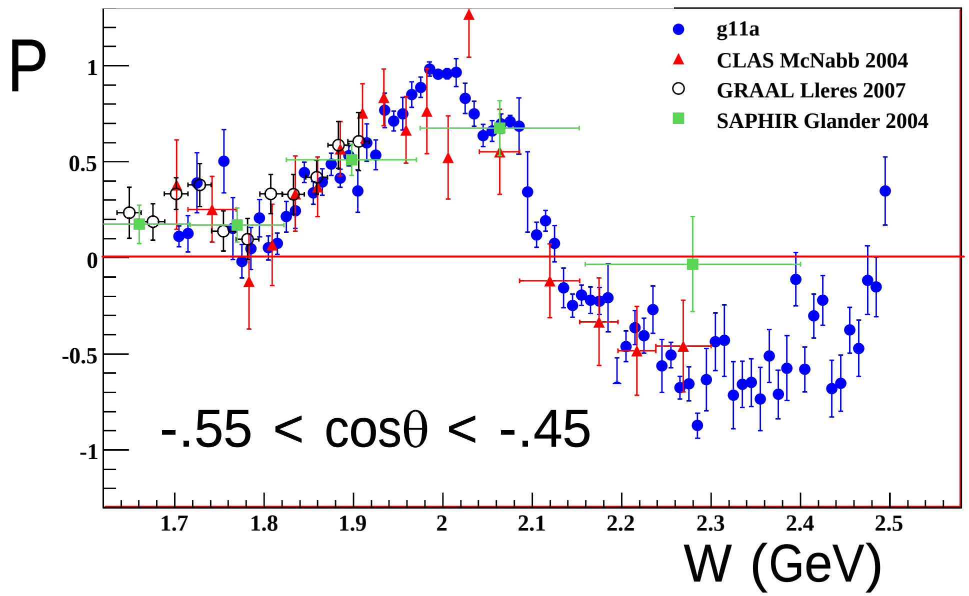

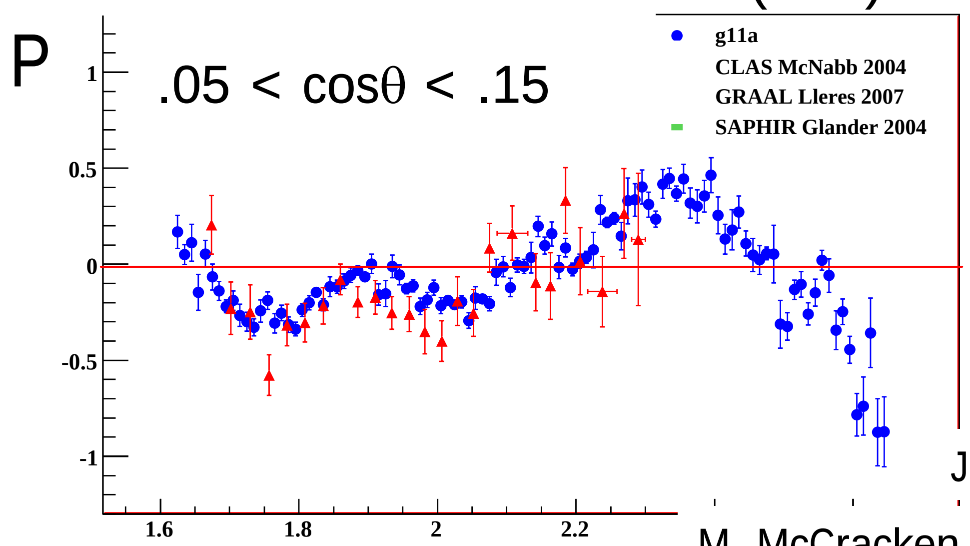

- Recent CLAS results show fine structure in P_Λ
- Good agreement among older CLAS results (McNabb g1c, Paterson g8b), and GRAAL
- PWA analysis underway

J. McNabb *et al.* Phys Rev C **69** 042201 (2004)

M. McCracken et al, (CLAS) Phys. Rev. C **81**, 025201 (2010)

Polarization comparison

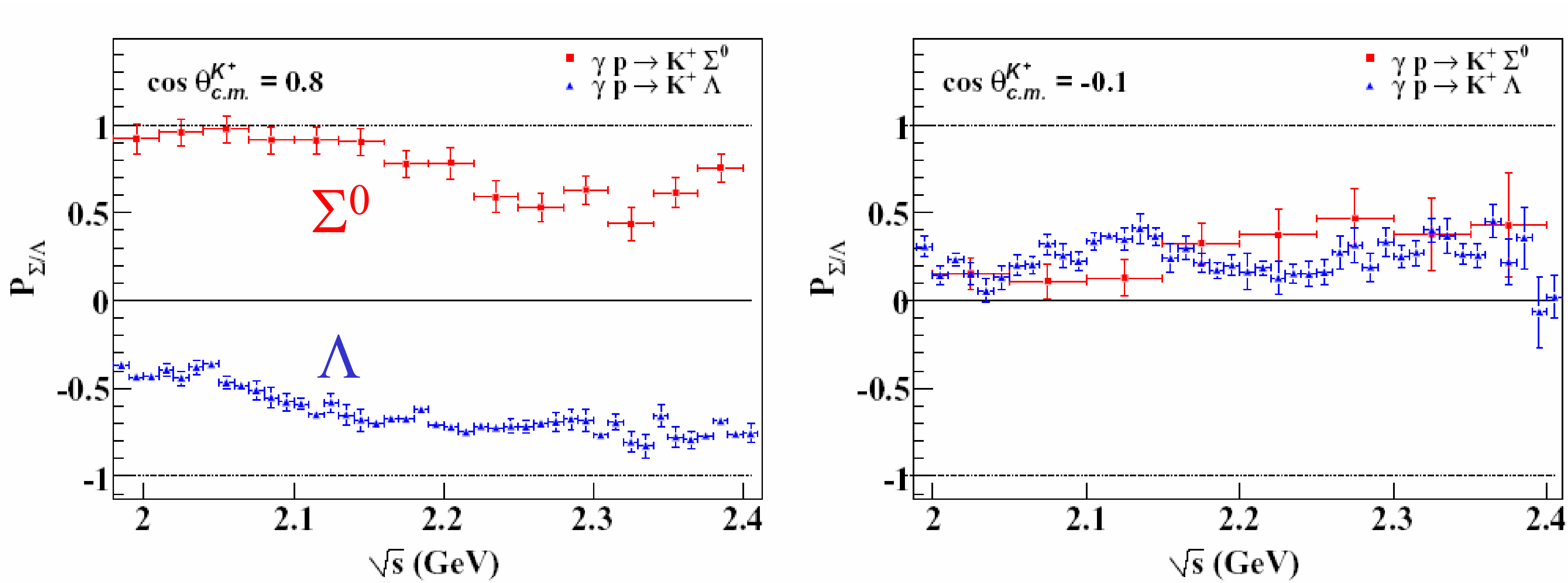

- Naïve SU(6) expectation: $P_{\Lambda} \simeq -P_{\Sigma^0}$
- True in forward direction
- False in backward direction

B. Dey *et al.* (CLAS) Phys Rev C **82** 025202 (2010)

Beam Asymmetry

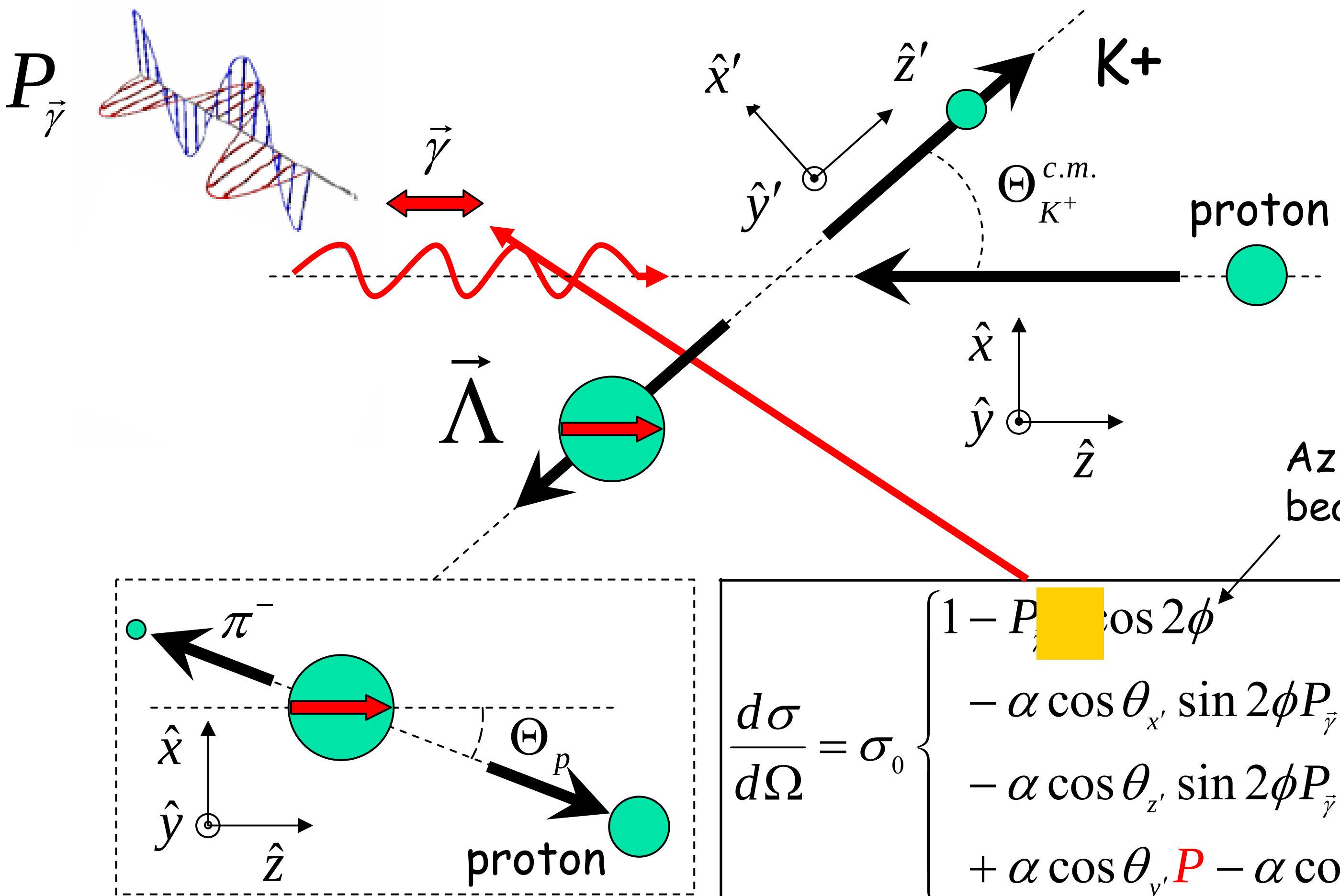

Azimuthal angle w.r.t. beam polarization

$$\frac{d\sigma}{d\Omega} = \sigma_0 \begin{Bmatrix} 1 - P_{\vec\gamma}\,\text{[illegible]}\cos 2\phi \\ -\alpha\cos\theta_{x'}\sin 2\phi P_{\vec\gamma} O_{x'} - \alpha\cos\theta_{x'} P_{\odot} C_{x'} \\ -\alpha\cos\theta_{z'}\sin 2\phi P_{\vec\gamma} O_{z'} - \alpha\cos\theta_{z'} P_{\odot} C_{z'} \\ +\alpha\cos\theta_{y'} P - \alpha\cos\theta_{y'} P_{\vec\gamma} T\cos 2\phi \end{Bmatrix}$$

$\gamma p \rightarrow K^+\Lambda$ Photon Beam Asymmetry

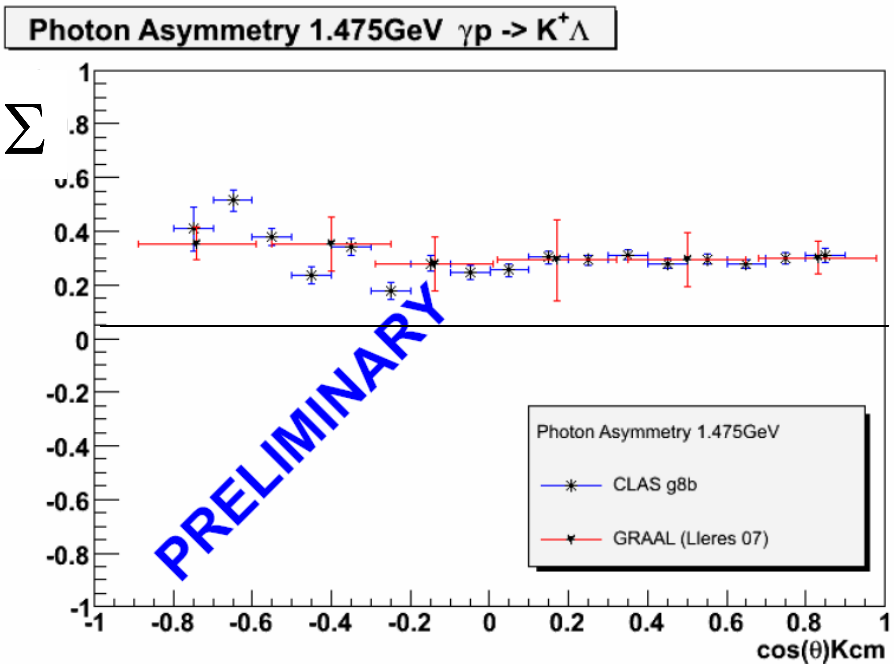

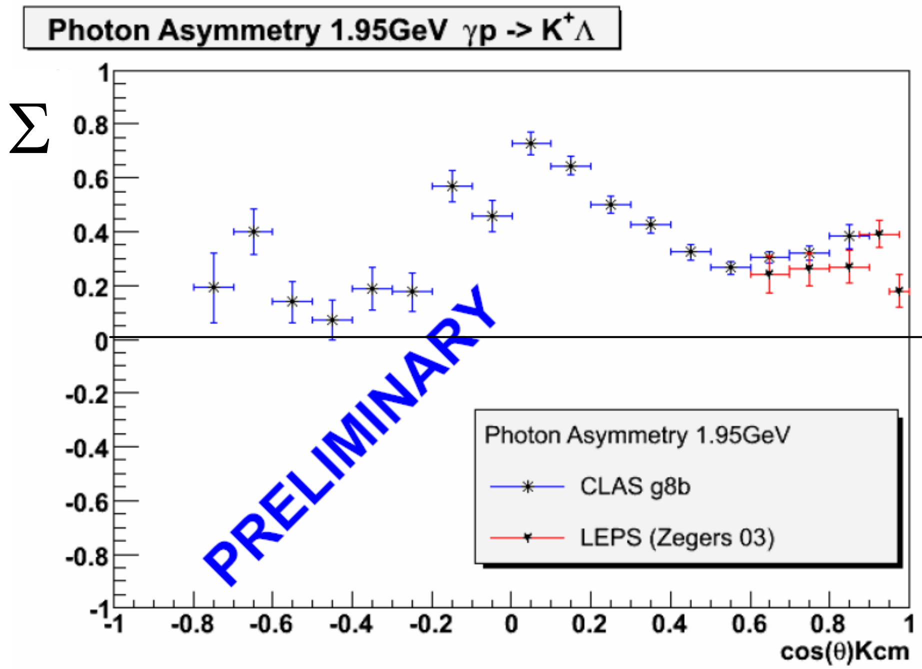

- Good agreement among CLAS, GRAAL and LEPS
- Results for $\gamma p \rightarrow K^+\Sigma^0$ coming as well

Craig Paterson (Glasgow)

Polarization Transfer for Linear Beam Polarization

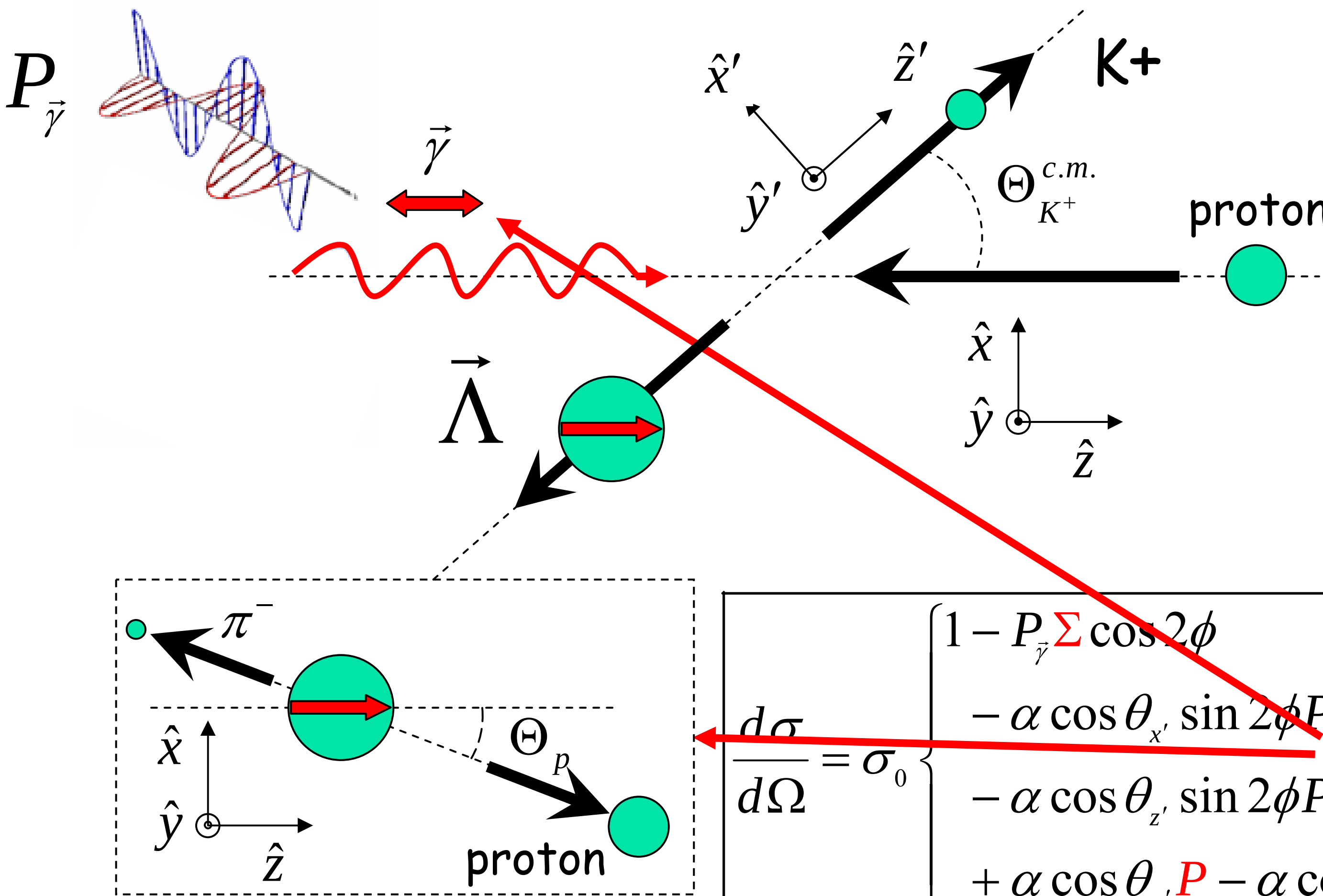

$$\frac{d\sigma}{d\Omega} = \sigma_0 \left\{ \begin{array}{l} 1 - P_{\vec{\gamma}} \Sigma \cos 2\phi \\ -\alpha \cos\theta_{x'} \sin 2\phi P_{\vec{\gamma}} \boxed{} - \alpha \cos\theta_{x'} P_{\odot} C_{x'} \\ -\alpha \cos\theta_{z'} \sin 2\phi P_{\vec{\gamma}} \boxed{} - \alpha \cos\theta_{z'} P_{\odot} C_{z'} \\ +\alpha \cos\theta_{y'} P - \alpha \cos\theta_{y'} P_{\vec{\gamma}} T \cos 2\phi \end{array} \right\}$$

$\gamma p \rightarrow K^+\Lambda$ Beam-Recoil O_x and O_z

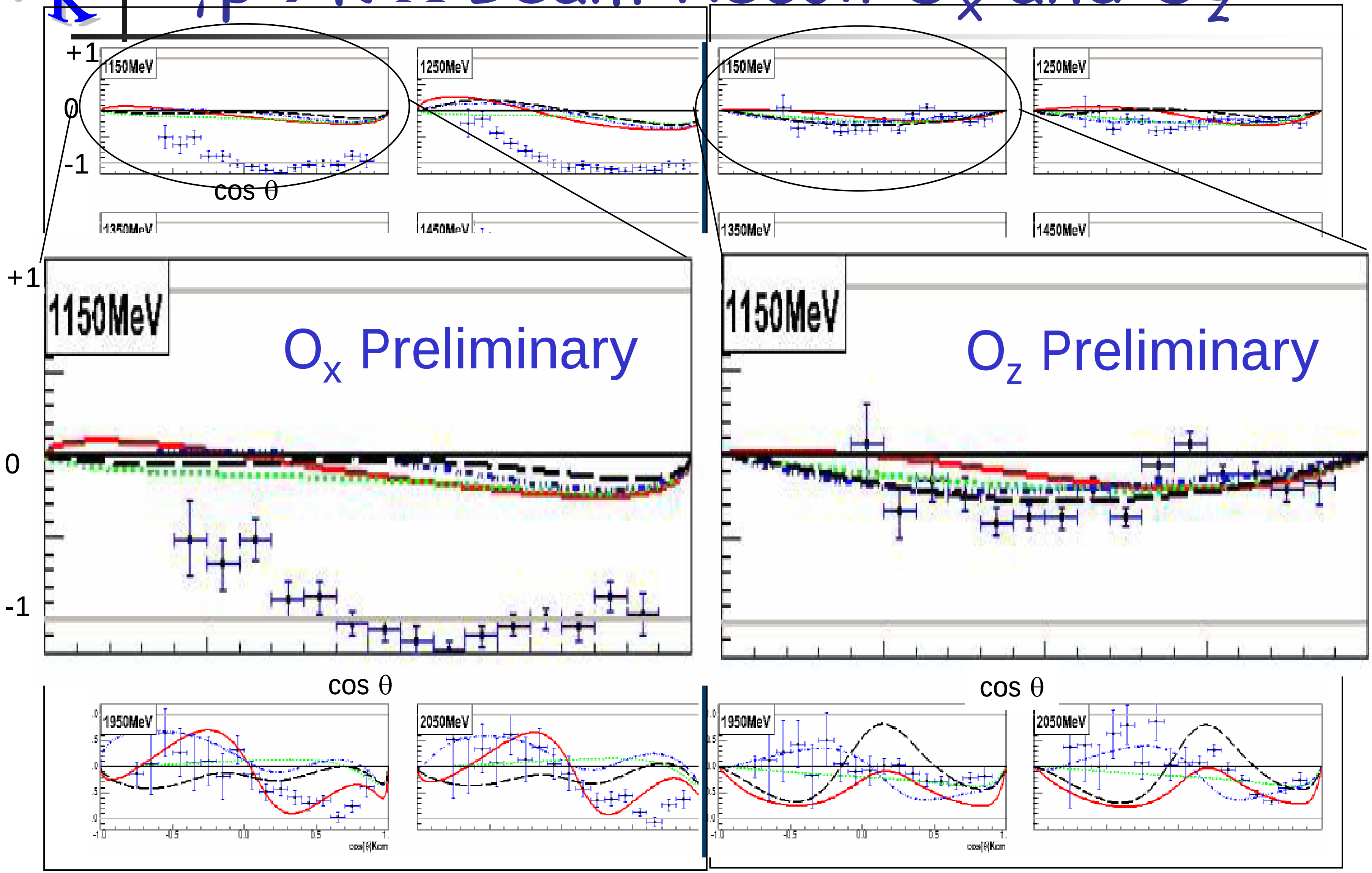

KaonMAID; RPR2-Regge only; RPR2-core; RPR2-w/D13

Craig Paterson (Glasgow)

Polarization Transfer for Circular Beam Polarization

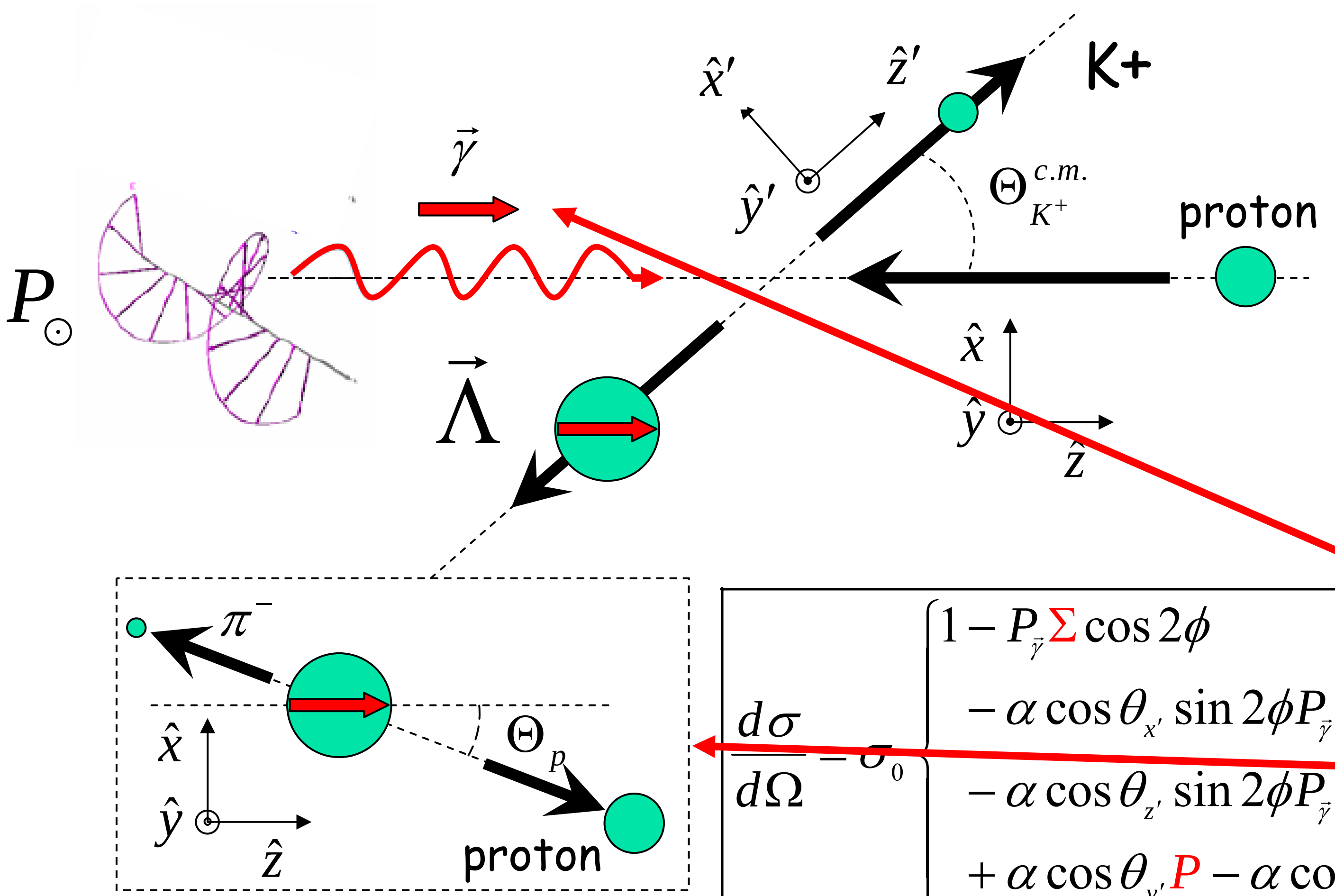

$$\frac{d\sigma}{d\Omega} = \sigma_0 \left\{ \begin{array}{l} 1 - P_{\vec{\gamma}}\Sigma\cos 2\phi \\ -\alpha\cos\theta_{x'}\sin 2\phi P_{\vec{\gamma}} O_{x'} - \alpha\cos\theta_{x'} P_{\odot} \\ -\alpha\cos\theta_{z'}\sin 2\phi P_{\vec{\gamma}} O_{z'} - \alpha\cos\theta_{z'} P_{\odot} \\ +\alpha\cos\theta_{y'} P - \alpha\cos\theta_{y'} P_{\vec{\gamma}} T\cos 2\phi \end{array} \right\}$$

C_z vs. W: Results for Λ

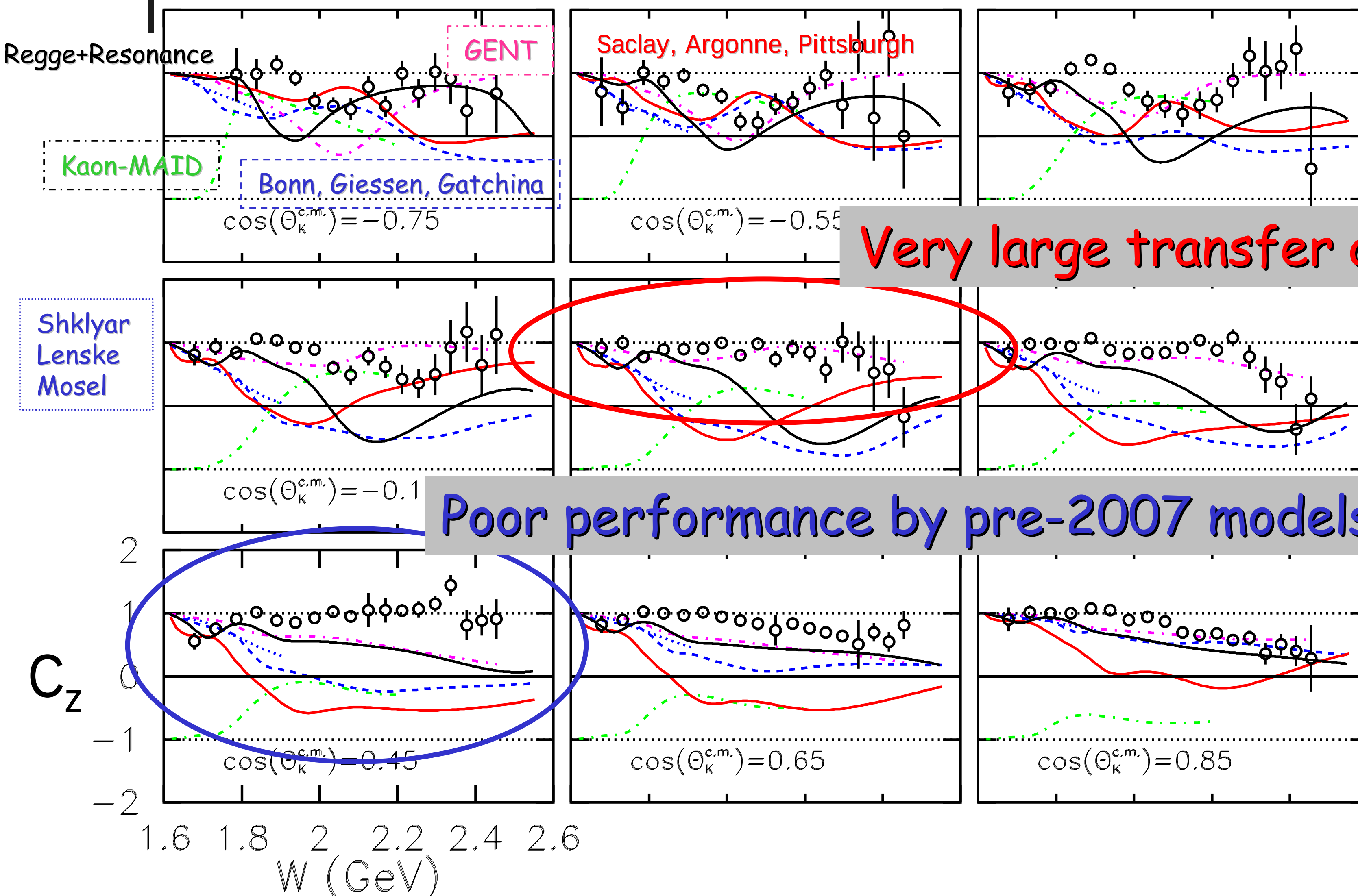

R. Bradford *et al.*, Phys. Rev. C **75**, 035205 (2007).

C_x vs. W: Results for Λ

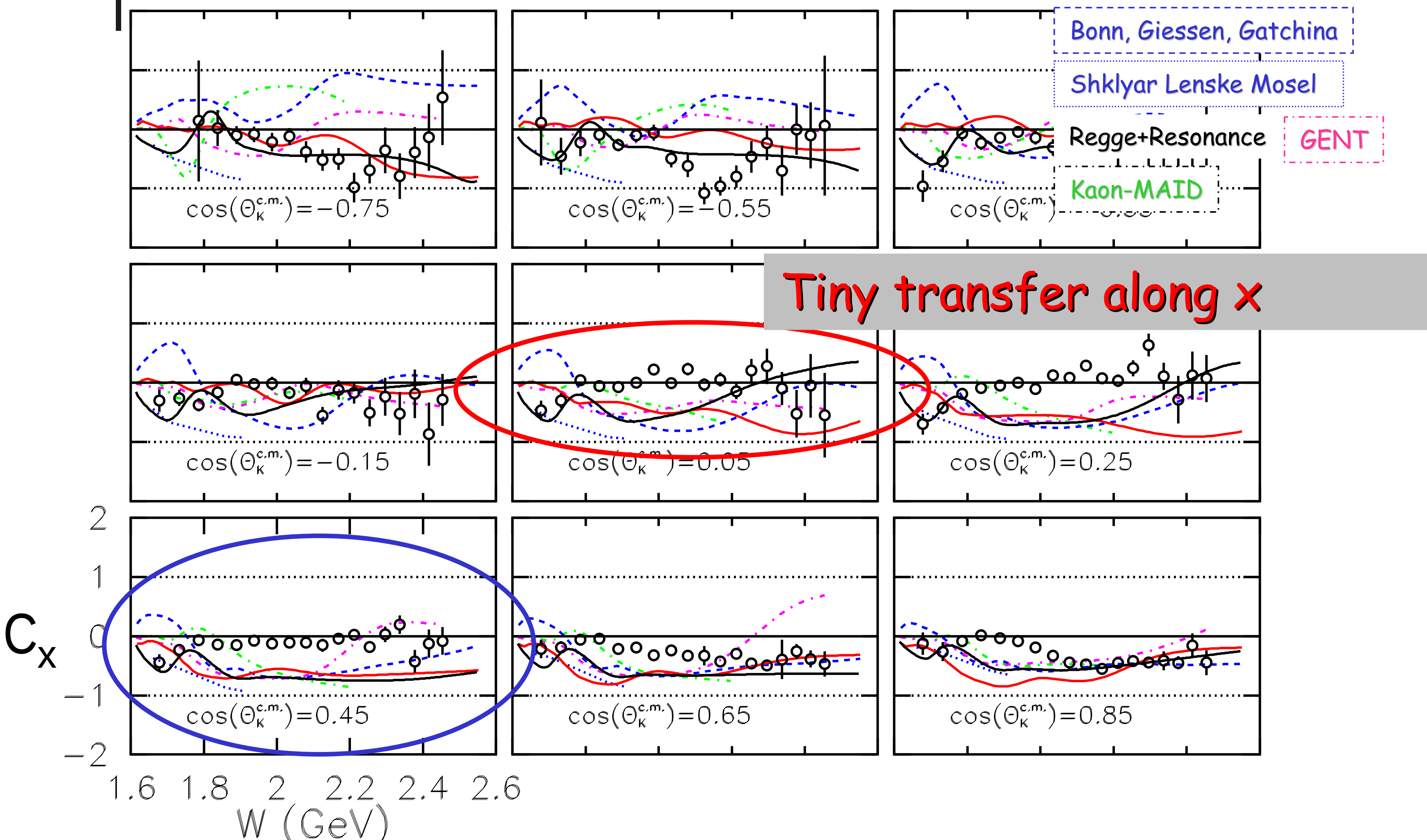

R. Bradford *et al.*, Phys. Rev. C **75**, 035205 (2007).

Model Comparisons

- Effective Lagrangian Models
  - Kaon-MAID; Mart, Bennhold, Haberzettl, Tiator
    - $S_{11}(1650)$, $P_{11}(1710)$, $P_{13}(1720)$, $D_{13}(1895)$, $K^*(892)$, $K_1(1270)$
  - GENT: Janssen, Ryckebusch *et al.*; Phys Rev C **65**, 015201 (2001)
    - $S_{11}(1650)$, $P_{11}(1710)$, $P_{13}(1720)$, $D_{13}(1895)$, $K^*(892)$, $\Lambda^*(1800)$, $\Lambda^*(1810)$
  - RPR (Regge plus Resonance) Corthals, Rychebusch, Van Cauteren, Phys Rev C **73**, 045207 (2006).
- Coupled Channels or Multi-channel fits
  - SAP (Saclay, Argonne, Pittsburgh) Julia-Diaz, Saghai, Lee, Tabakin; Phys Rev C **73**, 055204 (2006).
    - rescattering of KN and πN
    - $S_{11}(1650)$, $P_{13}(1900)$, $D_{13}(1520)$, $D_{13}(1954)$, $S_{11}(1806)$, $P_{13}(1893)$
  - BG (Bonn, Gachina): Sarantsev, Nikonov, Anisovich, Klempt, Thoma; Eur. Phys. J. A **25**, 441 (2005)
    - multichannel (pion, eta, Kaon) PWA
    - $P_{11}(1840)$, $D_{13}(1875)$, $D_{13}(2170)$
  - SLM: Shklyar, Lenske, Mosel; Phys Rev C **72** 015210 (2005)
    - coupled channels
    - $S_{11}(1650)$, $P_{13}(1720)$, $P_{13}(1895)$, but NOT $P_{11}(1710)$, $D_{13}(1895)$
- Regge Exchange Model
  - M. Guidal, J.M. Laget, and M. Vanderhaeghen; Phys Rev C 61, 025204 (2000)
    - K and K*(892) trajectories exchanged

R Values for the Λ

$$R \equiv \sqrt{P^2 + C_x^2 + C_z^2}$$

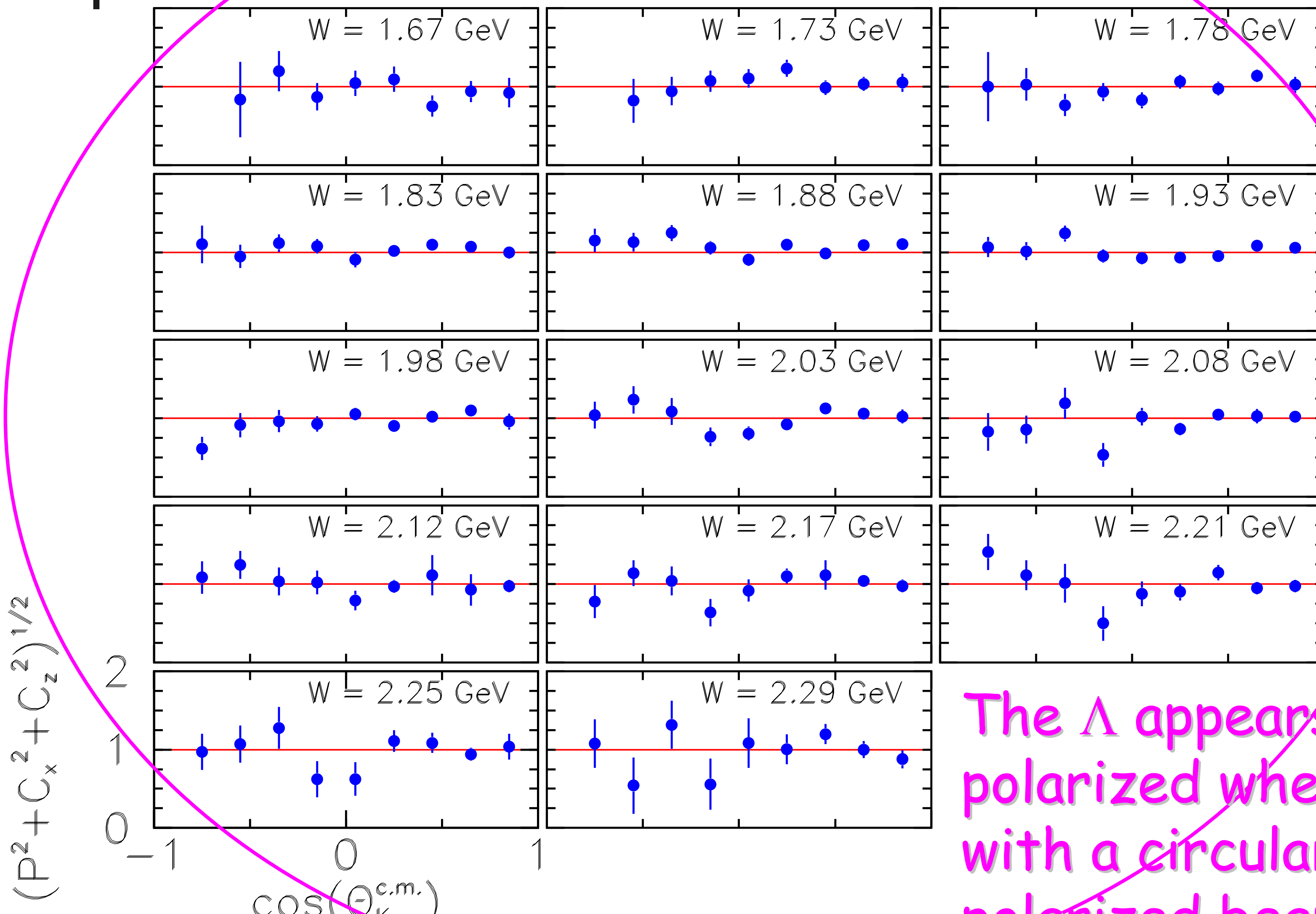

The Λ appears 100% polarized when created with a circularly polarized beam.

R. Bradford *et al.*, Phys. Rev. C **75**, 035205 (2007).

Average R Values for the Λ

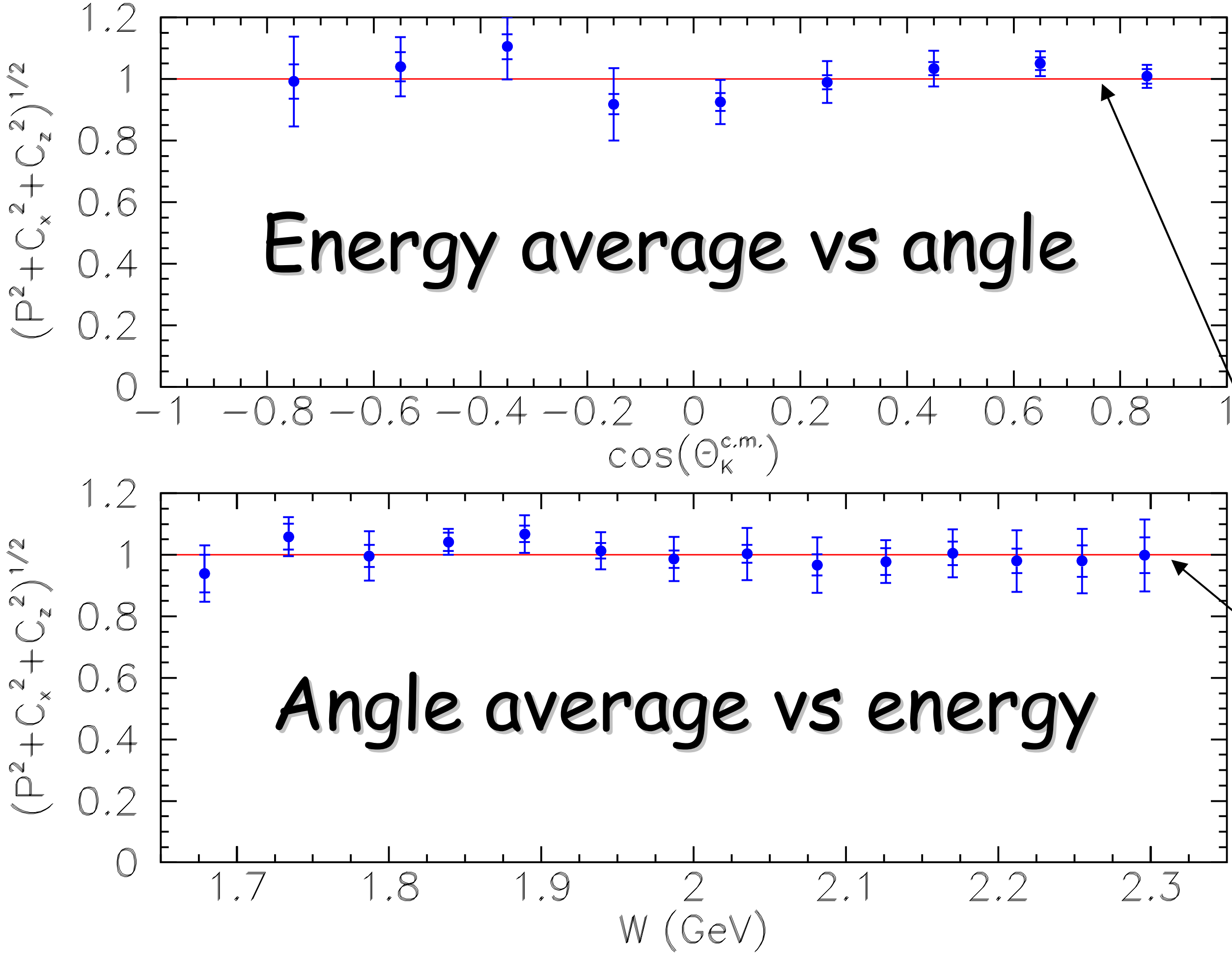

$$R \equiv \sqrt{P^2 + C_x^2 + C_z^2}$$

$$\bar{R} = 1.01 \pm 0.01$$

"Fully Polarized Λ"

Energy and angle averages are consistent with unity.

No model predicted this CLAS result.

Confirmed by GRAAL:
A. Lleres *et al.* Eur. Phys. J. **A 39**, 149 (2009).

R. Schumacher, Eur.Phys.J.A35, 299 (2008)

Quark-Picture Explanation

Quark-level dynamics manifest at the baryonic level.

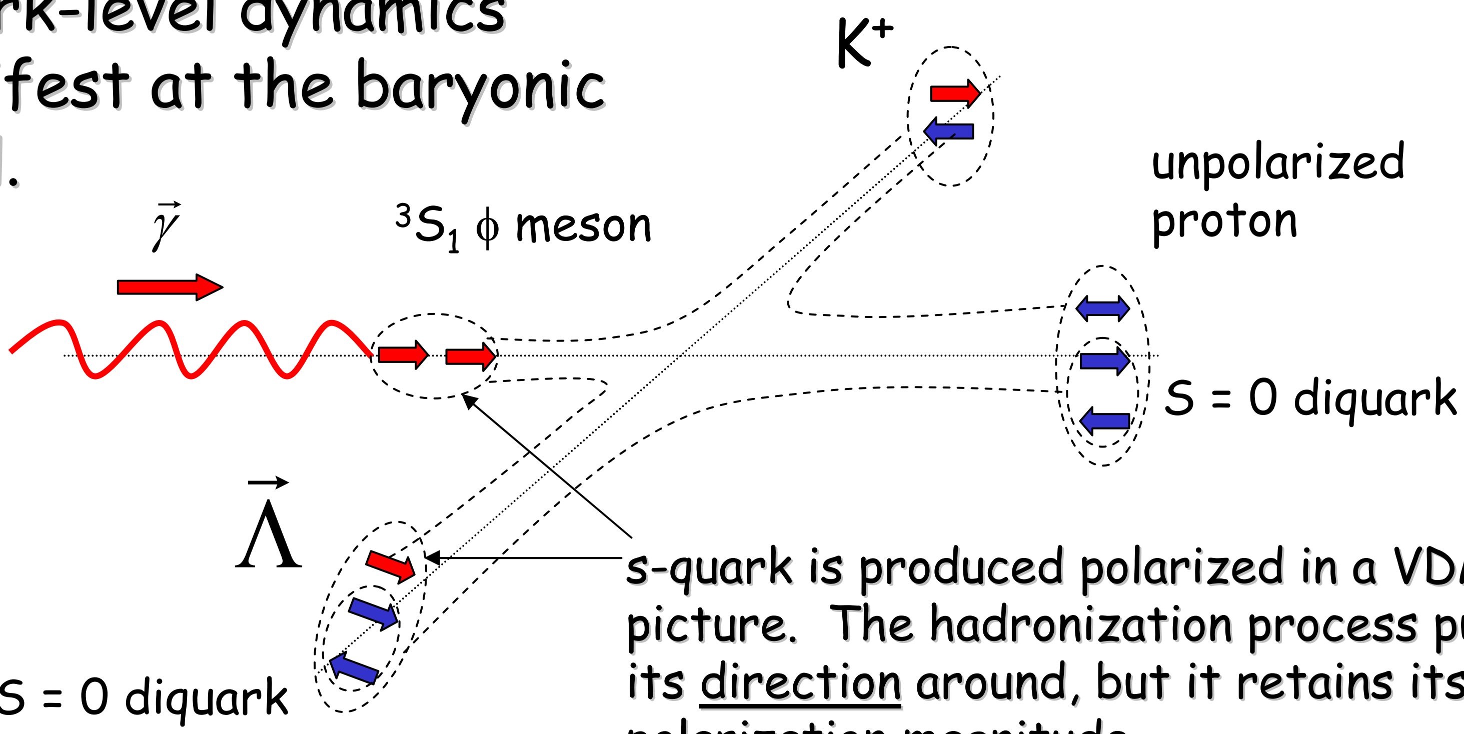

s-quark is produced polarized in a VDM $^3S_1$ picture. The hadronization process pushes its direction around, but it retains its full polarization magnitude.

R. S., Eur.Phys.J. A**35**, 299 (2008)

Alternative quark-level S=0 (spin singlet) scenario:
D. Carman *et al.*, Phys Rev. Lett 90 131804 (2003).

Hadronic-Model Explanation

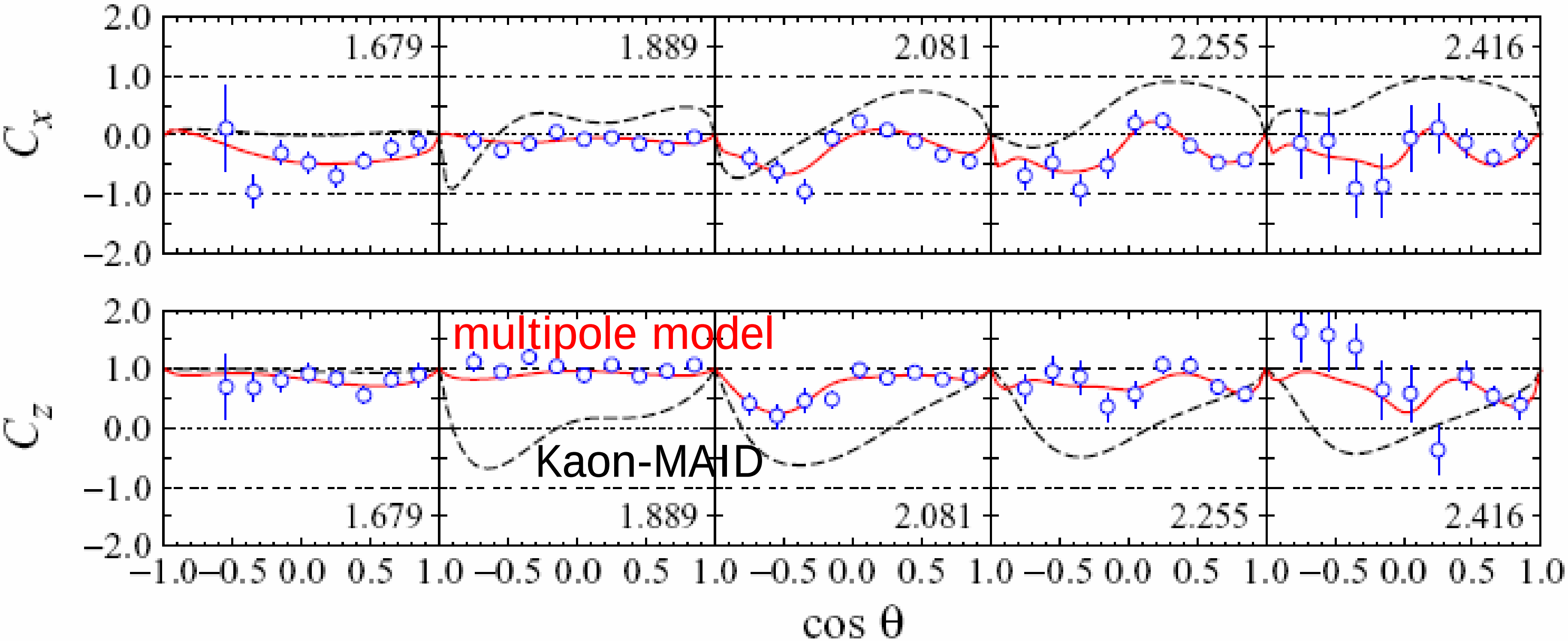

- Mart *et al.*'s refit of isobar and multipole models
- mix includes: $S_{11}(1650)$, $P_{11}(1710)$, $P_{13}(1720)$, $P_{13}(1900)$
- second resonance "bump" no longer consistent with a $D_{13}(2080)$

T. Mart, nucl-th 0808.0771 (Aug 2008)

Effect of including C_x C_z in Models

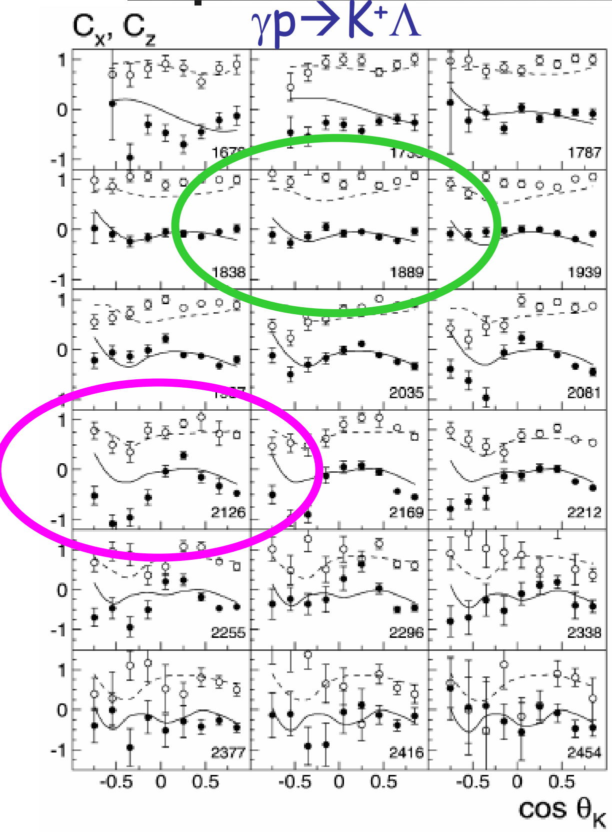

C_xC_z without N*(1900)P_{13}

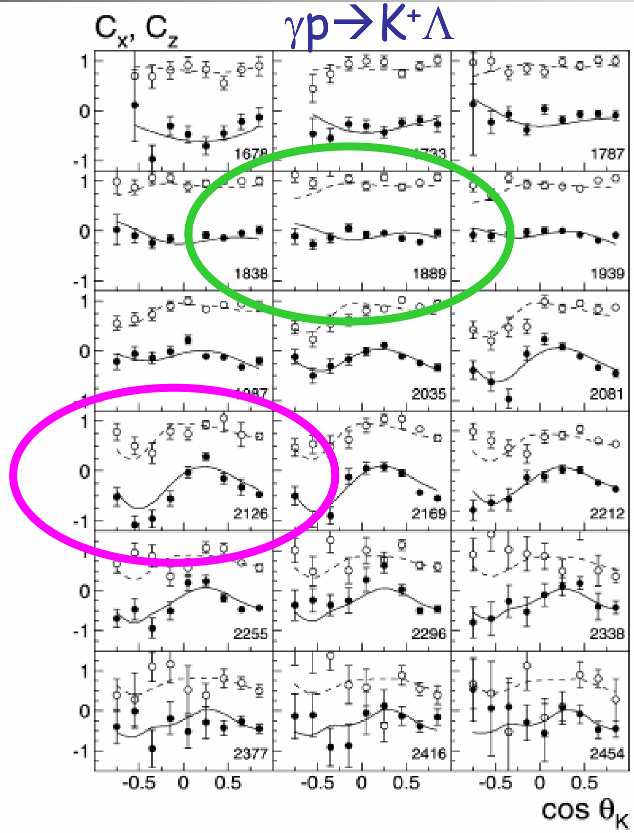

C_xC_z with N*(1900)P_{13}

- Nikanov *et al.*'s refit of Bonn-Gachina coupled-channel isobar model
- mix includes: S_{11}-wave, $P_{13}(1720)$, $P_{13}(1900)$, $P_{11}(1840)$
- $K^+\Sigma^0$ cross sections also better described with $P_{13}(1900)$
- Promote this "missing" resonance from ** to **** status.
- $P_{13}(1900)$ is not found in quark-diquark models.*

V. A. Nikanov *et al.*, Phys Lett. B **662**, 246 (2008).
see also: A.V. Anisovich *et al.*, Eur. Phys J. A **25** 427 (2005).

* E. Santopinto Phys Rev. C **72**, 02201(R), (2005).

Future prospects: n*'s

- CLAS "g13" data set – analysis in progress…
  - 40cm LD_2 DEUTERON target
  - Circular polarized beam, 20G two-sector triggers
    - E_γ up to 2.6 GeV (2006)
  - Linear polarized beam, 30G one-track triggers
    - E_γ in 6 bins between 1.1 and 2.3 GeV (2007)
- γ n (p)→K^0 $\{\Lambda,\Sigma^0\}$ (p) neutron cross sections, spin observables
  - Completes the set of isospin channels (P. Nadel-Turonski)
- γ n (p) → K^{0*} Λ, K^{+*} $\Sigma^{-*}(1385)$ (p) neutron target cross sections
- γ p (n)→K^+ $\{\Lambda,\Sigma^0\}$ (n) quasi-free proton cross sections, spin obs.
  - Raw linear polarization asymmetries seen (R. Johnstone PhD work)
  - ΛN potential from rescattering: high missing momentum

Further future prospects

- FroST (g9b)
  - Polarized target (C_4H_9OH)
  - Polarized photon beams: $\vec{\gamma}\ \vec{p}$
  - "complete" experiments
  - Runs 3-10 to 7-10 (recently…)
- HD-ice (g14)
  - New polarized target ($\vec{H}\vec{D}$)
  - Neutron target: $\vec{\gamma}\ \vec{n}$
  - Runs 2011 spring…
- CLAS12
  - RICH detector in discussion stage

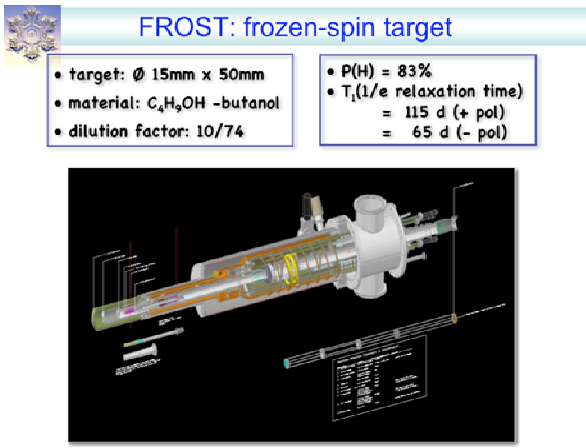

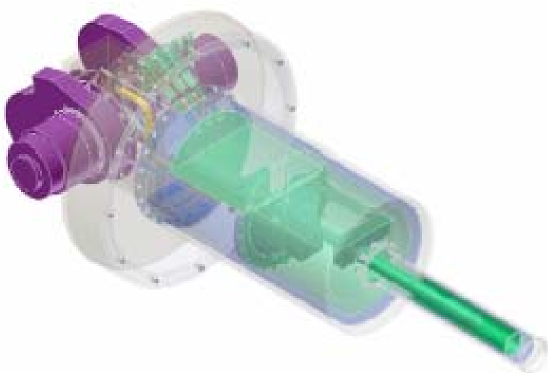

Seeking New S=0 Baryons via Mesons off the Proton:

published, acquired, FroST(g9b)

	σ	Σ	T	P	E	F	G	H	T_x	T_z	L_x	L_z	O_x	O_z	C_x	C_z	CLAS run Period
$p\pi^0$	✓	✓	✓		✓	✓	✓	✓									g1, g8, g9
$n\pi^+$	✓	✓	✓		✓	✓	✓	✓									g1, g8, g9
$p\eta$	✓	✓	✓		✓	✓	✓	✓									g1, g11, g8, g9
$p\eta'$	✓	✓	✓		✓	✓	✓	✓									g1, g11, g8, g9
$p\omega$	✓	✓	✓		✓	✓	✓	✓									g11, g8, g9
$K^+\Lambda$	✓	✓	✓	✓	✓	✓	✓	✓	✓	✓	✓	✓	✓	✓	✓	✓	g1, g8, g11
$K^+\Sigma^0$	✓	✓	✓	✓	✓	✓	✓	✓	✓	✓	✓	✓	✓	✓	✓	✓	g1, g8, g11
$K^{0*}\Sigma^+$	✓										✓	✓			✓	✓	g1, g8, g11

Source: V. D. Burkert

Seeking New S=0 Baryons via Mesons off the Neutron:

published, acquired, HD-ice

	σ	Σ	T	P	E	F	G	H	T_x	T_z	L_x	L_z	O_x	O_z	C_x	C_z	CLAS run Period
$p\pi^-$	✓	✓	✓		✓	✓	✓	✓									g2, g10, g13, g14
$p\rho^-$	✓	✓	✓		✓	✓	✓	✓									g2, g10, g13, g14
$K^0\Lambda$	✓	✓	✓	✓	✓	✓	✓	✓	✓	✓	✓	✓	✓	✓	✓	✓	g13, g14
$K^0\Sigma^0$	✓	✓	✓	✓	✓	✓	✓	✓	✓	✓	✓	✓	✓	✓	✓	✓	g13, g14
$K^+\Sigma^-$	✓	✓	✓		✓	✓	✓	✓									g10, g13, g14
$K^{0*}\Sigma^0$	✓	✓															g10, g13

The combination of all of these measurements on proton and neutron targets represents an extremely powerful tool in the search for new baryon states.

Source: V. D. Burkert

Summary: Hyperon Photoproduction

- KY photo- (and electro-) production offer kinematic and analysis benefits in N* searches
- Published CLAS KY results on proton (σ, P, C_x, C_z) have favored a $P_{13}(1900)$ (not $P_{11}(1900)$ or $D_{13}(2080)$)
- More observables to be published soon (more σ, P; Σ, O_x, O_z); others (G, E, L_x, L_z) are in the analysis pipeline (FroST)
- Results on the neutron (D) coming in 1-2 years (g13, HD-ice...)

End of Day 1 Talk

Outline /Overview

- DAY 1
  - History of Strangeness Electromagnetic Physics
    - Strangeness
    - Earliest experiments
  - Physics issues
    - N* searches
    - Reaction mechanisms
    - Amplitudes
    - Spin observables
  - Photoproduction of elementary hyperons

- DAY 2
  - Electroproduction of elementary hyperons
  - Electroproduction of hypernuclei
  - Structure of the $\Lambda(1405)$
  - Y* (S=-1) production
  - Cascade (S=-2) production

Strangeness Electroproduction

- Moving toward $Q^2=q^2-\nu^2 > 0$: "massive" virtual photon

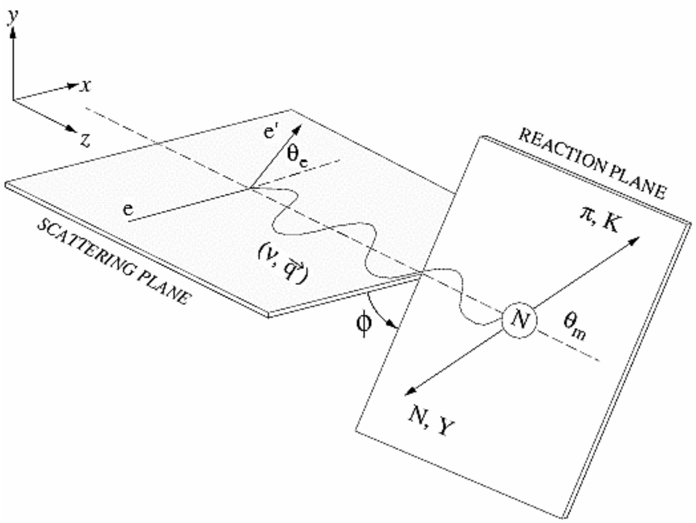

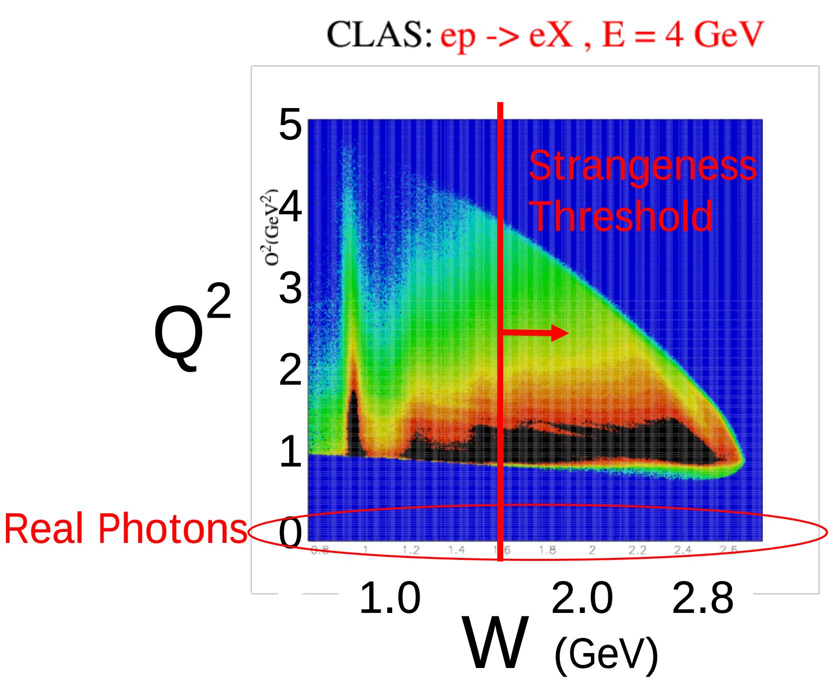

- First Measurements of σ_{LT} and σ_{TT}
- First Polarization Transfer: $\vec{e} \to \vec{\Lambda}$
- $\Lambda(1520)$ $J^\pi=3/2^+$ Decay Angular Distribution

Electroproduction Formalism

With unpolarized beam, target, recoil, we have five kinematic variables:

$$Q^2,\ W,\ \cos(\theta_K),\ \phi,\ \varepsilon.$$

Given Q^2 and W, for any pseudo–scalar meson, the (virtual) one–photon exchange cross section is:

$$\frac{d\sigma}{d\Omega_K} = \sigma_T + \epsilon_L \sigma_L + \epsilon\, \sigma_{TT} \cos(2\phi) + \sqrt{2\epsilon\ (\epsilon+1)}\ \sigma_{TL} \cos(\phi)$$

σ_u

where

$$\sigma_i = \frac{d\sigma_i}{d\Omega_K}(Q^2, W, \Theta_K)$$

are the Transverse, Longitudinal, LT–interference, and TT–interference virtual photon structure functions.

Kinematic factors:

$$\epsilon = \left(1 + 2\,\frac{\vec{q}^{\,2}}{Q^2}\,\tan^2\frac{\Theta_{e'}}{2}\right)^{-1}$$

$$\epsilon_L = \frac{Q^2}{\nu^2}\epsilon\ ;\ \nu = (E_e - E_{e'})_{lab}\ ;\ \vec{q} = (\vec{p}_e - \vec{p}_{e'})_{lab}$$

With CLAS one detects:

$$\frac{d^4\sigma}{dQ^2\,dW\,d\Omega_K} = \Gamma(Q^2, W)\,\frac{d\sigma}{d\Omega_K}(Q^2, W, \Theta_K, \phi)$$

where the virtual photon flux, Γ, is

$$\Gamma(Q^2, W) = \frac{\alpha}{4\pi}\,\frac{W}{E_e^2 m_N^2}\,(W^2 - m_N^2)\,\frac{1}{Q^2}\,\frac{1}{1-\epsilon}$$

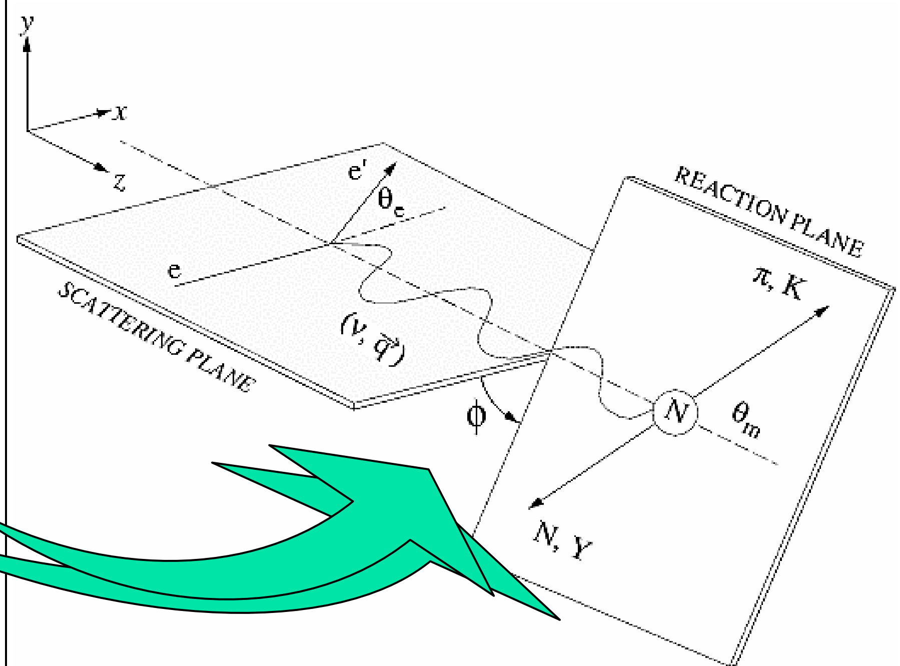

A look at p(e,e'K+)Λ...

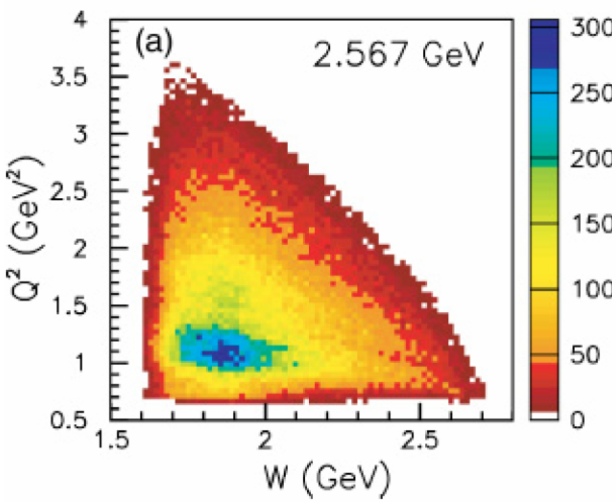

Kinematic Coverage in Q^2 and W

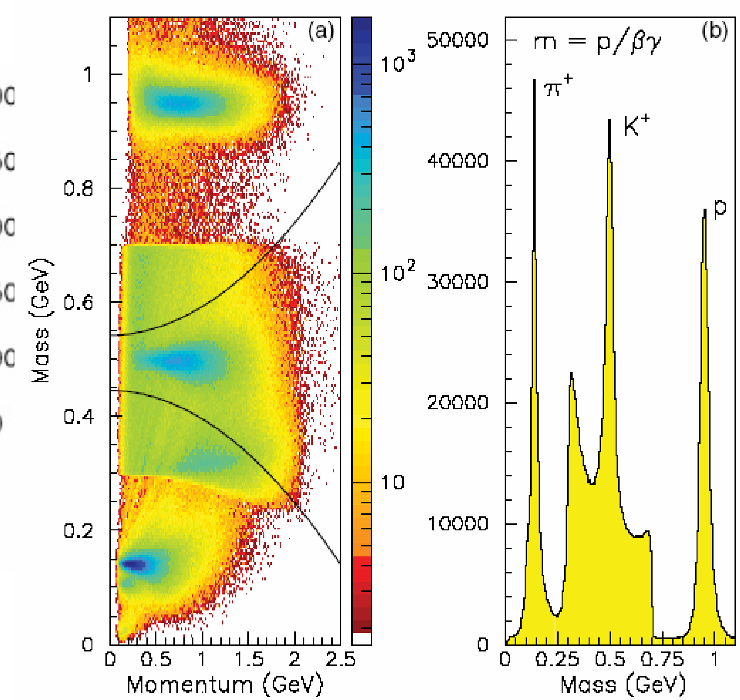

Masses from "Time of Flight" and Momentum

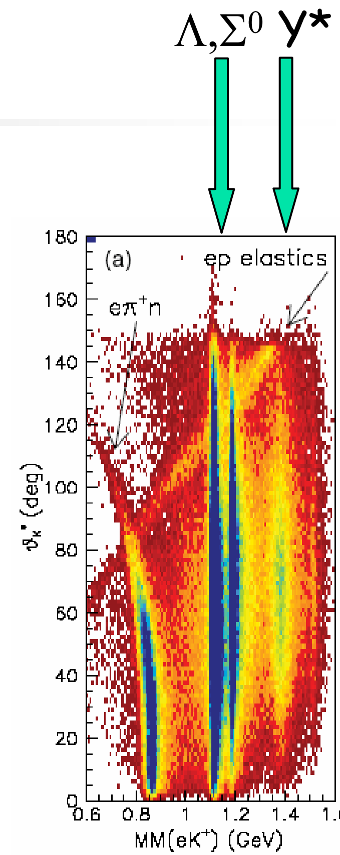

Hyperons revealed in Missing Mass Off e,e'K+

P. Ambrozewicz et al. (CLAS), Phys. Rev. C **75** 045203 (2007)

Fitting 'radiated' lineshapes

- Hyperon mass distribution affected by (computable) photon radiation off electrons

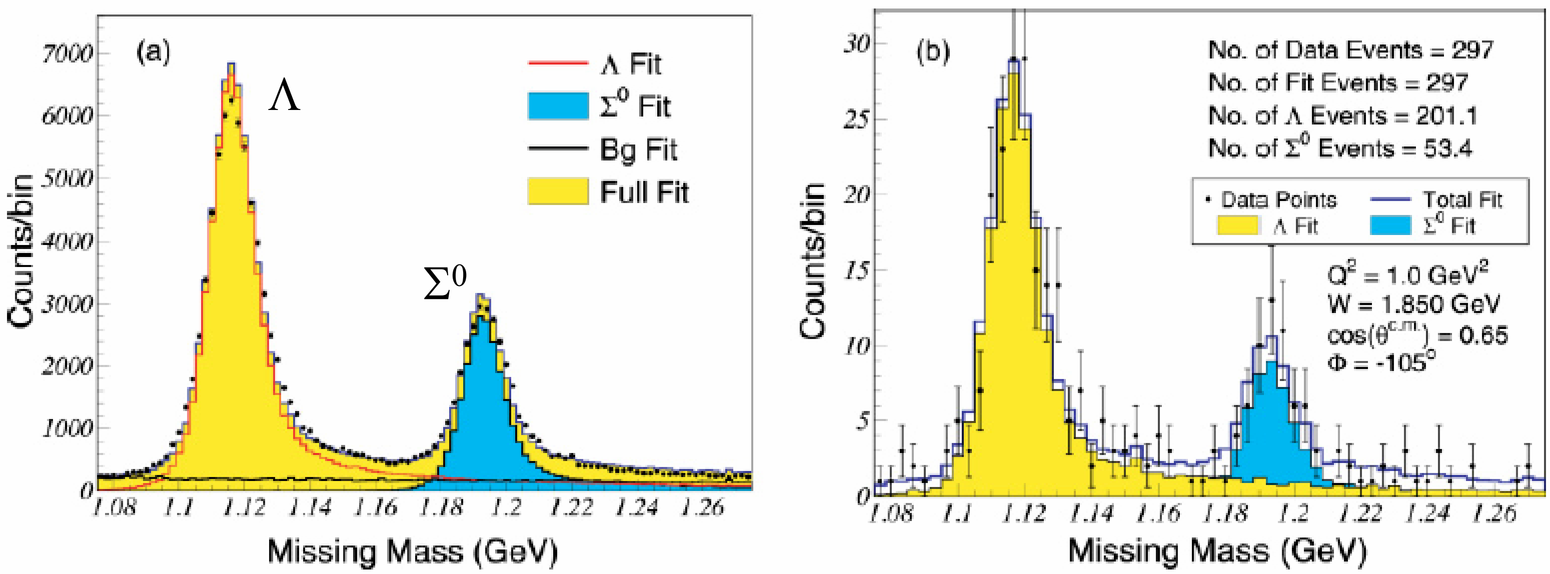

FIG. 6. (Color online) Signal and background fits from the 2.567 GeV data for the $e'K^+$ missing mass spectrum (a) summed over all kinematics and (b) for a typical $\cos\theta_K^*/\Phi$ bin at $Q^2 = 1.0$ GeV^2 and $W = 1.85$ GeV to demonstrate the typical fit quality in our data.

P. Ambrozewicz et al. (CLAS), Phys. Rev. C **75** 045203 (2007)

Results for p(e,e'K$^+$) Λ

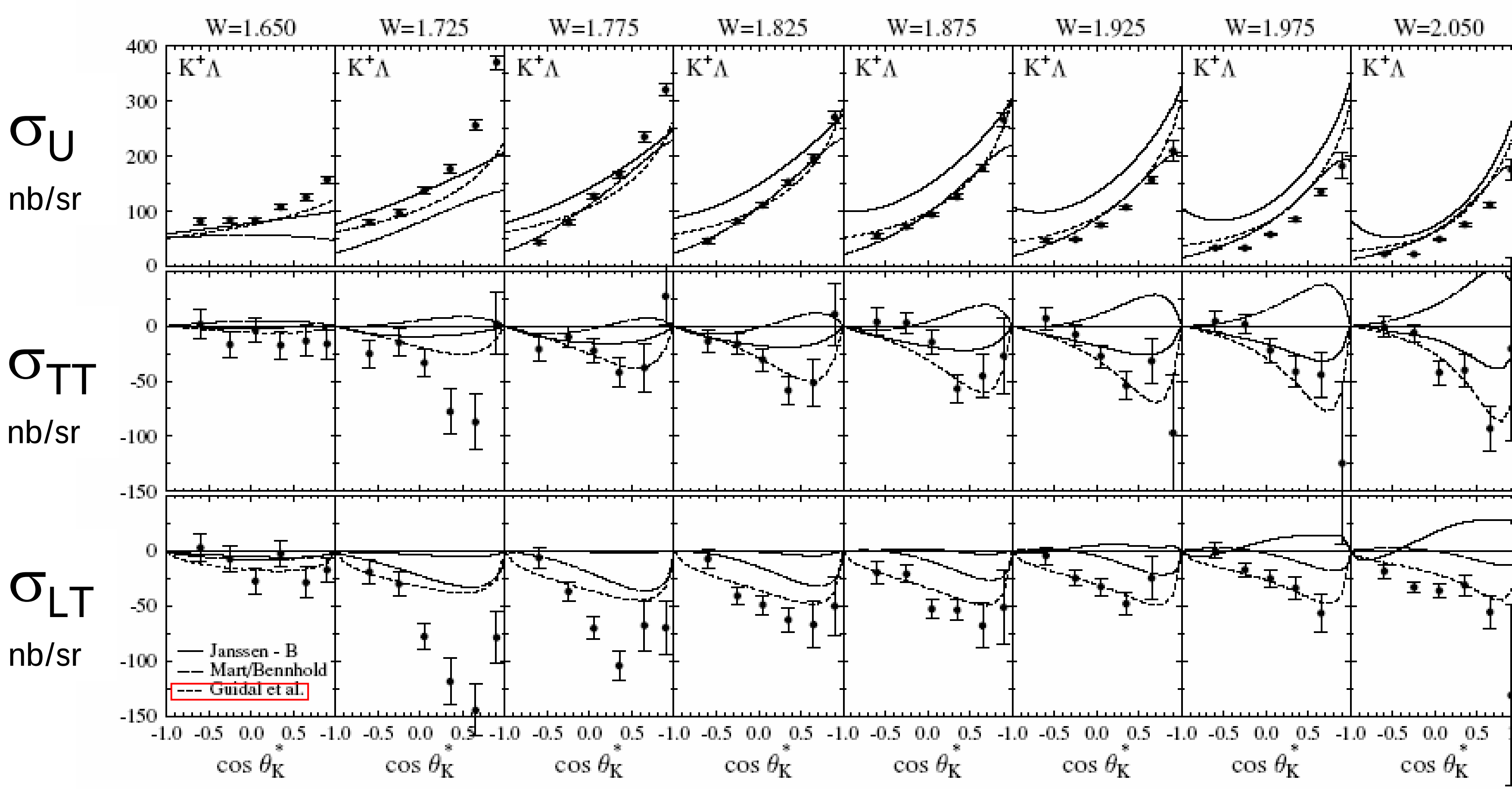

Q^2 = 0.65 GeV^2

Simple Regge exchange model works best

P. Ambrozewicz et al. (CLAS), Phys. Rev. C **75** 045203 (2007)

Results for p(e,e'K$^+$) Σ^0

σ_U
nb/sr

σ_{TT}
nb/sr

σ_{LT}
nb/sr

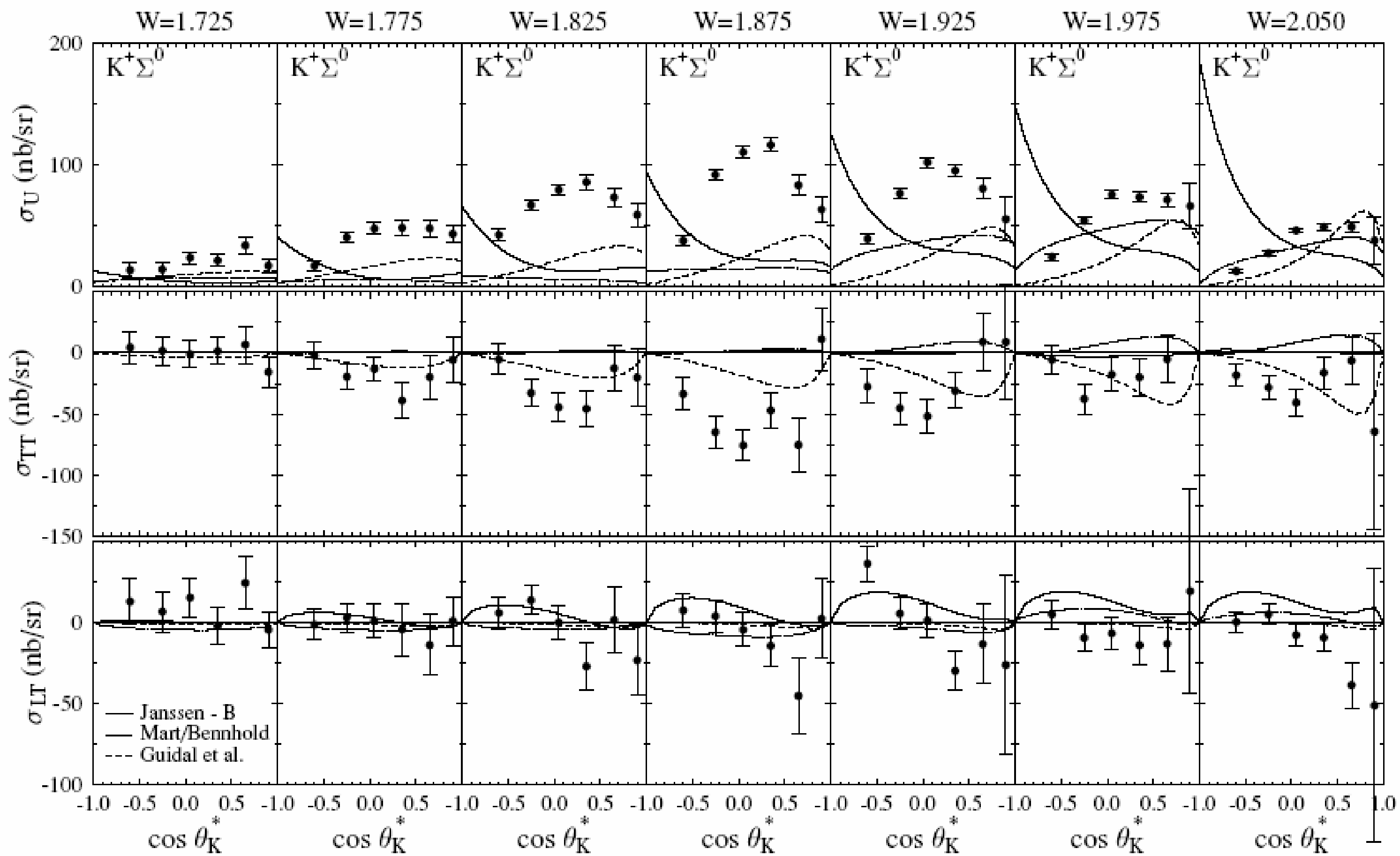

$Q^2 = 0.65\ GeV^2$

All models fail…

P. Ambrozewicz et al. (CLAS), Phys. Rev. C **75** 045203 (2007)

W Dependence Λ

σ_U nb/sr

σ_{TT} nb/sr

σ_{LT} nb/sr

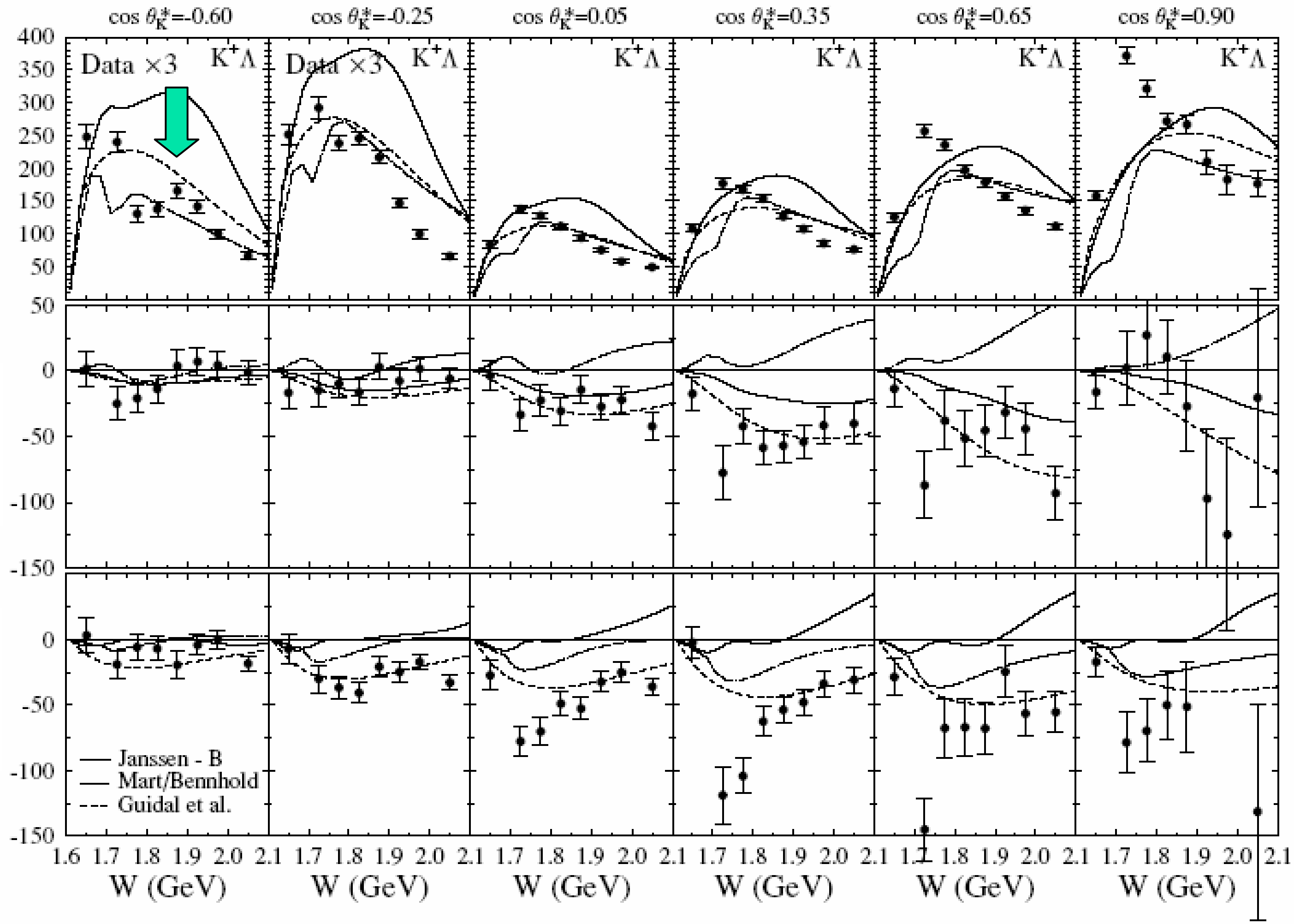

$Q^2 = 0.65\ GeV^2$

Qualitatively, σ_u similar to photoproduction

P. Ambrozewicz et al. (CLAS), Phys. Rev. C **75** 045203 (2007)

W Dependence Σ^0

σ_U
nb/sr

σ_{TT}
nb/sr

σ_{LT}
nb/sr

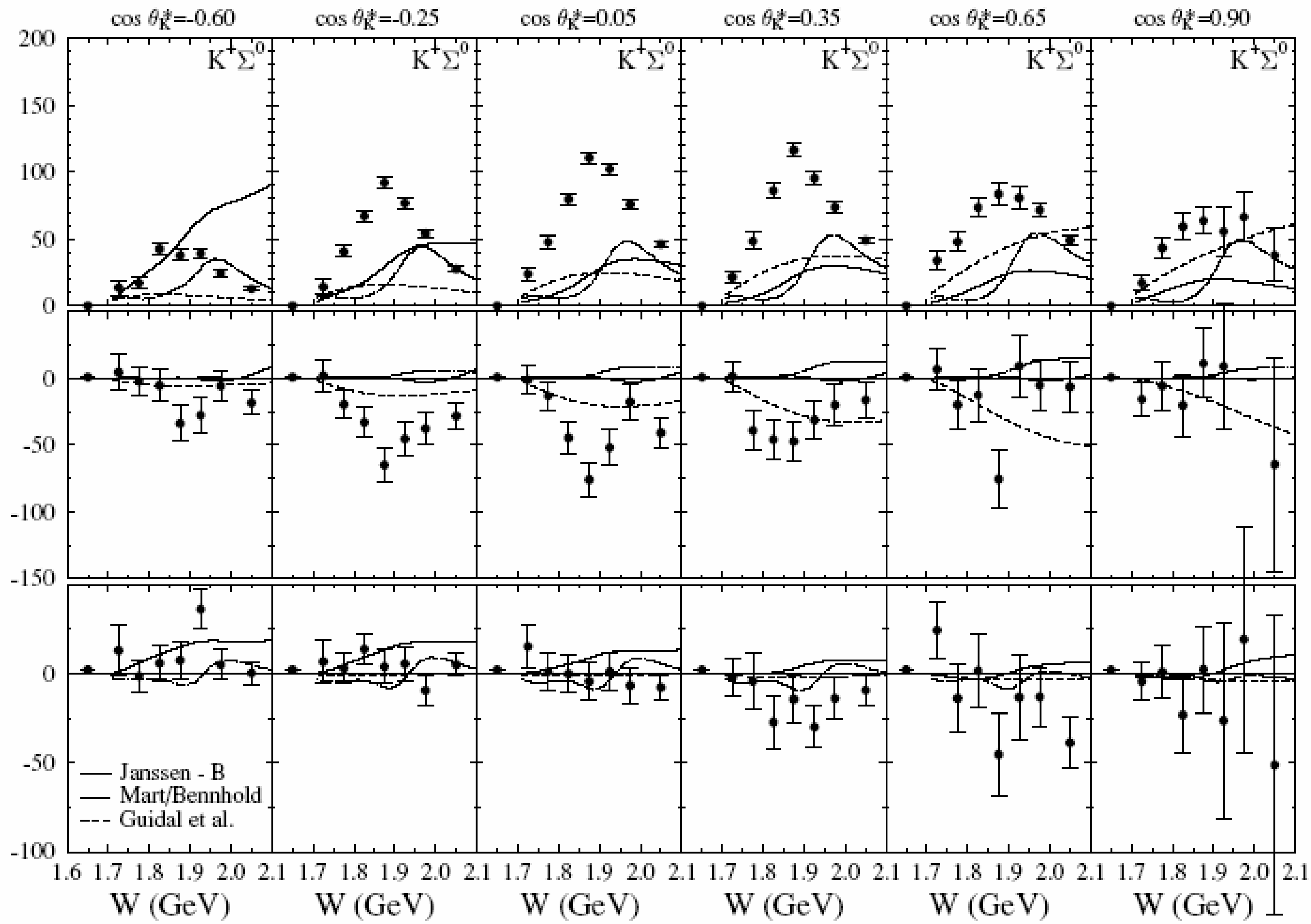

Q^2 = 0.65 GeV^2

P. Ambrozewicz et al. (CLAS), Phys. Rev. C **75** 045203 (2007)

Q^2 dependences

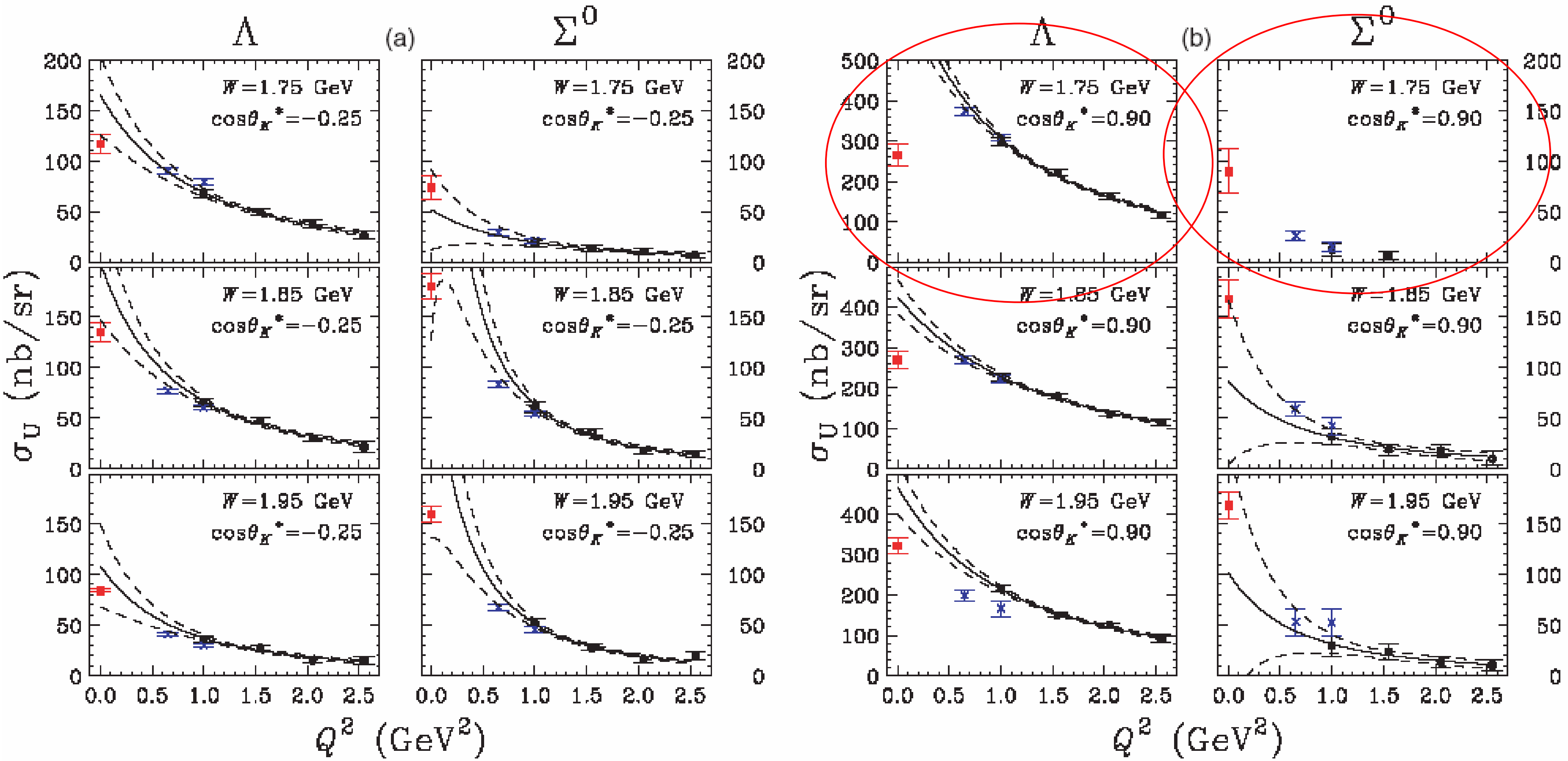

- Observe that Q^2 dependence of Σ^0 "falls faster" than for Λ at forward angles $\rightarrow$ large role for longitudinal piece of cross section(?)

P. Ambrozewicz et al. (CLAS), Phys. Rev. C **75** 045203 (2007)

Separation of L and T Responses

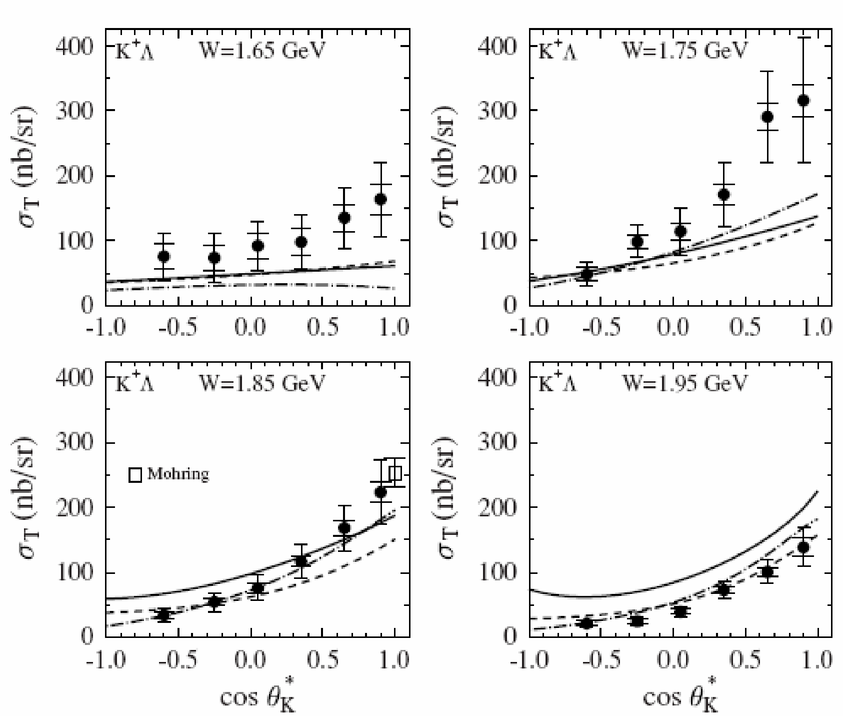

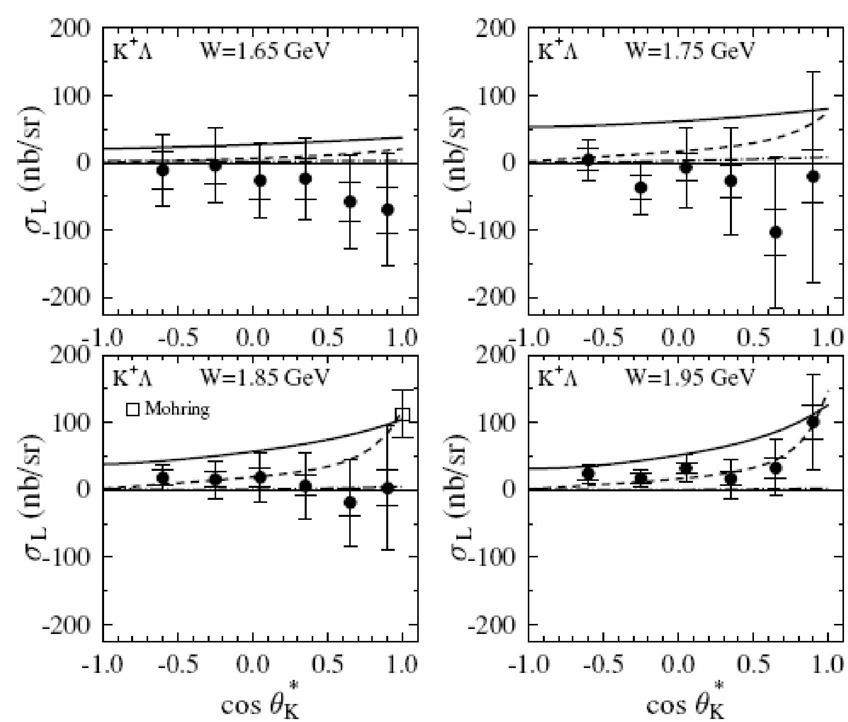

FIG. 23. Structure function σ_T vs $\cos\theta_K^*$ for the $K^+\Lambda$ final state for our different W points at $\boxed{Q^2 = 1.0\ \text{GeV}^2}$ from the ϵ-Φ fit. Inner error bars are statistical only; outer error bars are combined statistical and systematic. Curves are from calculations of MB [44] (dot-dashed), JB [45] (solid), and GLV (dashed) models. The parallel kinematics data point comes from Mohring *et al.* [14] (open square).

Rosenbluth separation:

-Measure at multiple ε at same Q^2

-Longitudinal part is <u>small</u>

P. Ambrozewicz et al. (CLAS), Phys. Rev. C **75** 045203 (2007)

CLAS $p(\vec{e},e'K^+)\vec{\Lambda}$ Transferred Polarization

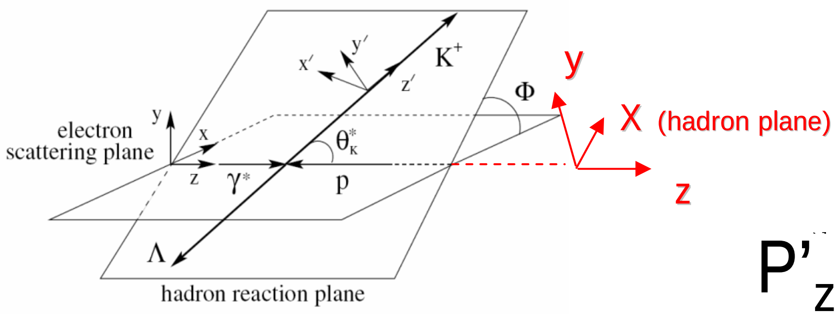

- Electro-production analog $C_x \rightarrow P_x'$ and $C_z \rightarrow P_z'$
- Large polarization transfer *along virtual photon direction* (not the z' helicity axis)
- Beam depolarization (~0.6) is not divided out in figures.
- Qualitatively consistent with photoproduction: hints at "simple" reaction mechanism

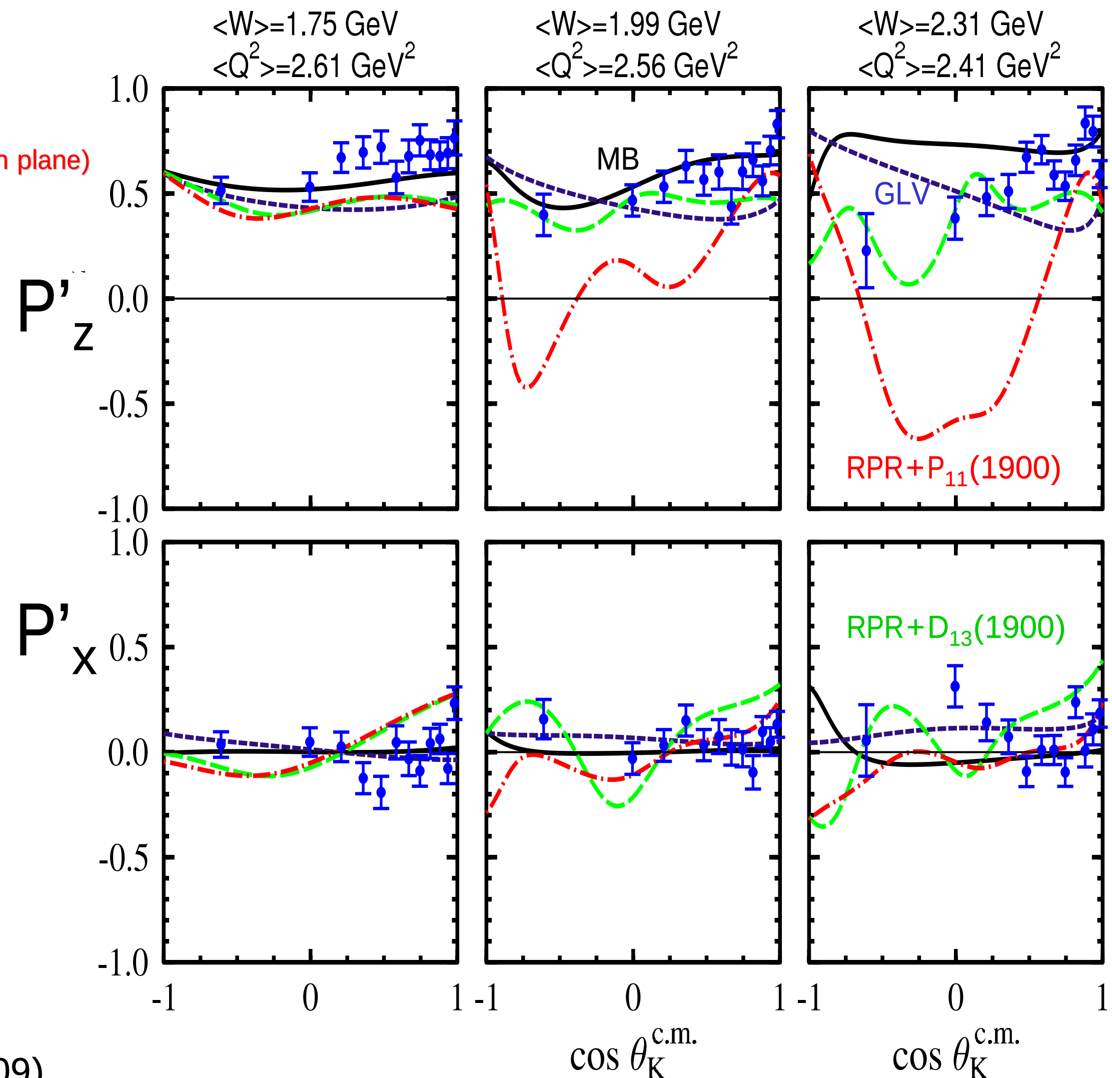

D. Carman *et al.*, Phys Rev. C **79** 065205 (2009).

D. Carman *et al.*, Phys Rev. Lett. **90** 131804 (2003).

Elementary Electroproduction Summary

- Electroproduction ($Q^2 > 0$) "looks like" photoproduction ($Q^2 = 0$), to a good approximation
  - Q^2 fall-off of Λ and Σ^0 are not the same
  - W dependences are similar
- Role of the longitudinal response is not settled
- Interference response functions are substantial
- Modeling effort has lagged in recent years

Hypernuclear Electroproduction

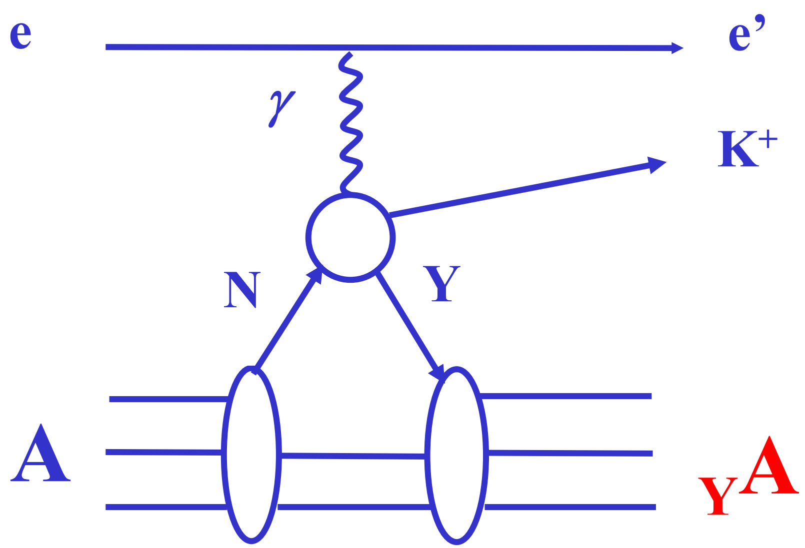

Experimental Physics Issues…

- Strong Q^2 dependence of cross section
  - Minimize electron scattering angle, Θ_{lab}~6°
- Minimize momentum transfer to target
  - Detect kaon along virtual photon direction
  - q > ~250 MeV/c
- Tiny Electroproduction cross sections
  - Order of mb for (π,K) and (K,π); μb for (e,e′K)
  - Compensate with high beam intensity
    - ~100 milliAmps for (e,e′), vs. ~10^7/sec for (K, π)
    - Rate limitations of detectors
  - Particle ID crucial: K/π separation
- Sub-MeV resolution has been achieved

YN Interaction & Light Hypernuclei

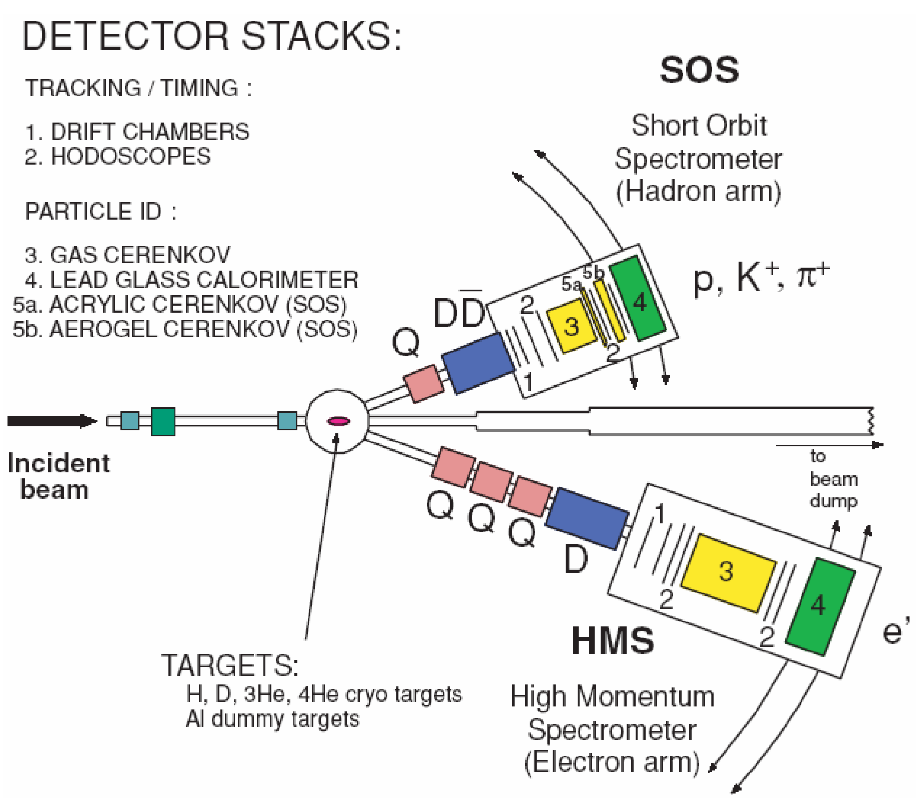

- E91-016 Collaboration, Hall C
  - HMS and SOS used in "standard" setup
  - ^{2}H, ^{3}He, ^{4}He, and C targets
- First demonstration of the feasibility of light hypernuclear electroproduction

F. Dohrmann et al., Phys. Rev. C 76, 054004 (2007).

Electroproduction on the Deuteron

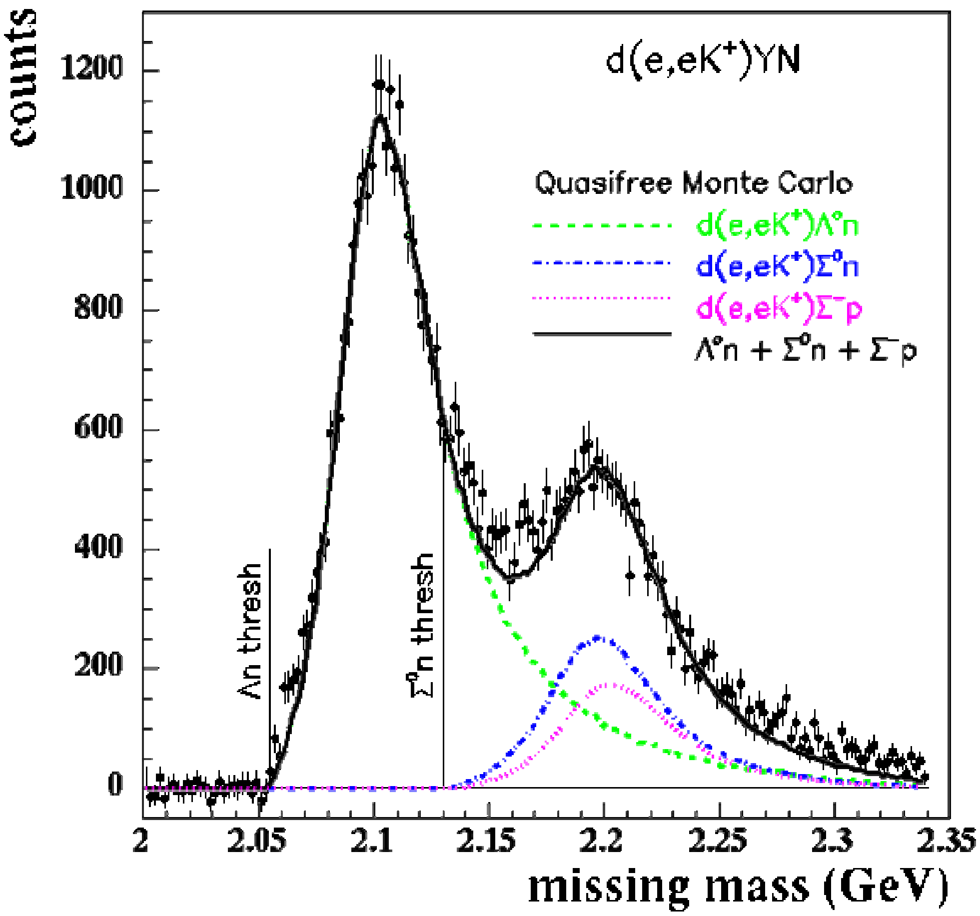

- Quasi-free production
  - E = 3.245 GeV
  - Q^2 = 0.38 GeV^2
- Access to Λ, Σ^0, and Σ^- cross section
- Access to YN final state interaction → scattering lengths and effective ranges
- No "cusps" or "dibaryons" seen near the Σ^0 threshold

YN Interaction and Hypernuclear Structure

Λn FSI from ^{2}H(e,e'K^{+})

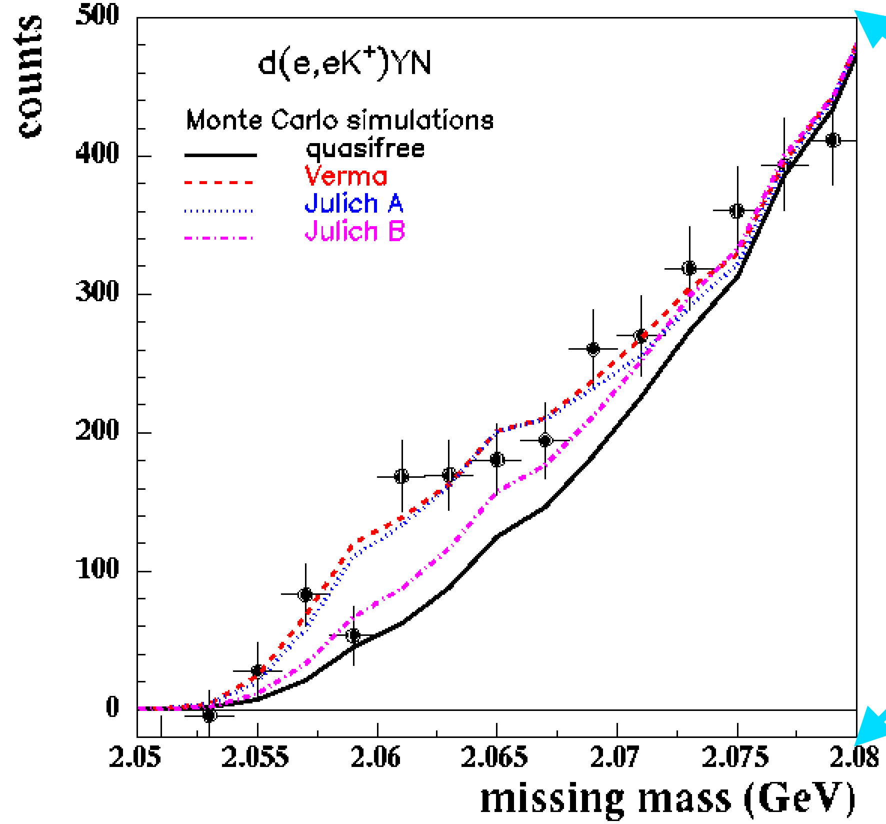

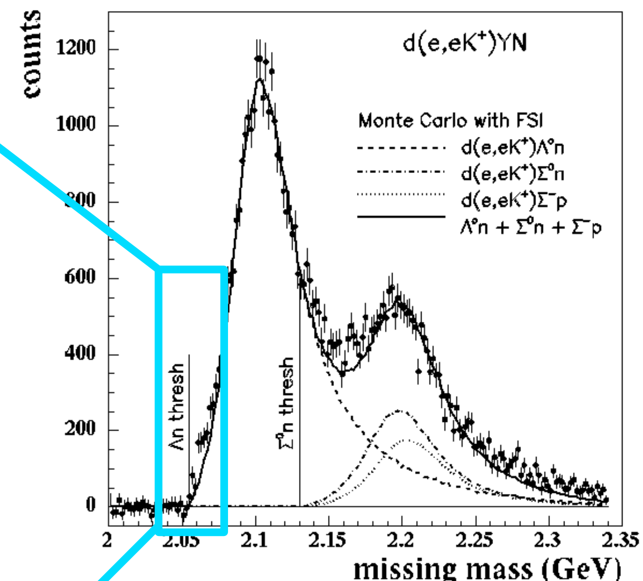

Table 1: Scattering length and effective range for the three hyperon-nucleon potentials used in the simulations.

Model	State	a (fm)	r (fm)
Verma	$^1S_0$	-2.29	3.15
	$^3S_1$	-1.77	3.25
Jülich A	$^1S_0$	-1.60	1.33
	$^3S_1$	-1.60	3.15
Jülich B	$^1S_0$	-0.57	7.65
	$^3S_1$	-1.94	2.42

YN Interaction & Light Hypernuclei

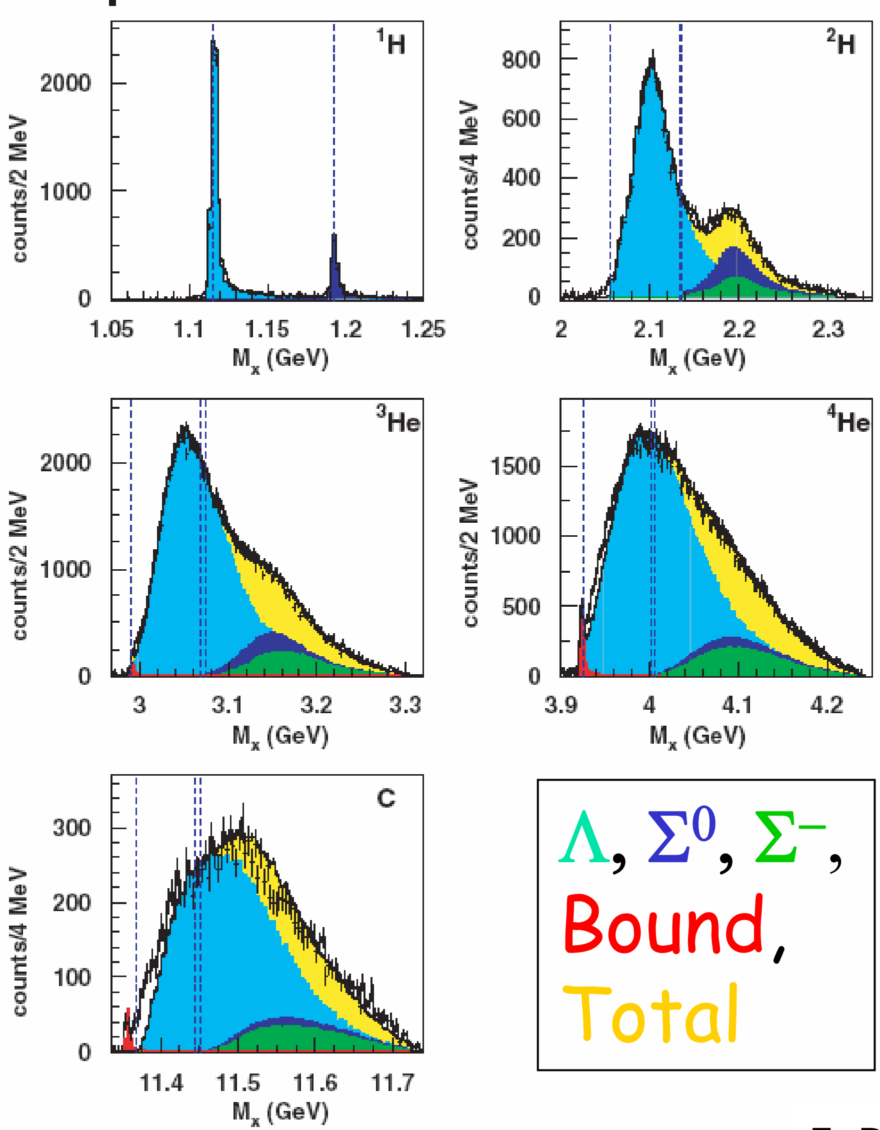

- Quasi-free Hyperon electroproduction on light nuclei
- Simple QF model fits data well
- Bound states seen
  - First non-emulsion “reaction” data for $^3{}_\Lambda$H and $^4{}_\Lambda$H.

F. Dohrmann et al., Phys. Rev. C **76**, 054004 (2007).

$^{3,4}He(e,e' K^{+})^{3,4}{}_{\Lambda}H$ Hypernuclear States

Q^2=0.35 GeV^2
W=1.91 GeV
t ~t_{min}

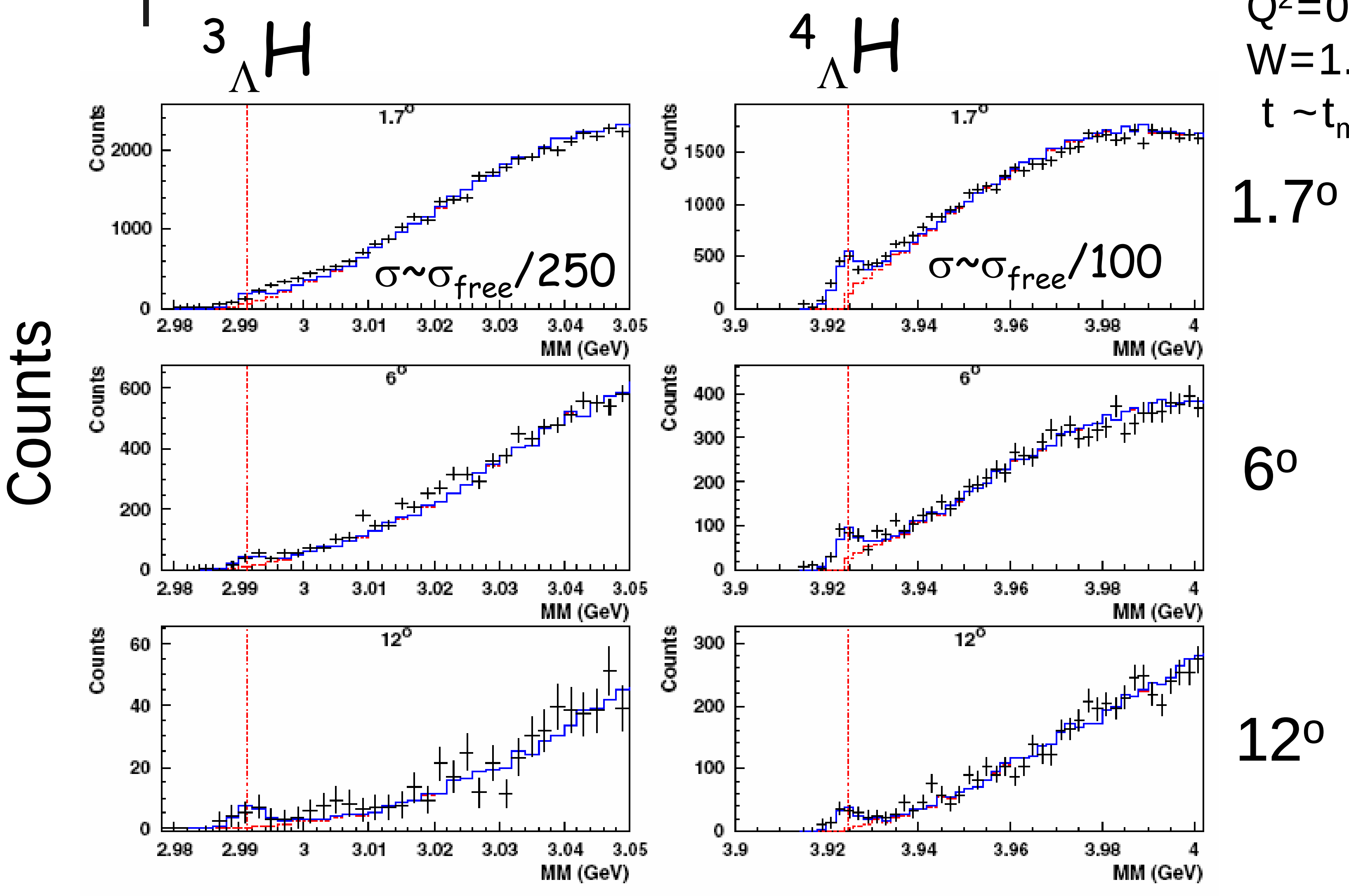

F. Dohrmann et al., Phys. Rev. Lett. **93**, 242501 (2004).

High Resolution Hypernuclear Electroproduction

- Physics goals:
  - Measure *P*-shell ΛN spin-orbit splitting – not achieved…
  - (γ_v, K^+) spectra favor high J, unnatural parity (spin flip) states
  - Precision binding energy measurements
- Hall C: E89-009 L. Tang, E. Hungerford, R. Chrien *et al.*
  - Showed $A(e,e'K^+)_\Lambda A$ with δE ~ 900 keV is possible
  - Tour-de-Force demonstration of $^{12}C(e, e' K^+)^{12}{}_\Lambda B$
- Hall A: E97-107 P. Markowitz, F. Frullani *et al.*
  - High resolution using 2 HMS spectrometers; septa; RICH
- Hall C: E01-011, E05-015 O.Hashimoto, J.Reinhold, L.Tang *et al.*
  - Strive for x250 in event rate, δE < 400 keV
  - Replaced SOS with "HKS" built by Japanese team; Enge "tilt" method (E01-011) → HES spectrometer (E05-015)

Hall C: E89-009 Setup

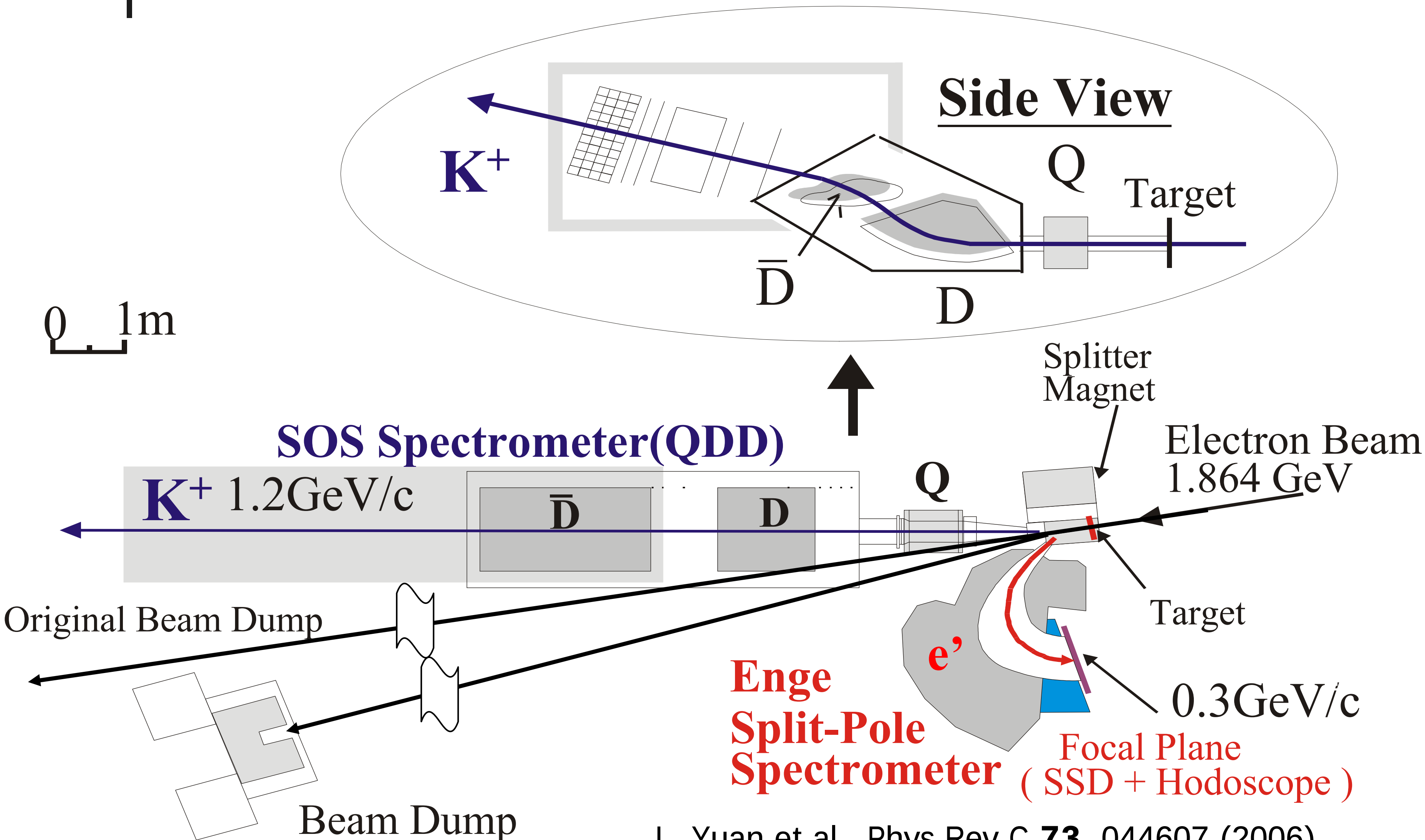

L. Yuan et al., Phys Rev C **73**, 044607 (2006).
T. Miyoshi et al., Phys. Rev. Lett. **90**, 232502 (2003).

Calibration on Hydrogen

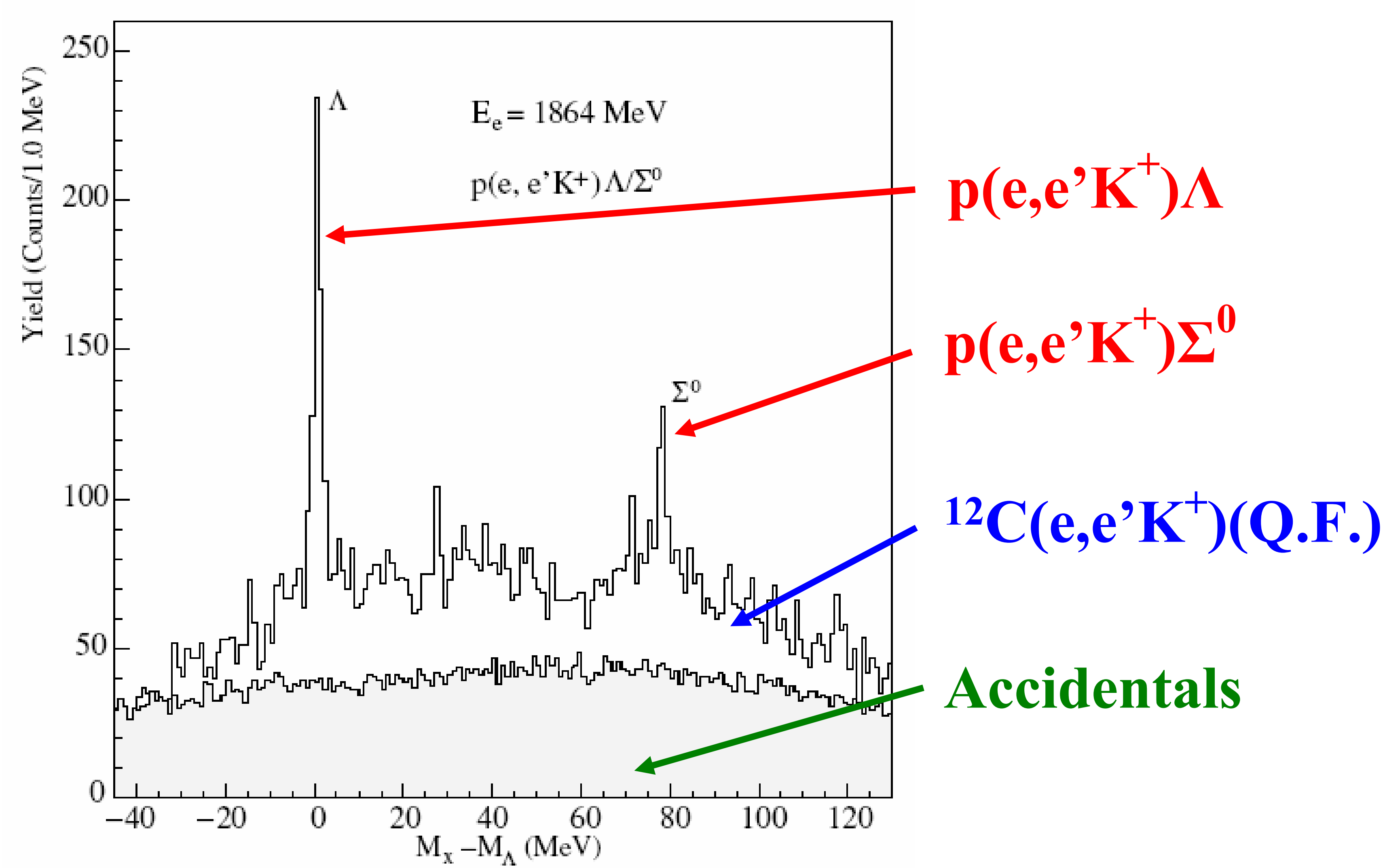

$^{12}C(e, e' K^+)^{12}{}_{\Lambda}B$ (E89-009)

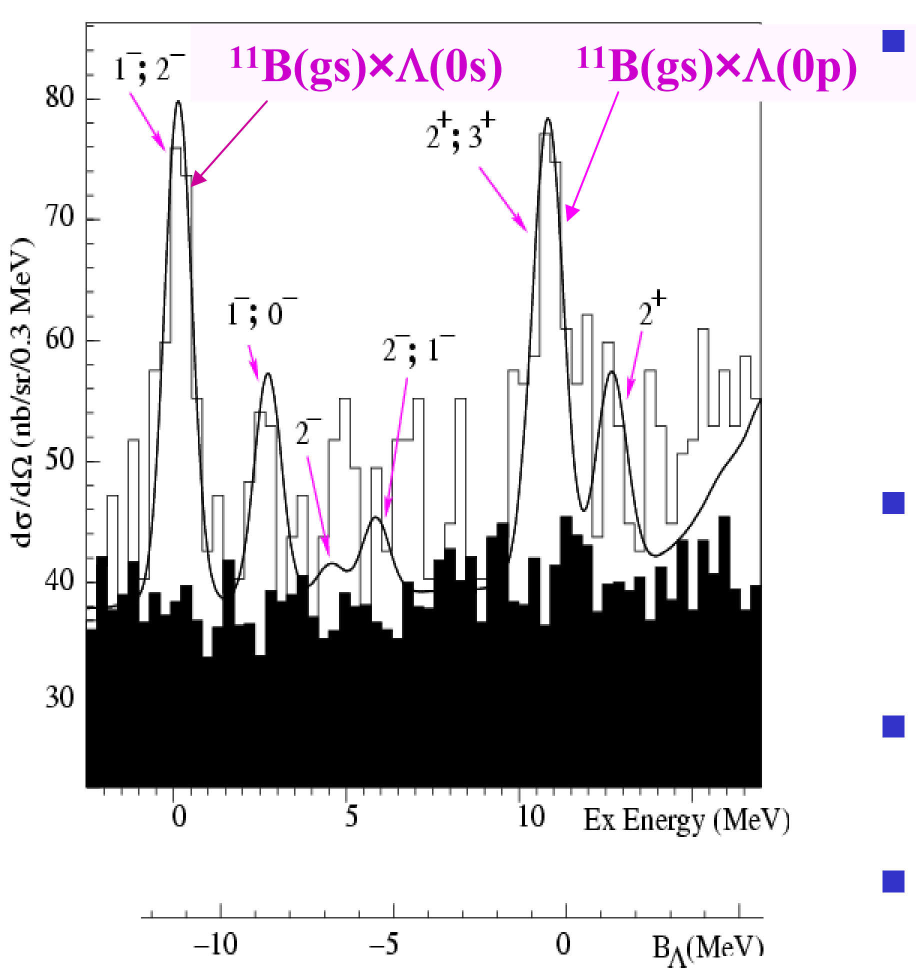

- Bound states resolved!
  - $\delta E \sim 0.75$ MeV FWHM
  - Compare to 1.5 MeV using (π^+, K^+) reaction
  - 1 month data taking
  - Calculation by Motoba & Millener
- Λ in S-shell doublet (^{11}B ground state)
  - $3/2^- + 1/2^+ = 1^-, 2^-$
- Λ in P-shell states
  - $3/2^- + \{1/2^-, 3/2^-\} = 1^+, 2^+, 3^+$
- Core excited states

L. Yuan et al., Phys Rev C **73**, 044607 (2006).
T. Miyoshi et al., Phys. Rev. Lett. **90**, 232502 (2003).

$^{12}C(e, e' K^+)^{12}_{\Lambda}B$ (E89-009)

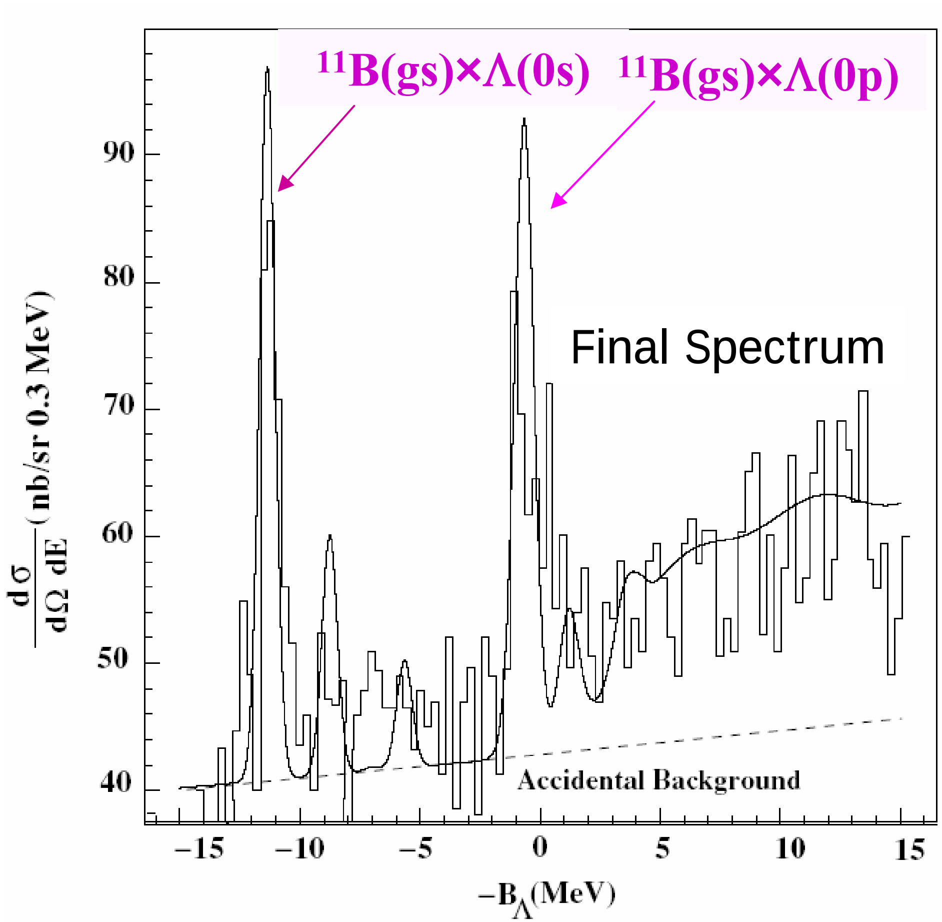

- Bound states resolved
  - $\delta E \sim 0.75$ MeV FWHM
  - Compare to 1.5 MeV using (π^+,K^+) reaction
  - 1 month data taking
  - Calculation by Motoba & Millener
- Λ in S-shell doublet (^{11}B ground state)
  - $3/2^- + 1/2^+ = 1^-, 2^-$
- Λ in P-shell states
  - $3/2^- + \{1/2^-, 3/2^-\} = 1^+, 2^+, 3^+$
- Core excited states

L. Yuan et al., Phys Rev C **73**, 044607 (2006).
T. Miyoshi et al., Phys. Rev. Lett. **90**, 232502 (2003).

Hall A: E94-107 Setup

The two High Resolution Spectrometer (HRS) in Hall A @ JLab

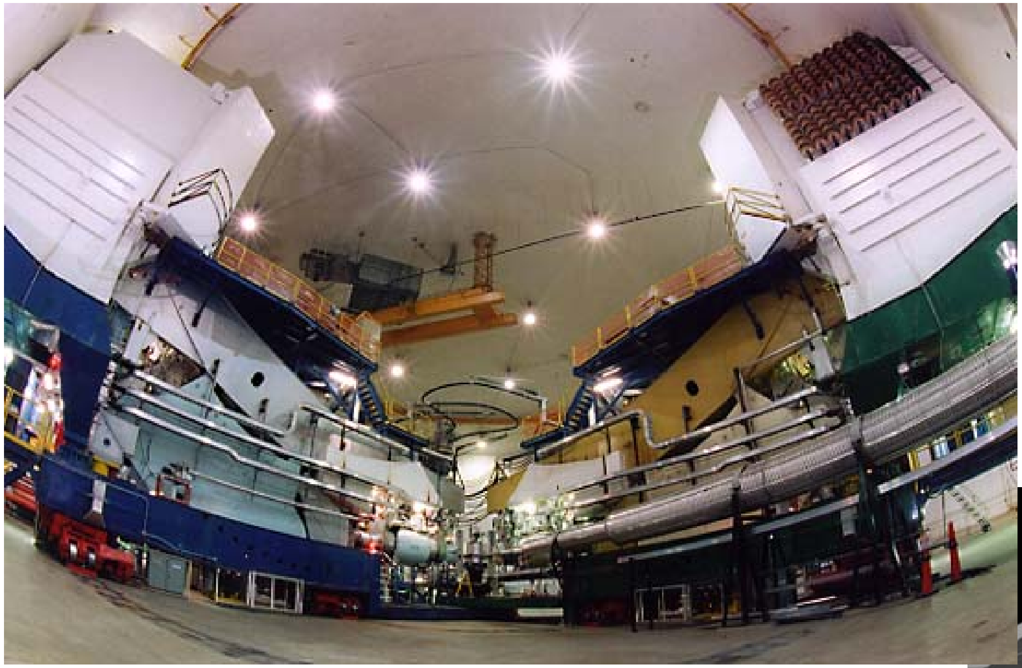

HRS – QDQ characteristics:
Momentum range: 0.3-4.0GeV/c
Δp/p (FWHM): 10^{-4}
Δp: ±5 %
$\Delta\Omega$: 5–6 msr
Minimum Angle : 12.5°

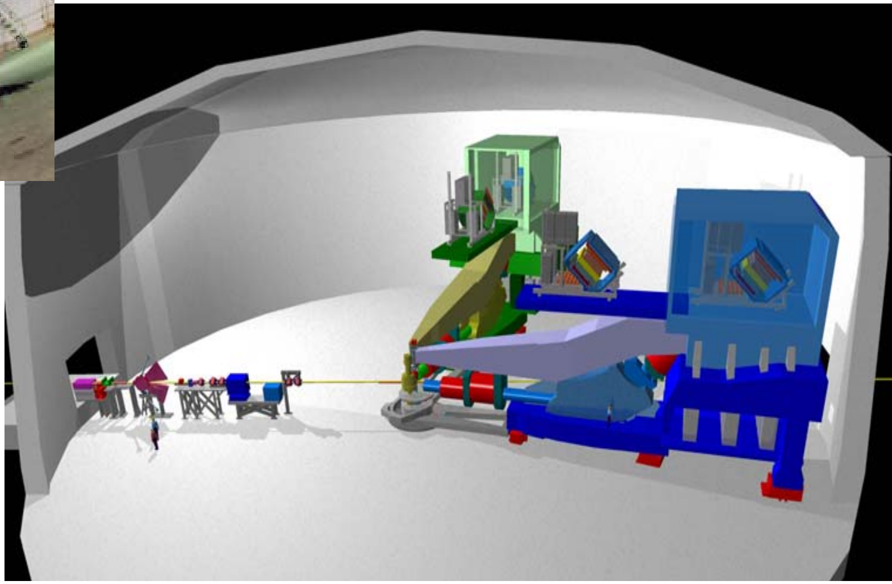

E94-107 collaboration added:

- 2 superconducting septa
- Ring Imaging Cherenkov

P. Markowitz, Florida International, private comm.

Hall A Results: $^{12}{}_{\Lambda}B$

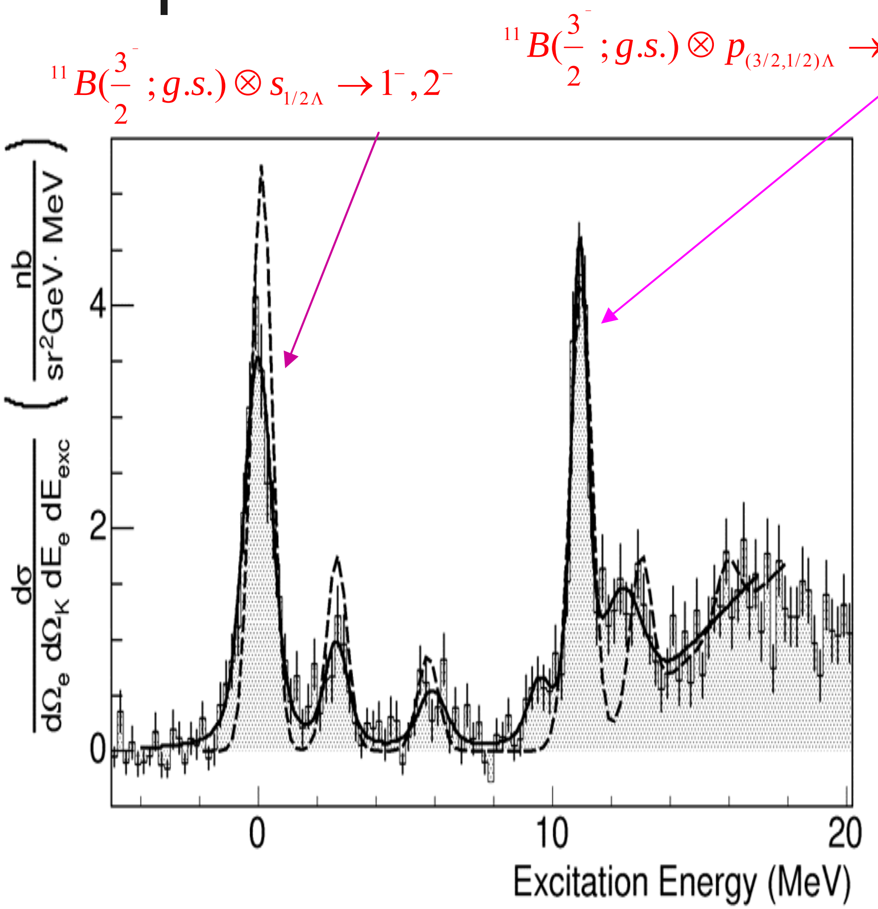

Ex (MeV)	Width (FWHM, MeV)	S/N ratio	Cross section [nb/sr²/GeV]
0.0 ± 0.03	1.15 ± 0.18	19.7	4.48 ± 0.29 ± 0.63
2.65 ± 0.10	0.95 ± 0.43	7.0	0.75 ± 0.16 ± 0.63
5.92 ± 0.13	1.13±0.29	5.3	0.45± 0.13 ± 0.09
9.54 ± 0.16	0.93±0.46	4.4	0.63 ± 0.20 ± 0.13
10.93 ±0.03	0.67±0.15	20.0	3.42 ± 0.50 ± 0.55
12.36 ±0.13	1.58 ±0.29	7.3	1.19 ± 0.36 ± 0.35

P. Markowitz, Florida International, private comm.
M. Iodice et al., Phys. Rev. Lett. 99, 052501 (2007).

Results on ^{16}O target – Hypernuclear Spectrum of $^{16}{}_{\Lambda}$N

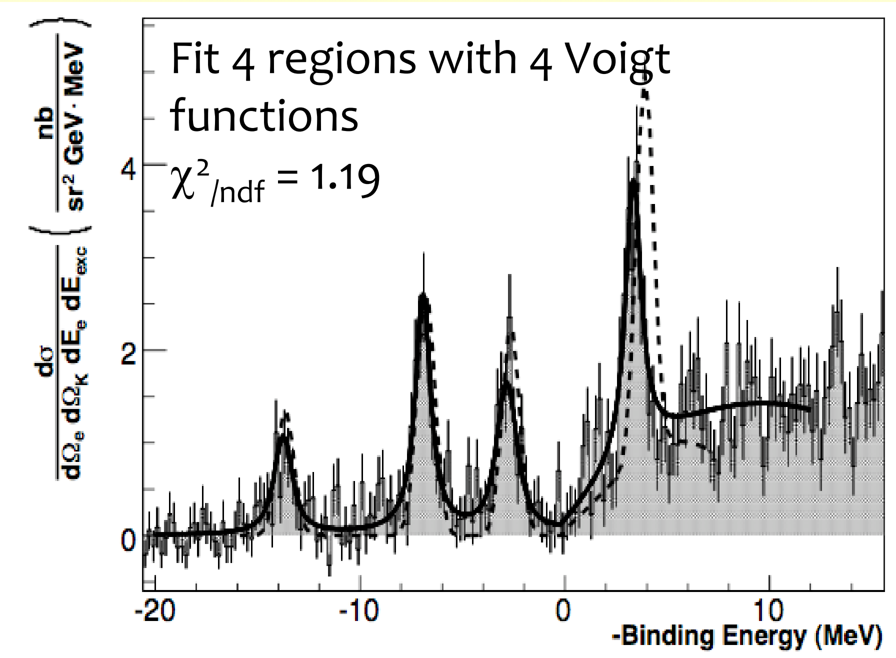

Binding Energy B_{Λ}=13.76±0.16 MeV
Accuracy for $^{16}{}_{\Lambda}$N unmatched!
(ambiguous interpretation from emulsion data; interaction involving Λ production on *n* more difficult to normalize)

Within errors, the binding energy and the excited levels of the mirror hypernuclei $^{16}{}_{\Lambda}$O and $^{16}{}_{\Lambda}$N (this experiment) are in agreement, giving no strong evidence of charge-dependent effects

E_x (MeV)	Width (FWHM, MeV)	Cross section ($nb/sr^2/GeV$)	E_x (MeV)	Wave function	J^π	Cross section ($nb/sr^2/GeV$)
0.0/13.76±0.16	1.71	1.45 ± 0.26	0.00	$p_{1/2}^{-1} \otimes s_{1/2\Lambda}$	0^-	0.002
			0.03	$p_{1/2}^{-1} \otimes s_{1/2\Lambda}$	1^-	1.45
6.83 ± 0.06	0.88	3.16 ± 0.35	6.71	$p_{3/2}^{-1} \otimes s_{1/2\Lambda}$	1^-	0.80
			6.93	$p_{3/2}^{-1} \otimes s_{1/2\Lambda}$	2^-	2.11
10.92 ± 0.07	0.99	2.11 ± 0.37	11.00	$p_{1/2}^{-1} \otimes p_{3/2\Lambda}$	2^+	1.82
			11.07	$p_{1/2}^{-1} \otimes p_{1/2\Lambda}$	1^+	0.62
17.10 ± 0.07	1.00	3.44 ± 0.52	17.56	$p_{3/2}^{-1} \otimes p_{1/2\Lambda}$	2^+	2.10
			17.57	$p_{3/2}^{-1} \otimes p_{3/2\Lambda}$	3^+	2.26

(cf. A. Gal talk discussion)

F. Cusanno *et al.*, Phys. Rev. Lett. **103**, 202501 (2009).

Results on ^{16}O target – Hypernuclear Spectrum of $^{16}{}_{\Lambda}$N

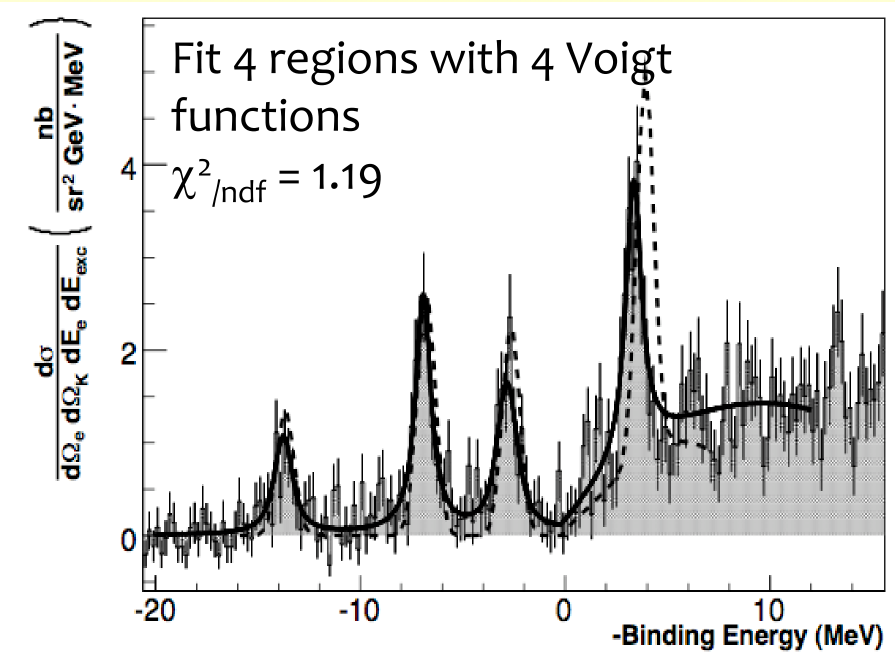

Theoretical model (D.J.Millener) based on :
SLA p(e,e'K$^+$)Λ (elementary process)
ΛN interaction fixed parameters from KEK and BNL $^{16}{}_{\Lambda}$O spectra

- Four peaks reproduced by theory
- The fourth peak (Λ in p state) position disagrees with theory. **This might be an indication of a large spin-orbit term S_Λ (under investigation)**

E_x (MeV)	Width (FWHM, MeV)	Cross section $(nb/sr^2/GeV)$	E_x (MeV)	Wave function	J^π	Cross section $(nb/sr^2/GeV)$
0.0/13.76±0.16	1.71	1.45 ± 0.26	0.00	$p_{1/2}^{-1} \otimes s_{1/2\Lambda}$	0^-	0.002
			0.03	$p_{1/2}^{-1} \otimes s_{1/2\Lambda}$	1^-	1.45
6.83 ± 0.06	0.88	3.16 ± 0.35	6.71	$p_{3/2}^{-1} \otimes s_{1/2\Lambda}$	1^-	0.80
			6.93	$p_{3/2}^{-1} \otimes s_{1/2\Lambda}$	2^-	2.11
10.92 ± 0.07	0.99	2.11 ± 0.37	11.00	$p_{1/2}^{-1} \otimes p_{3/2\Lambda}$	2^+	1.82
			11.07	$p_{1/2}^{-1} \otimes p_{1/2\Lambda}$	1^+	0.62
17.10 ± 0.07	1.00	3.44 ± 0.52	17.56	$p_{3/2}^{-1} \otimes p_{1/2\Lambda}$	2^+	2.10
			17.57	$p_{3/2}^{-1} \otimes p_{3/2\Lambda}$	3^+	2.26

(cf. A. Gal talk discussion)

F. Cusanno et al., Phys. Rev. Lett. **103**, 202501 (2009).

Results on ^{16}O target – Hypernuclear Spectrum of $^{16}{}_{\Lambda}N$

Evidence of a 5th peak in the quasi-free regions (already observed in KEK $^{16}{}_{\Lambda}O$ data) is now investigated. Results from newfits are PRELIMINARY.

Theoretical effort is ongoing to investigate $s_{1/2}\Lambda$ coupling to core excited states

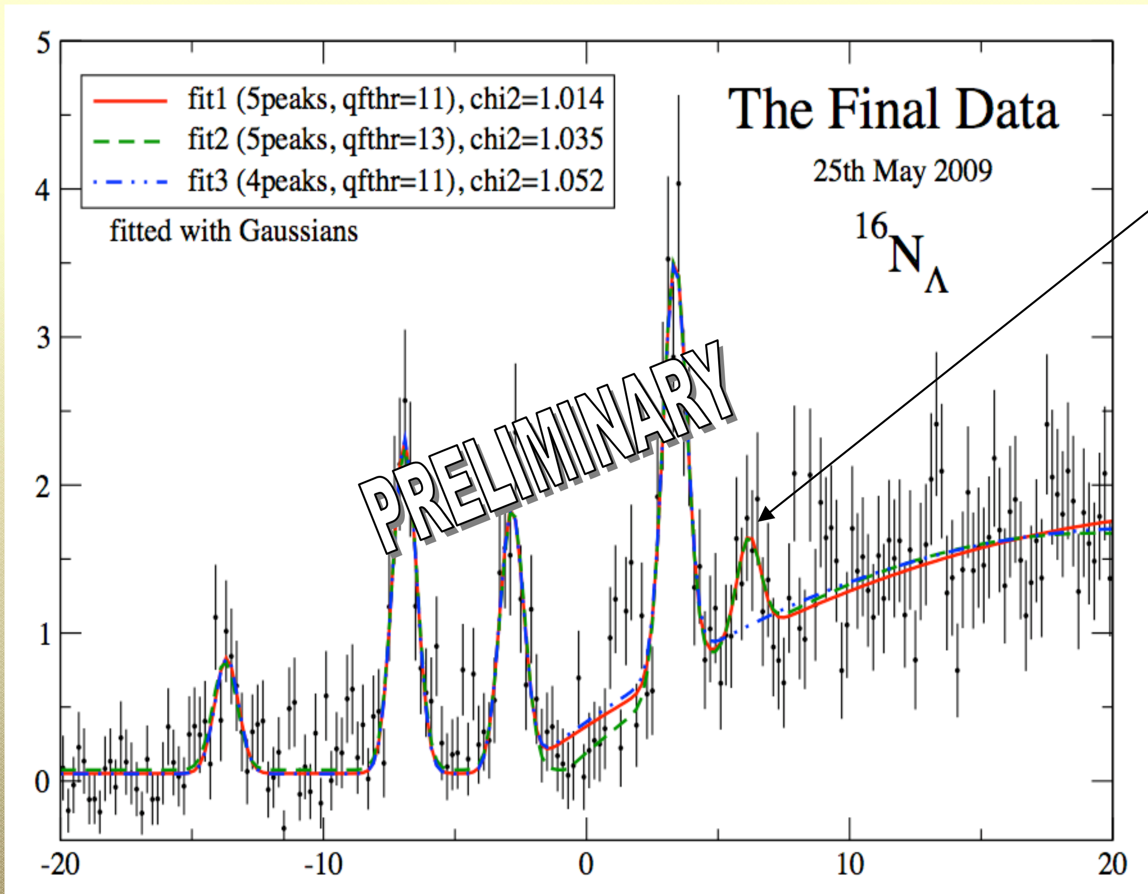

$CoreExcitedStates \otimes s_{1/2}\Lambda$

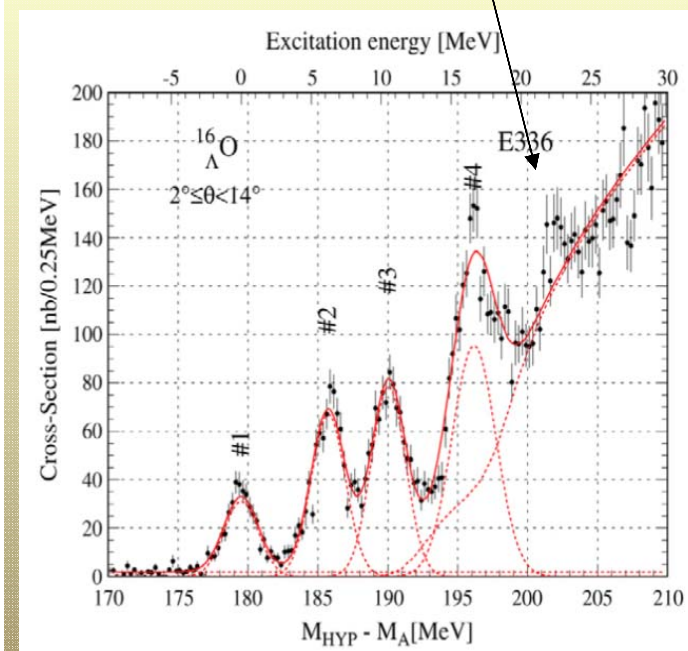

P. Markowitz, Florida International, private comm.

Hall C: E01-011

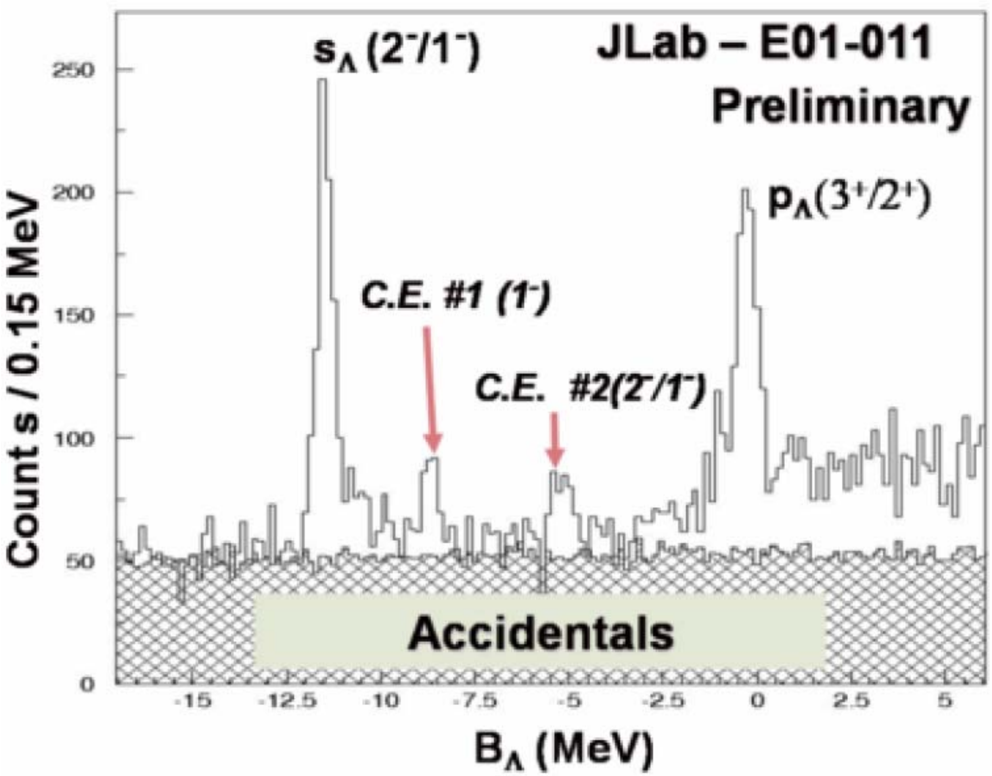

- Detector upgrades:
  - New splitter magnet
  - SOS→HKS for kaons (E01-011)
  - Enge→HES electron spectrometer (E05-015)
- Data (fall 2009) on ^{7}Li, ^{9}Be, ^{10}B, ^{12}C, ^{52}Cr (new)
  - Goal: precision ground state mass determinations (<200 keV), without resorting to emulsion information

- Hall A measured FWHM ~670 keV, almost background free
- Hall C measured FWHM ~465 keV, with twice the statistics!

(cf. T. Gogami talk discussion)

 P. Markowitz, Florida International, private comm.

Related Hypernuclei Compared

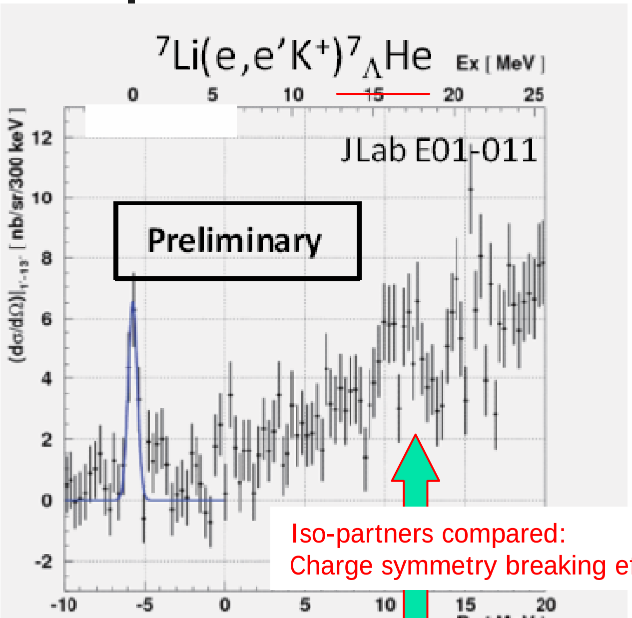

Iso-partners compared:
Charge symmetry breaking effects

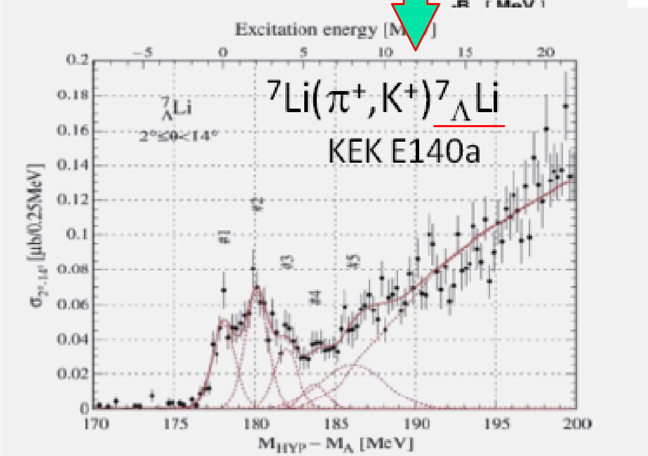

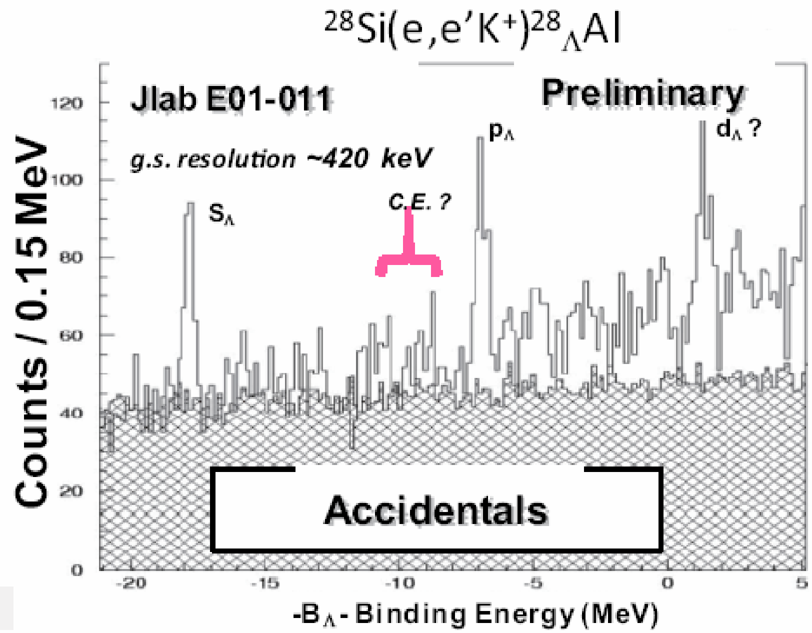

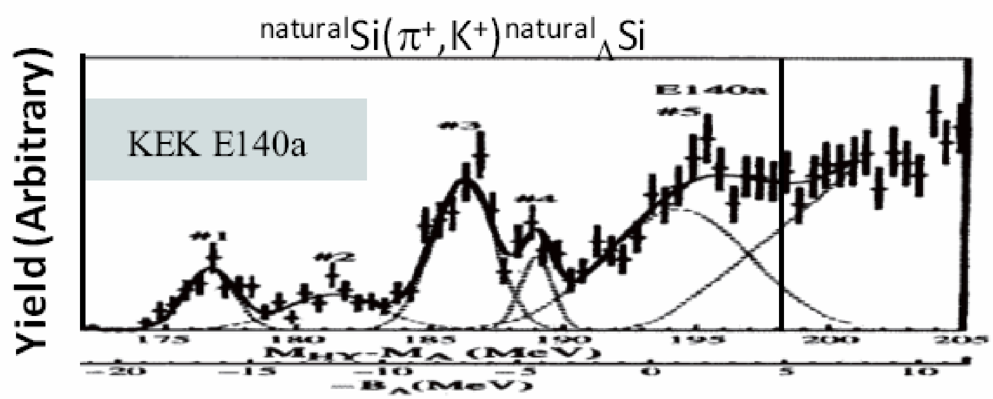

O. Hashimoto, Nucl. Phys. A **835**, 121 (2010).

Outlook for Hypernuclear Electroproduction

- Technical challenges have proven manageable for $(e,e' K^+)$
  - High resolution of ~500 keV achieved
  - High rates of > few 100/day for ${}^{12}_{\Lambda}B$ ground state (comparable to (π^+,K^+) work)
  - Medium-heavy targets, e.g. ${}^{28}Si(e,e'K^+){}^{28}_{\Lambda}Al$, are measurable
- Program Elements:
  - Precision ground state masses
  - Search for charge symmetry breaking effects
  - Production of particle continuum states not amenable to gamma spectroscopy

Creating Excited Strange States

- K^*
- $\Lambda(1405)$
- $\Lambda(1520)$
- Cascades…

$K^{*0}\ \Sigma^+$ Photoproduction measurement

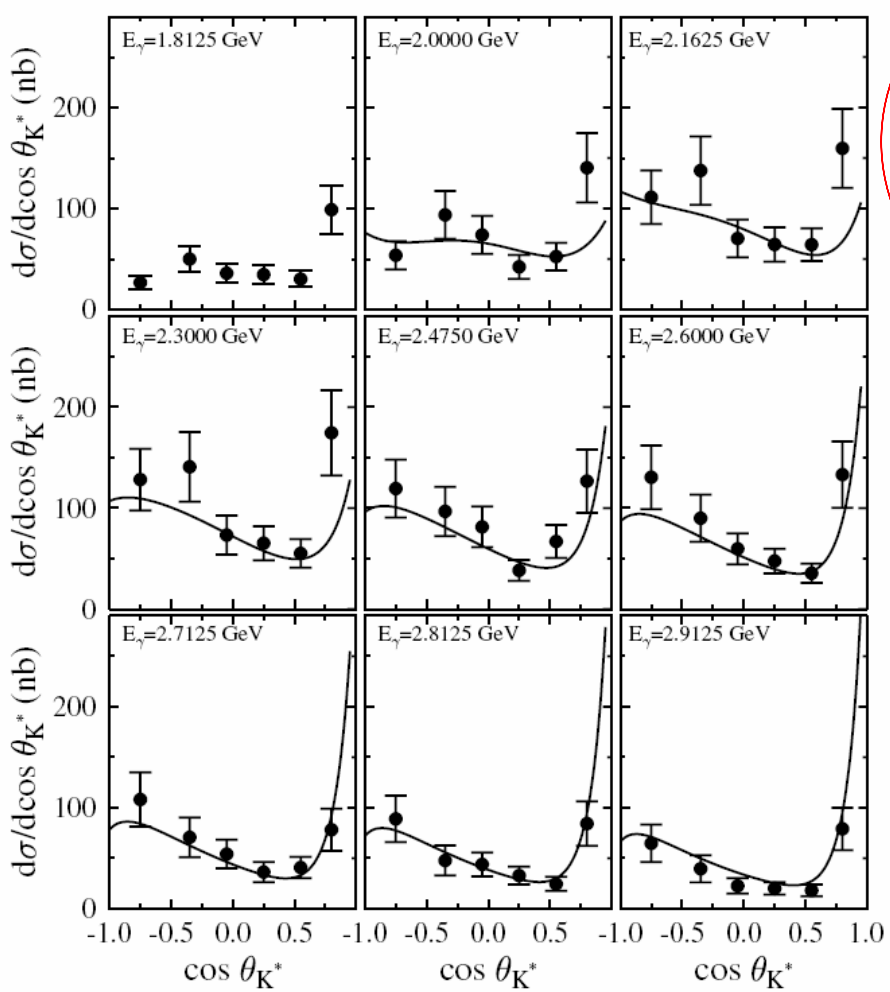

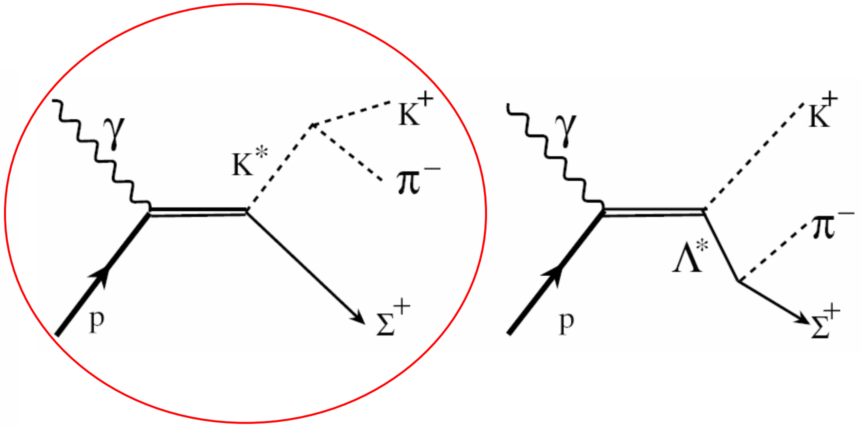

- Strange vector meson production: no t-channel Pomeron exchange allowed
- Two $K^*\Sigma N$ couplings set by SU(3)-flavor-blind quark-K^* interaction
  - Relate to ω, ρ photoproduction
  - no N* used in the model
- Test for the need for scalar $\kappa(800)$ exchange: conclude that none is needed.

 I. Hleiqawi *et al.*, Phys. Rev. C **75**, 042201 (2007).

What "is" the $\Lambda(1405)$?

- Structure – an issue since its discovery
  - SU(3) singlet 3q state
    I=0, $J^\pi = \frac{1}{2}^-$
  - $\bar{K}N$ sub-threshold bound state
  - Gluonic (udsg) hybrid $J^\pi = \frac{1}{2}^+$
    - O. Kittel & G.R.Farrar hep-ph/0010186
  - Dynamically generated resonance, via unitary meson-baryon channel coupling
    - R. Dalitz & S.F.Tuan, Phys. Rev. Lett. **2**, 425 (1959), Ann. Phys. **10**, 307 (1960).
    - J. C. Nacher, E. Oset, H. Toki, A. Ramos, Phys. Lett. B **455**, 55 (1999). ← inspired CLAS exp'ts

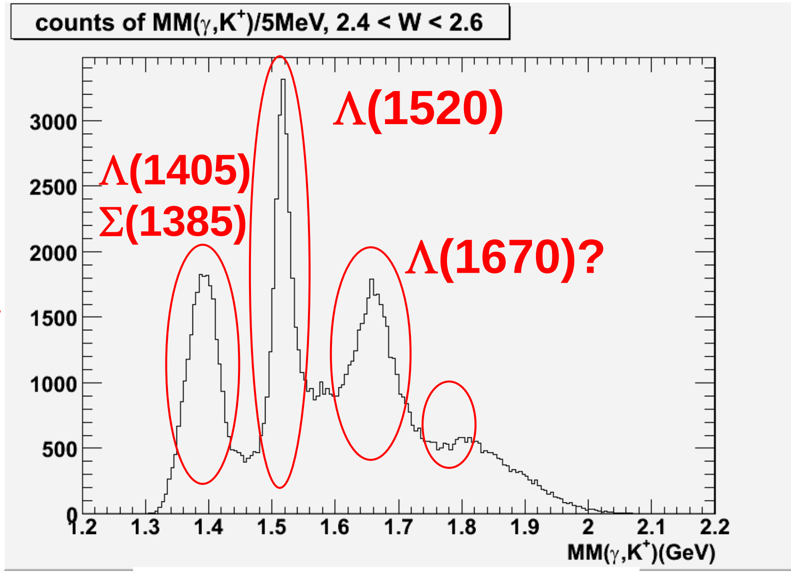

(γ,K) Missing Mass (GeV)

The Low-Mass S=-1 Hyperons

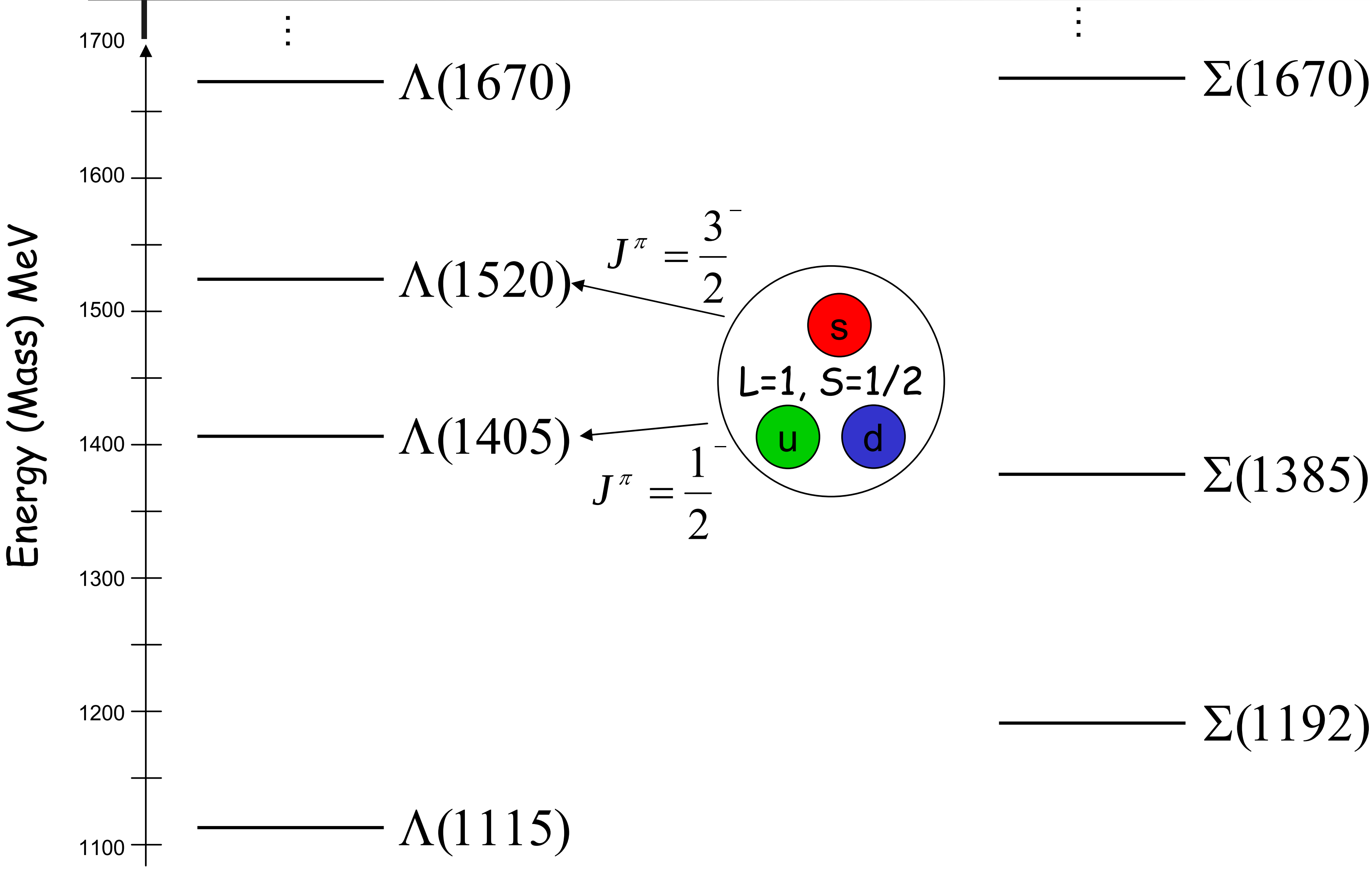

The Low-Mass S=-1 Hyperons

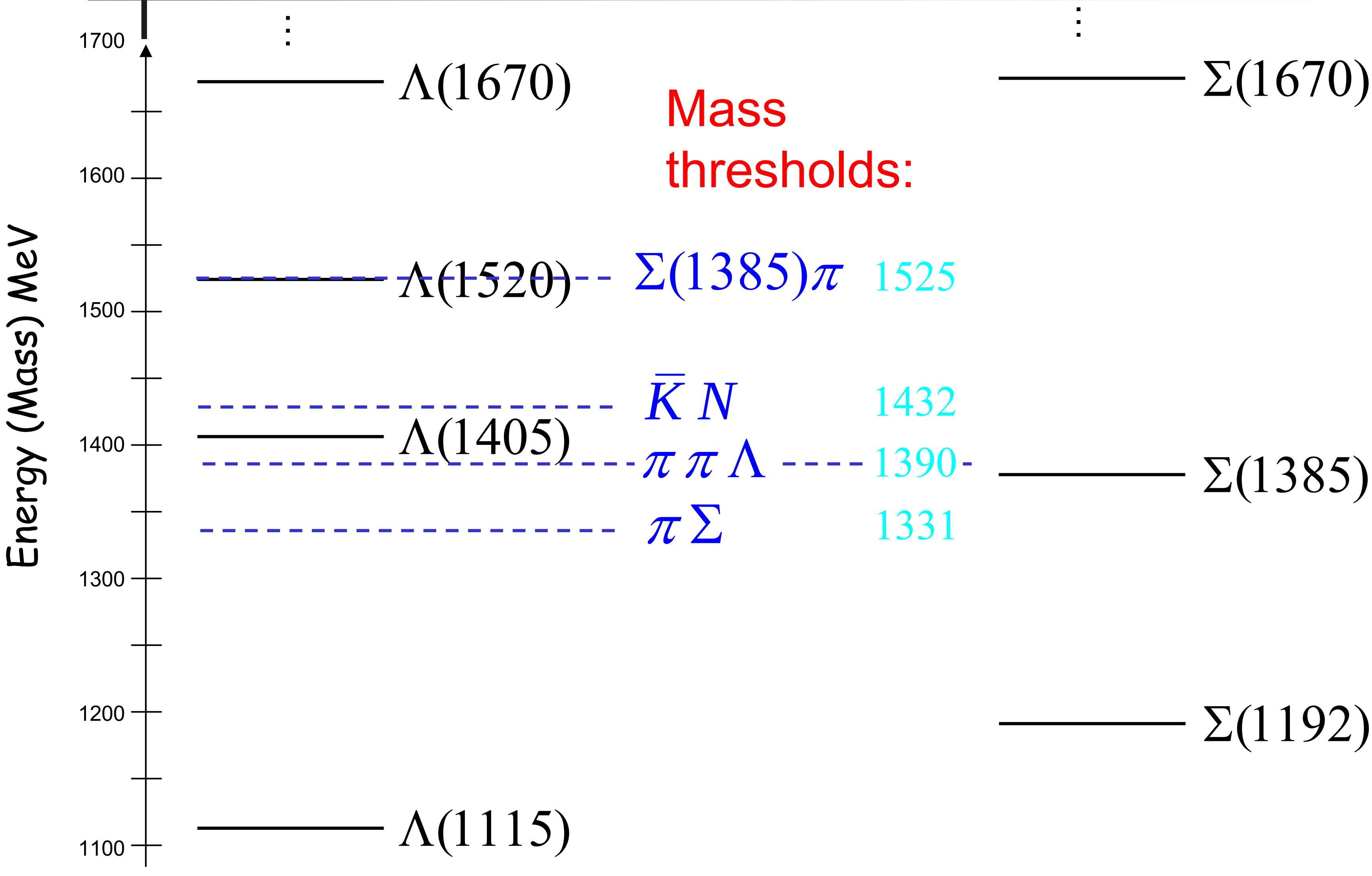

Dynamical State Generation

Do the "ground state" mesons and baryons attract strongly enough to form mB "molecular" bound states or unbound resonances?

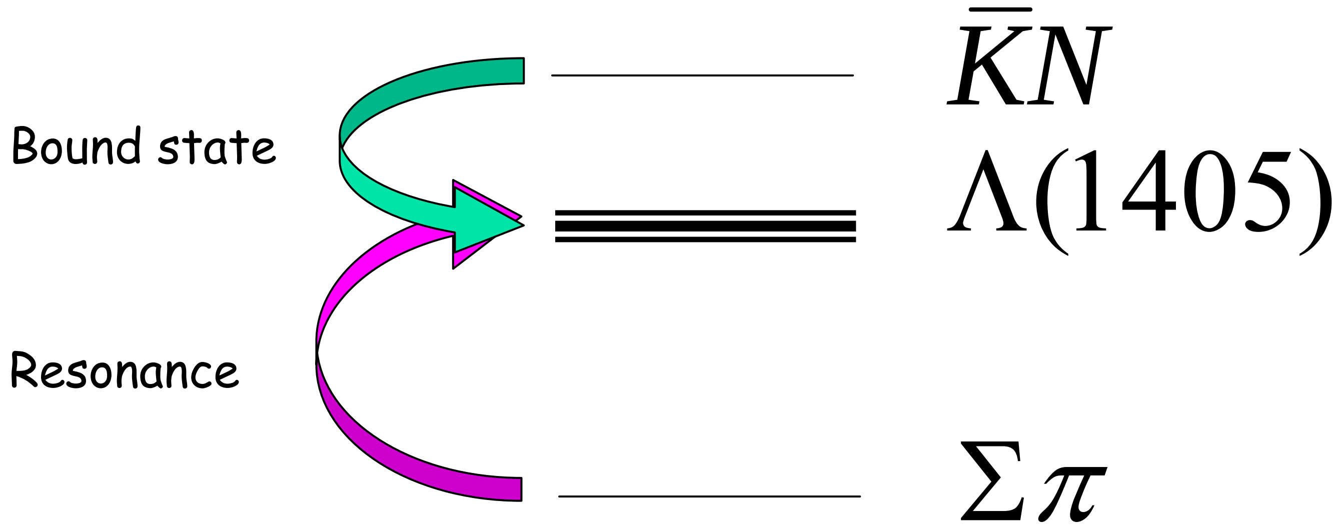

Unitary channel coupling via Bethe-Salpeter equation formalism

"Weinberg-Tomozawa" driving term… + higher chiral orders…

Chiral Unitary Model (example)

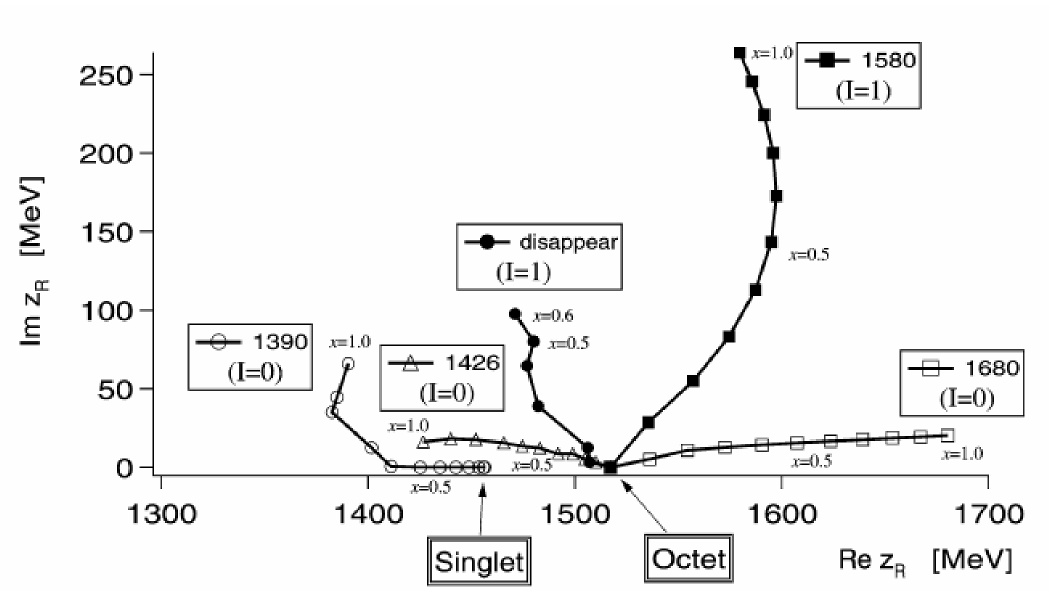

Fig. 1. Trajectories of the poles in the scattering amplitudes obtained by changing the SU(3) breaking parameter x gradually. At the SU(3) symmetric limit ($x = 0$), only two poles appear, one is for the singlet and the other for the octets. The symbols correspond to the step size $\delta x = 0.1$.

- SU(3) baryons irreps $1+8_s+8_a$ combine with 0^- Goldstone bosons to generate:
- Two octets and a singlet of $\frac{1}{2}^-$ baryons generated dynamically in SU(3) limit
- SU(3) breaking leads to two S=-1 I=0 poles near 1405 MeV
  - ~1420 mostly $\bar{K}N$
  - ~1390 mostly $\pi\Sigma$
- Possible weak I=1 pole also predicted

D. Jido, J.A Oller, E. Oset, A. Ramos, U-G Meissner Nucl. Phys. A 725 181 (2003)

Chiral Unitary Model (different example)

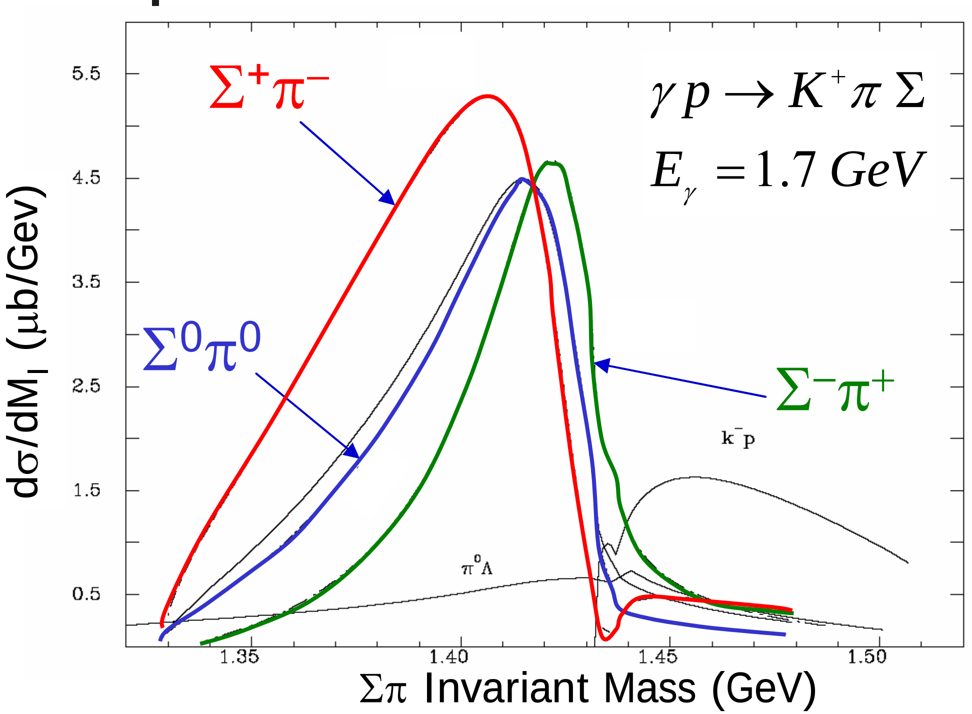

$$\frac{d\sigma(\pi^+\Sigma^-)}{dM_I} \propto \frac{1}{2}\left|T^{(1)}\right|^2 + \frac{1}{3}\left|T^{(0)}\right|^2 + \frac{2}{\sqrt{6}}\mathrm{Re}\left(T^{(0)}T^{(1)*}\right) + O\left(T^{(2)}\right)$$

$$\frac{d\sigma(\pi^-\Sigma^+)}{dM_I} \propto \frac{1}{2}\left|T^{(1)}\right|^2 + \frac{1}{3}\left|T^{(0)}\right|^2 - \frac{2}{\sqrt{6}}\mathrm{Re}\left(T^{(0)}T^{(1)*}\right) + O\left(T^{(2)}\right)$$

$$\frac{d\sigma(\pi^0\Sigma^0)}{dM_I} \propto \frac{1}{3}\left|T^{(0)}\right|^2 + O\left(T^{(2)}\right)$$

- Mass distribution of the "Λ(1405)" predicted to depend on πΣ decay channel
- J. C. Nacher, E. Oset, H. Toki, A. Ramos, Phys. Lett. B **455**, 55 (1999).
  - Chiral Lagrangian + mB FSI + Channel Coupling
  - I(π Σ) = {0,1,2} – not in an isospin eigenstate
  - I=2 contributions negligible
  - Interference between I=0 and I=1 amplitudes modifies mass distributions

Chiral Dynamics – some recent refs.

- Chiral dynamics of the two Λ(1405) states,
  D. Jido, J.A. Oller, E. Oset,A. Ramos, U-G. Meissner, Nucl Phys A 725, 181 (2003).
- Chiral dynamics of kaon-nucleon interactions, revisited, B. Borasoy, R. Nissler, W. Wiese, Eur. Phys. J. A 25 79 (2005).
- Low lying S=-1 excited baryons and chiral symmetry, E. Oset, A. Ramos, C. Bennhold, Phys. Lett. B 527 99 (2002).
- Non-perturbative chiral approach to s-wave KN ineractions,
  E. Oset, A. Ramos, Nucl. Phys. A 635 99 (1998).
- SU(3) chiral dynamics with coupled channels eta and kaon photoproduction,
  N. Kaiser, T. Waas, W. Weise, Nucl. Phys. A 612 297 (1997).

Getting the three final states:

$\gamma+p \rightarrow K^{+}+$ $\boxed{\Lambda(1405)}$

33% $\Sigma^{-}\,\pi^{+} \rightarrow \pi^{-}(n)\,\pi^{+}$ 100% Case 3

33% $\Sigma^{+}\,\pi^{-} \rightarrow p(\pi^{0})\,\pi^{-}$ 52% Case 2

$\rightarrow \pi^{+}(n)\,\pi^{-}$ 48% Case 3

33% $\Sigma^{0}\,\pi^{0} \rightarrow \Lambda(\gamma\,\pi^{0})$ 100% Case 2

$\gamma+p \rightarrow$ $\boxed{K^{*+,0}+\Sigma^{0,+}}$ Subtracted incoherently bin by bin using Monte Carlo model

Fit to Lineshape with MC Templates

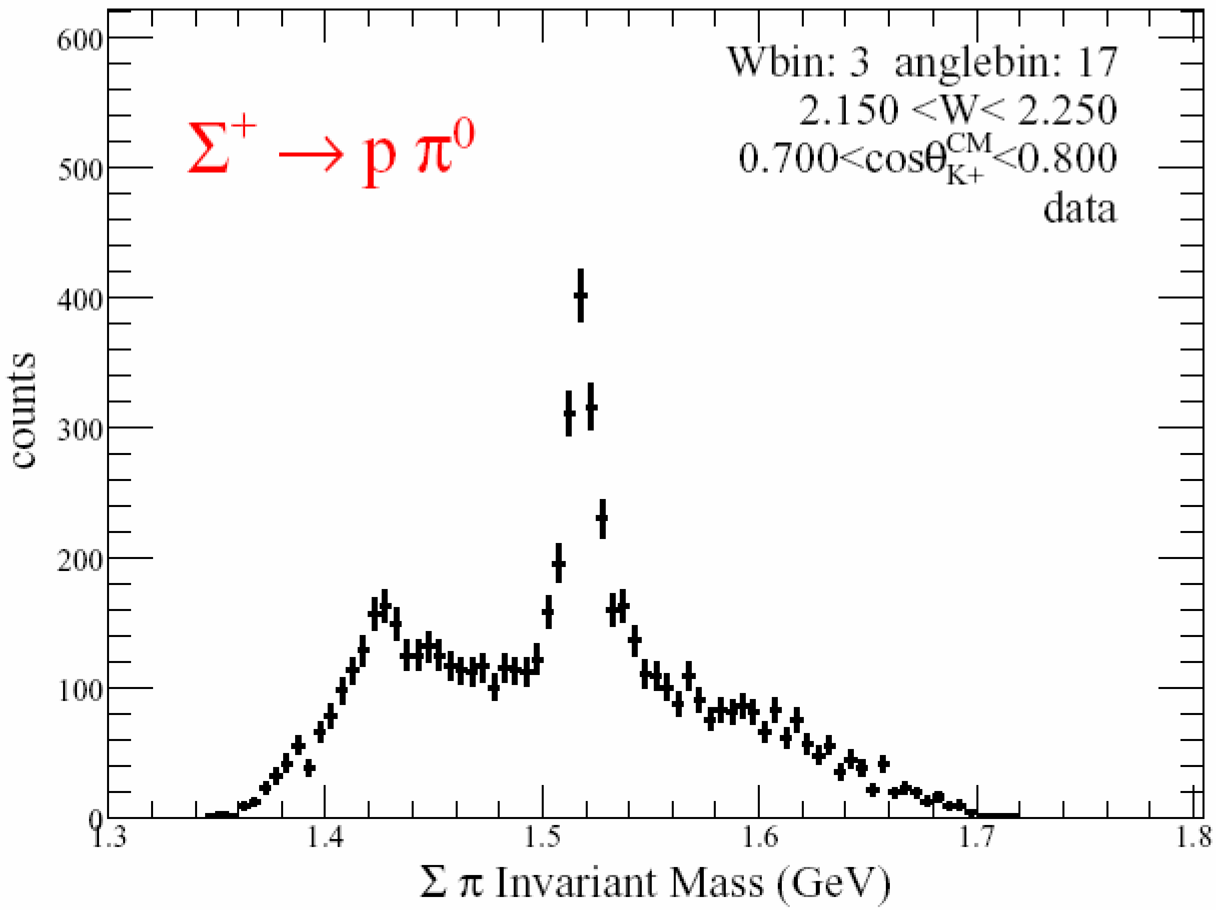

- Example of 1 bin out of 150:

Fit to Lineshape with MC Templates

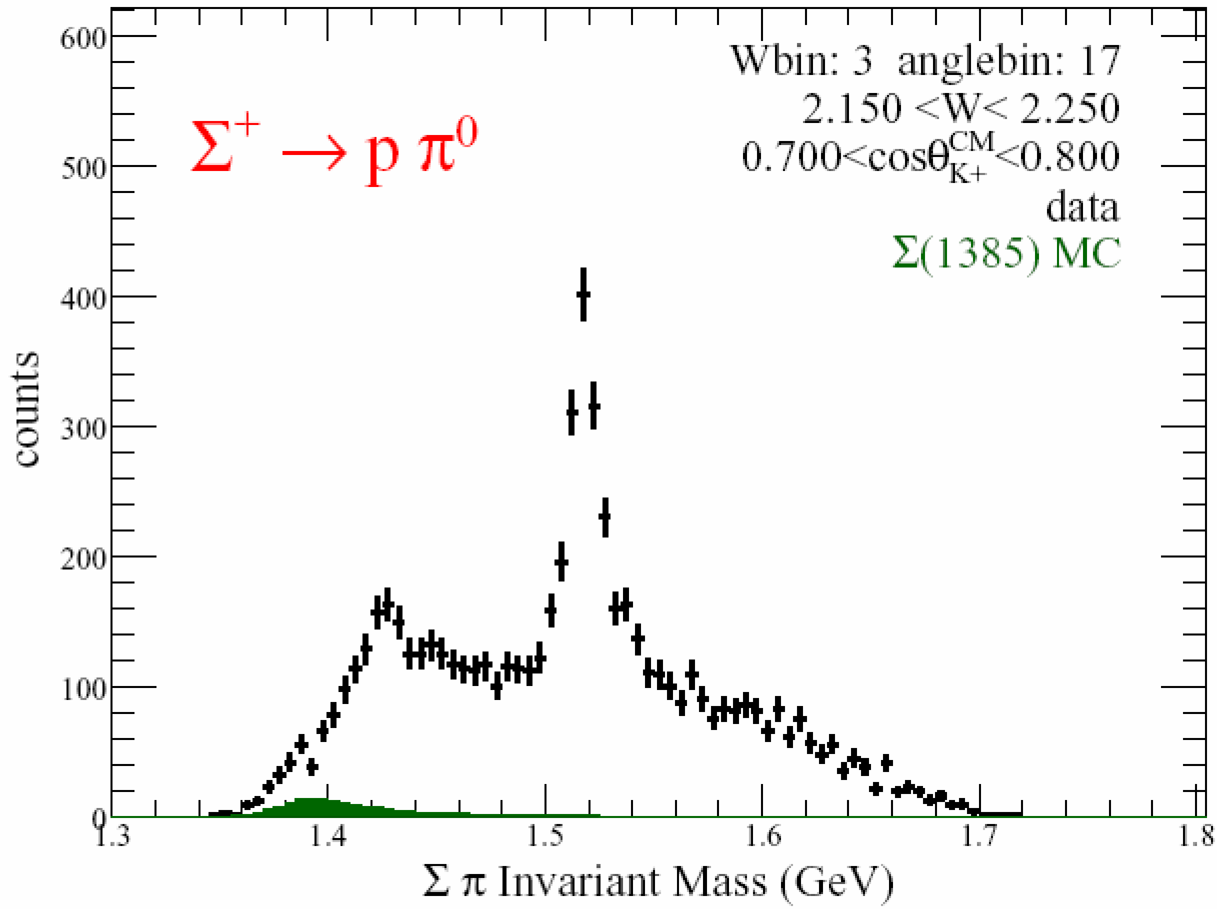

- Example of 1 bin out of 150:
- Subtract off $\Sigma^0(1385)$ (fixed by $\Lambda\pi^0$ decay mode)

Fit to Lineshape with MC Templates

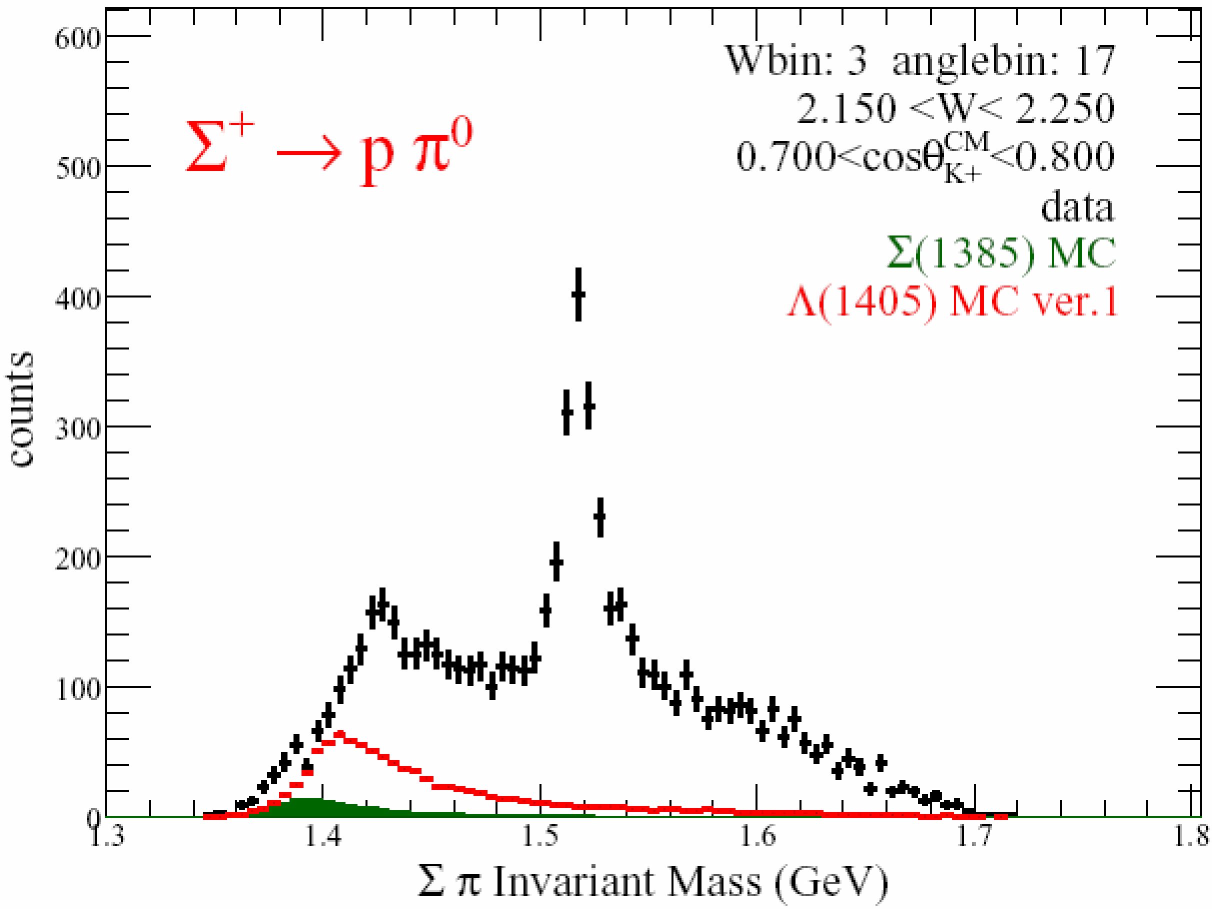

- Example of 1 bin out of 150:
- Subtract off Σ^0(1385) (fixed by $\Lambda\pi^0$ decay mode)
- Model Λ(1405) à la PDG (Iteration 0)

Fit to Lineshape with MC Templates

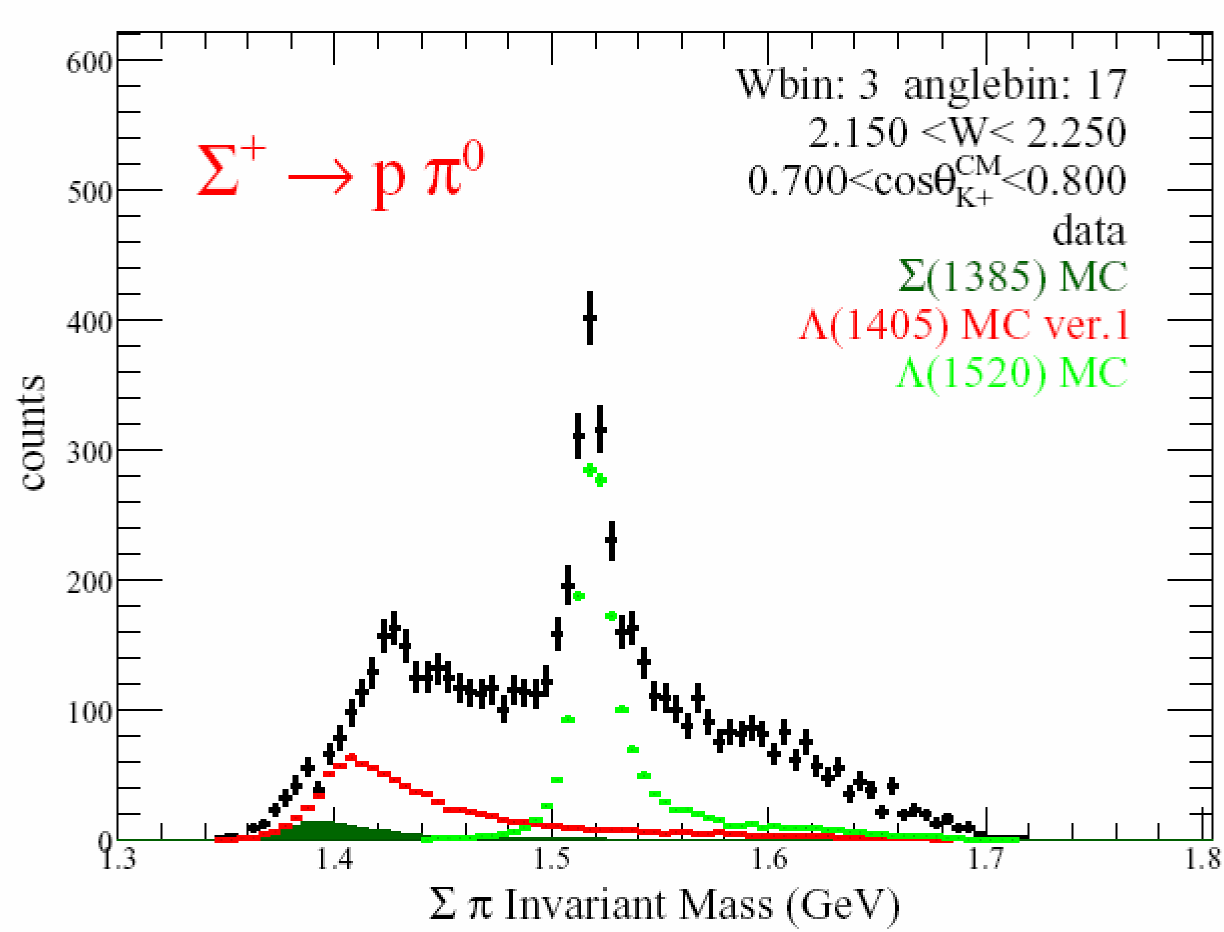

- Example of 1 bin out of 150:
- Subtract off Σ^0(1385) (fixed by $\Lambda\pi^0$ decay mode)
- Model Λ(1405) à la PDG (Iteration 0)
- Subtract off fitted Λ(1520)

Fit to Lineshape with MC Templates

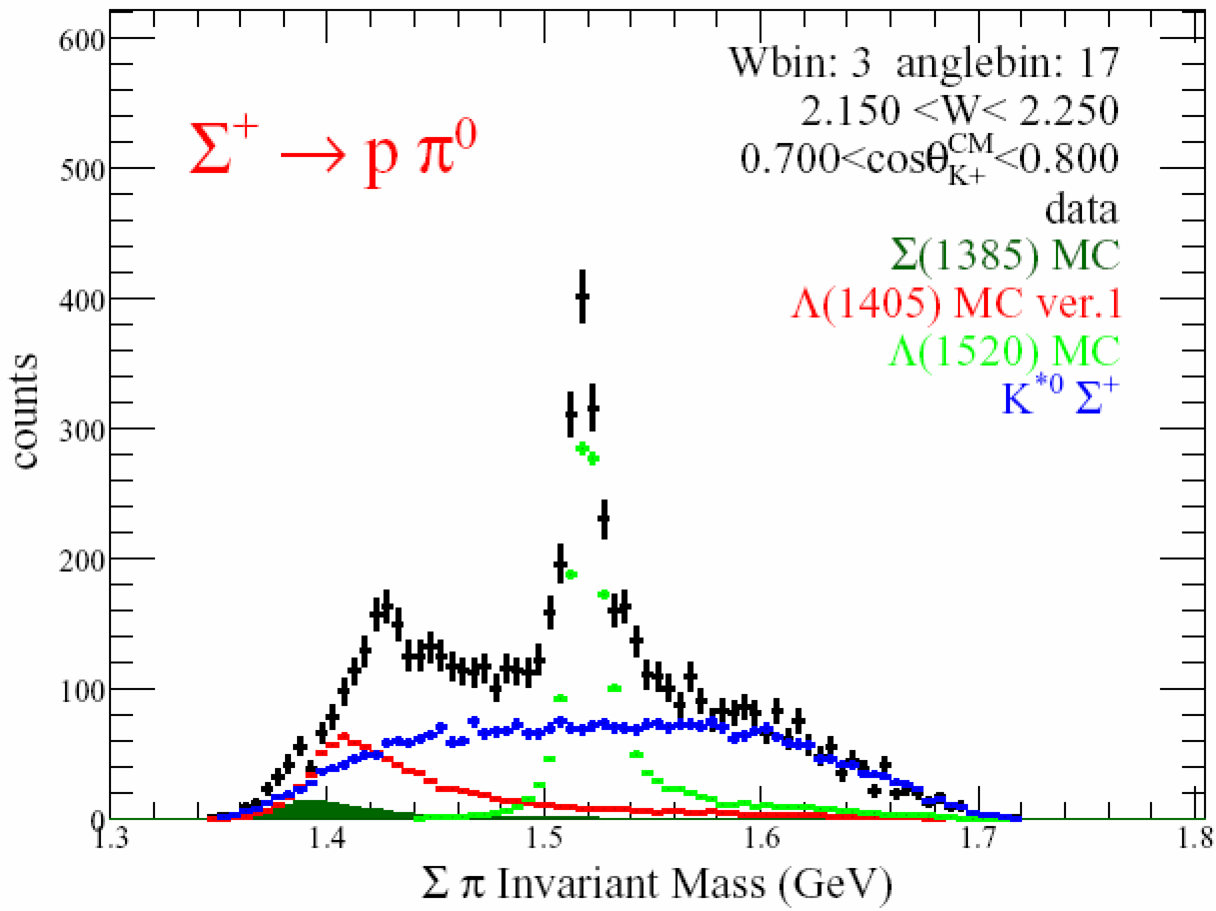

- Example of 1 bin out of 150:
- Subtract off $\Sigma^0(1385)$ (fixed by $\Lambda\pi^0$ decay mode)
- Model $\Lambda(1405)$ à la PDG (Iteration 0)
- Subtract off fitted $\Lambda(1520)$
- Subtract off fitted K^{*0} (incoherent)

Fit to Lineshape with MC Templates

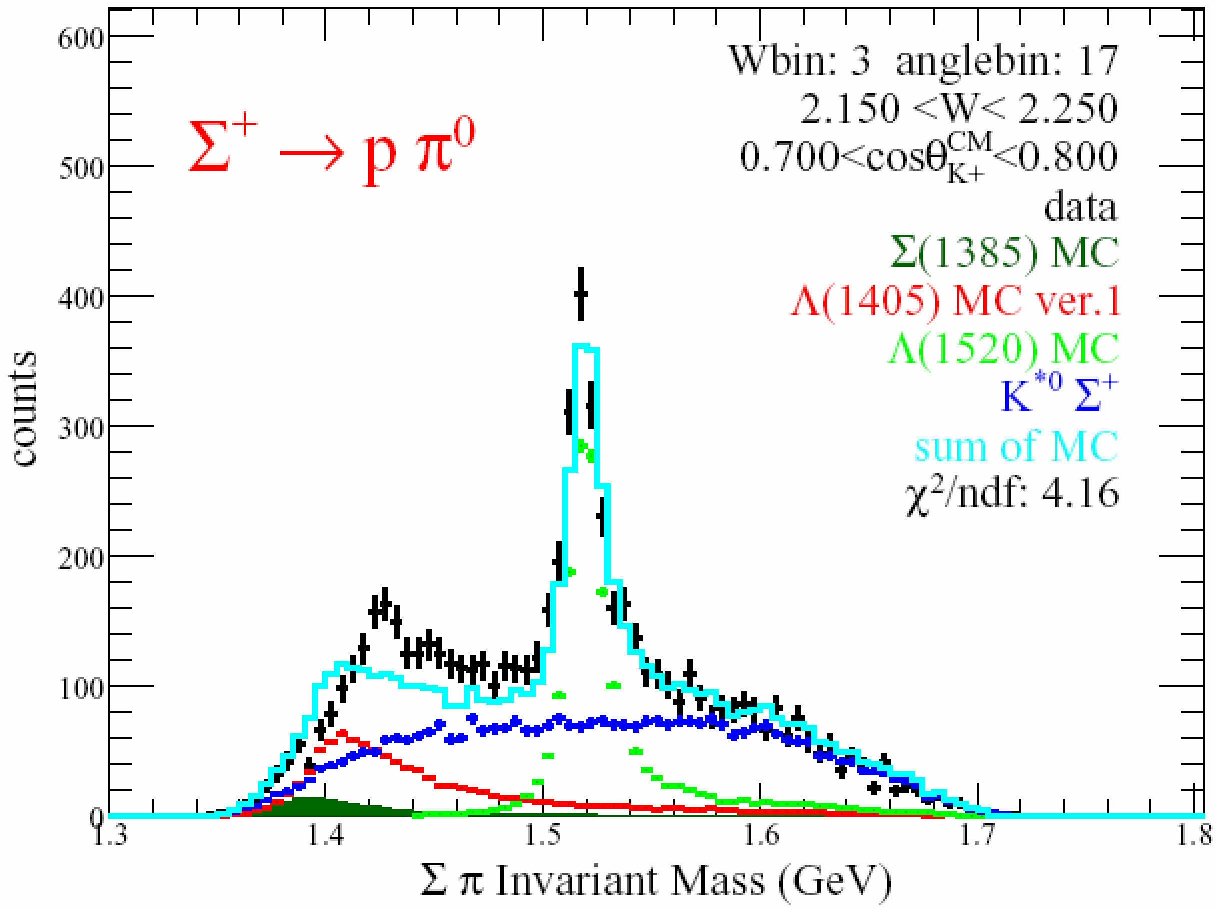

- Example of 1 bin out of 150:
- Subtract off $\Sigma^0(1385)$ (fixed by $\Lambda\pi^0$ decay mode)
- Model $\Lambda(1405)$ à la PDG (Iteration 0)
- Subtract off fitted $\Lambda(1520)$
- Subtract off fitted K^{*0} (incoherent)
- Fit looks bad: iteration $\Lambda(1405)$ lineshape

Fit to Lineshape with MC Templates

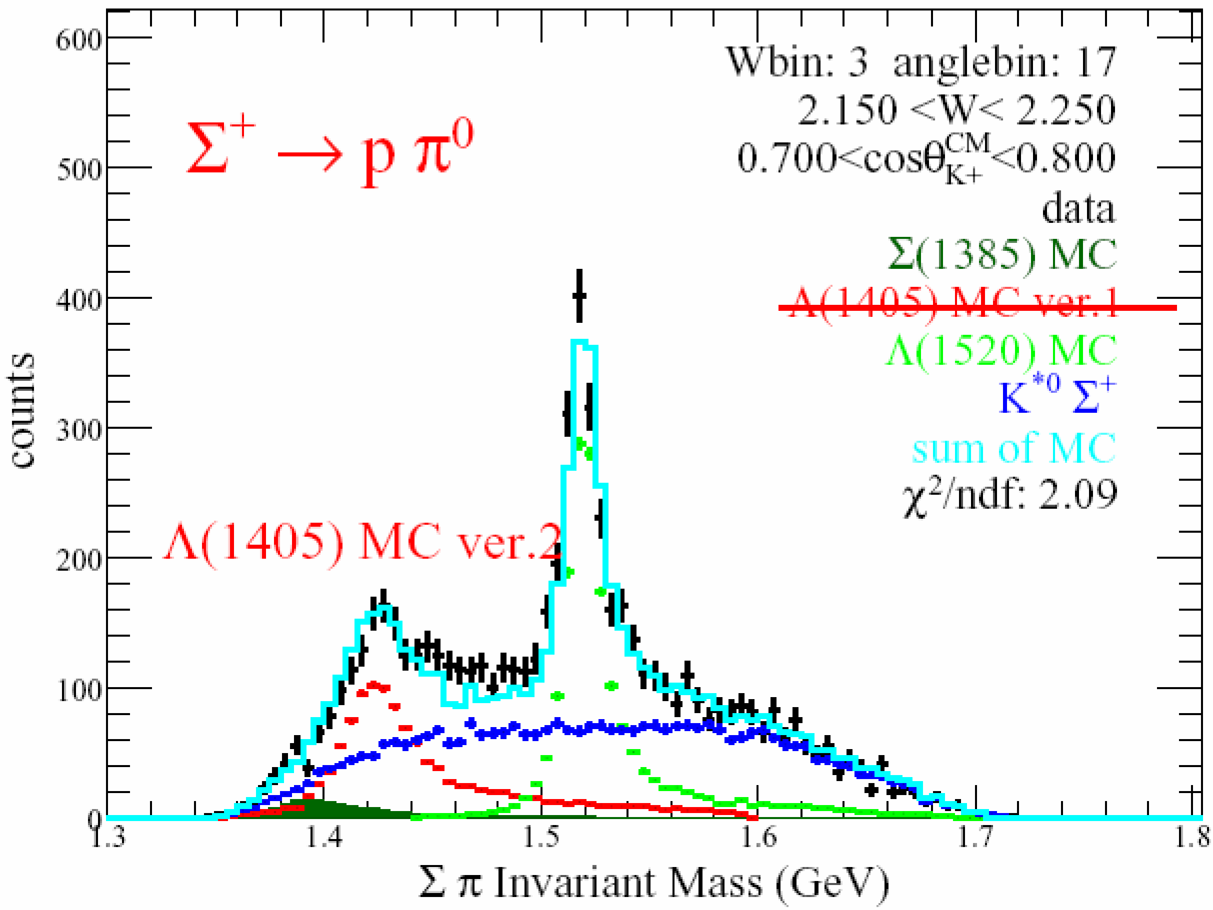

- Example of 1 bin out of 150:
- Subtract off Σ^0(1385) (fixed by $\Lambda\pi^0$ decay mode)
- Model Λ(1405) à la PDG (Iteration 0)
- Subtract off fitted Λ(1520)
- Subtract off fitted K^{*0} (incoherent)
- Fit looks bad: iteration Λ(1405) lineshape
- Fit looks good with iterated Λ(1405) lineshape

CLAS result for $\Lambda(1405)$

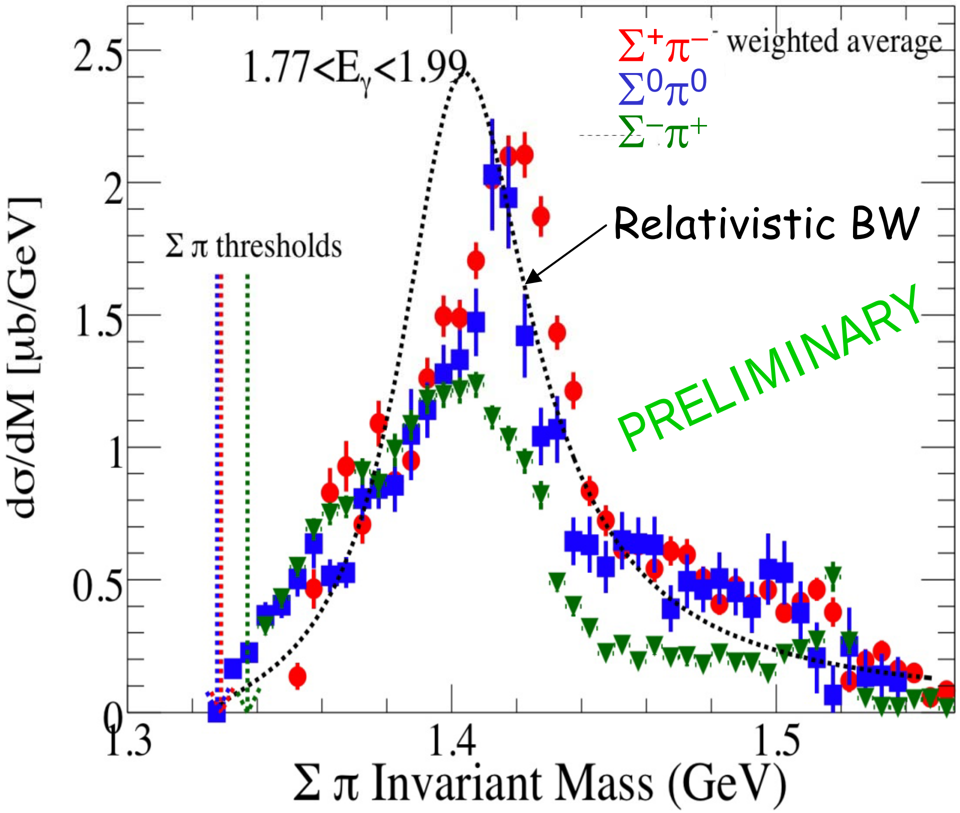

Note that "sign" of the charge asymmetry is opposite to Nacher *et al* prediction

- Decay-channel asymmetry of $\Lambda(1405)$ lineshape confirmed
- Asymmetric among the three charge states → isospin I=0 **and** I=1 processes contribute (decomposition in progress…)
- Subtracted back-grounds: $\Sigma(1385)$, $\Lambda(1520)$, $K^*(892)$
- Direct Spin-parity measurement: $J^\pi = \frac{1}{2}^-$

Isospin Decomposition

Separate $\{\Sigma^+\pi^-, \Sigma^0\pi^0, \Sigma^-\pi^+\}$ into I=0 and I=1 amplitude contributions

$$T^{(0)} \equiv \left\langle \{\Sigma\pi\}_{I=0} \,|\, \hat{T}^{(0)} \,|\, \gamma p \right\rangle$$

$$T^{(1)} \equiv \left\langle \{\Sigma\pi\}_{I=1} \,|\, \hat{T}^{(1)} \,|\, \gamma p \right\rangle$$

$$\cancel{T^{(2)} \equiv \left\langle \{\Sigma\pi\}_{I=2} \,|\, \hat{T}^{(2)} \,|\, \gamma p \right\rangle}$$

$$\left|A_{\Sigma^+\pi^-}\right|^2 = \frac{1}{3}\left|T^{(0)}\right|^2 + \frac{1}{2}\left|T^{(1)}\right|^2 - \frac{2}{\sqrt{6}}\left|T^{(0)}\right|\left|T^{(1)}\right|\cos\Delta\phi_{01}$$

$$\left|A_{\Sigma^0\pi^0}\right|^2 = \frac{1}{3}\left|T^{(0)}\right|^2$$

$$\left|A_{\Sigma^-\pi^+}\right|^2 = \frac{1}{3}\left|T^{(0)}\right|^2 + \frac{1}{2}\left|T^{(1)}\right|^2 + \frac{2}{\sqrt{6}}\left|T^{(0)}\right|\left|T^{(1)}\right|\cos\Delta\phi_{01}$$

$$\frac{d\sigma}{dm} = \frac{(\hbar c)^2}{16\pi}\frac{\alpha}{W^2}\frac{p_f(m)}{p_i(W)}\left|(I_{3\Sigma}, I_{3\pi}\,|\,0,0)T^{(0)} + (I_{3\Sigma}, I_{3\pi}\,|\,1,0)T^{(1)} + \cancel{(I_{3\Sigma}, I_{3\pi}\,|\,2,0)T^{(2)}}\right|^2$$

$$T^{(0,1,2)}(m) = g^{(0,1,2)}\frac{m\Gamma_0\dfrac{\rho}{\rho_0}}{(m_0^2 - m^2) - im\Gamma(q)}$$

$\rho = 2q/m$ — $\Sigma\,\pi$ phase space factor

$\Gamma(m) = \Gamma_0\dfrac{q(m)}{q_0}$ — Mass-dependent width for relativistic Breit Wigner

Isospin Decomposition

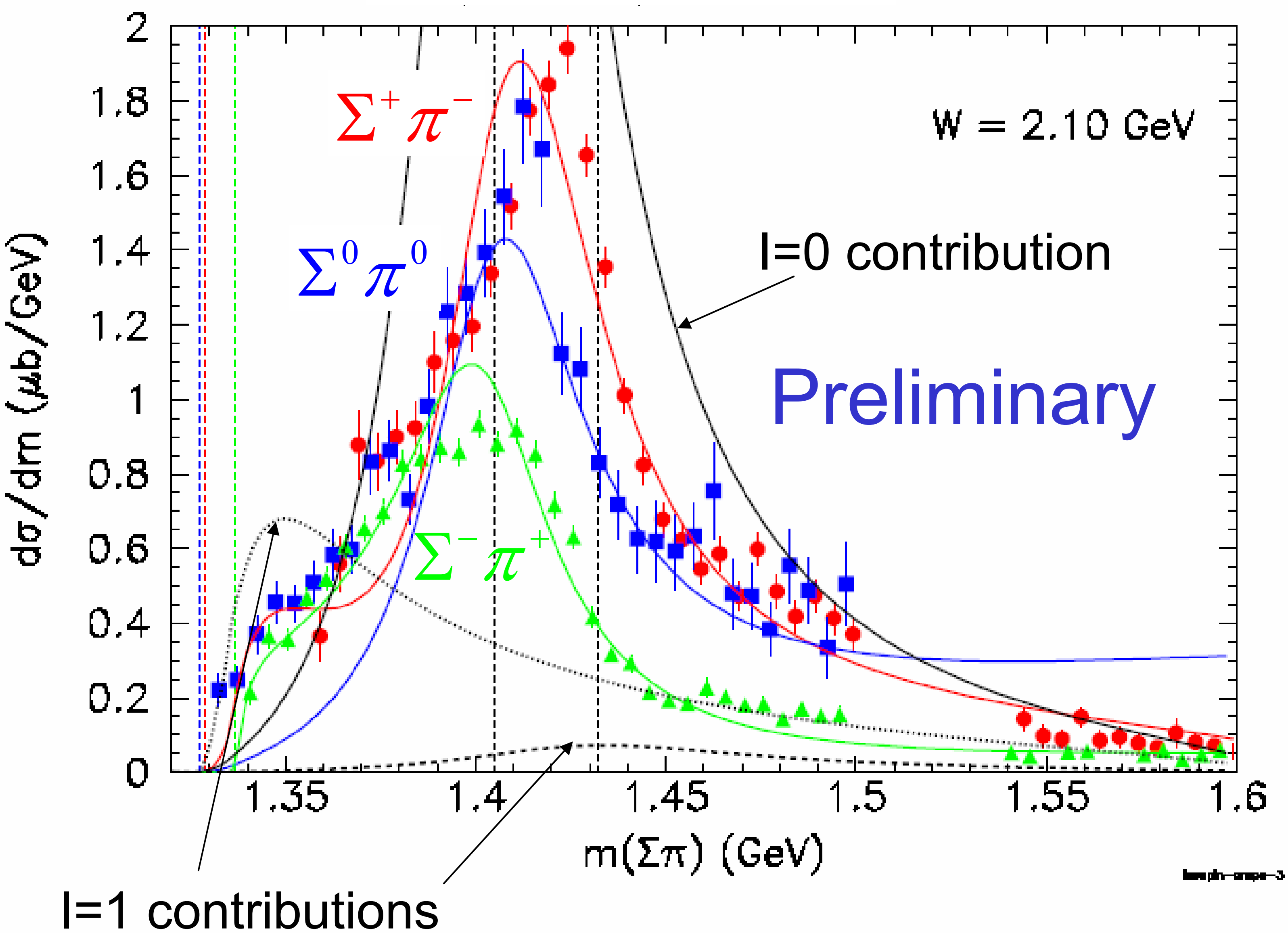

Jefferson Lab/CLAS/Carnegie Mellon University, February 2010

$\Lambda(1405)$ Differential Cross Section Results

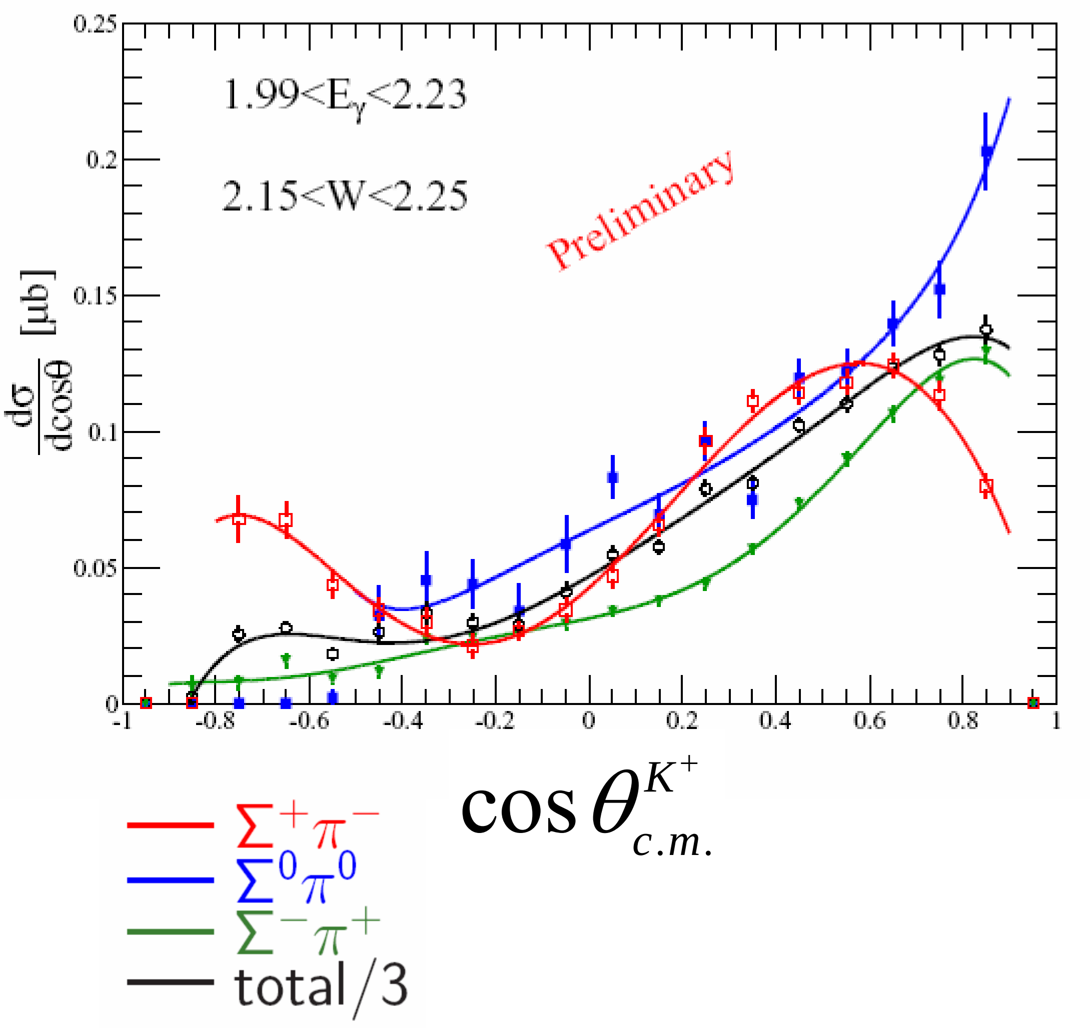

- γ+p → K^+ + $\Lambda(1405)$
- Clear turn-over for $\Sigma^+\pi^-$ channel at forward angles
  - Lines are just 6th order Legendre poly.
- Theory: contact term only, no angular dependence
- Experiment: see strong isospin AND angular interference effect

$\Lambda(1405)$ Differential Cross Section Results

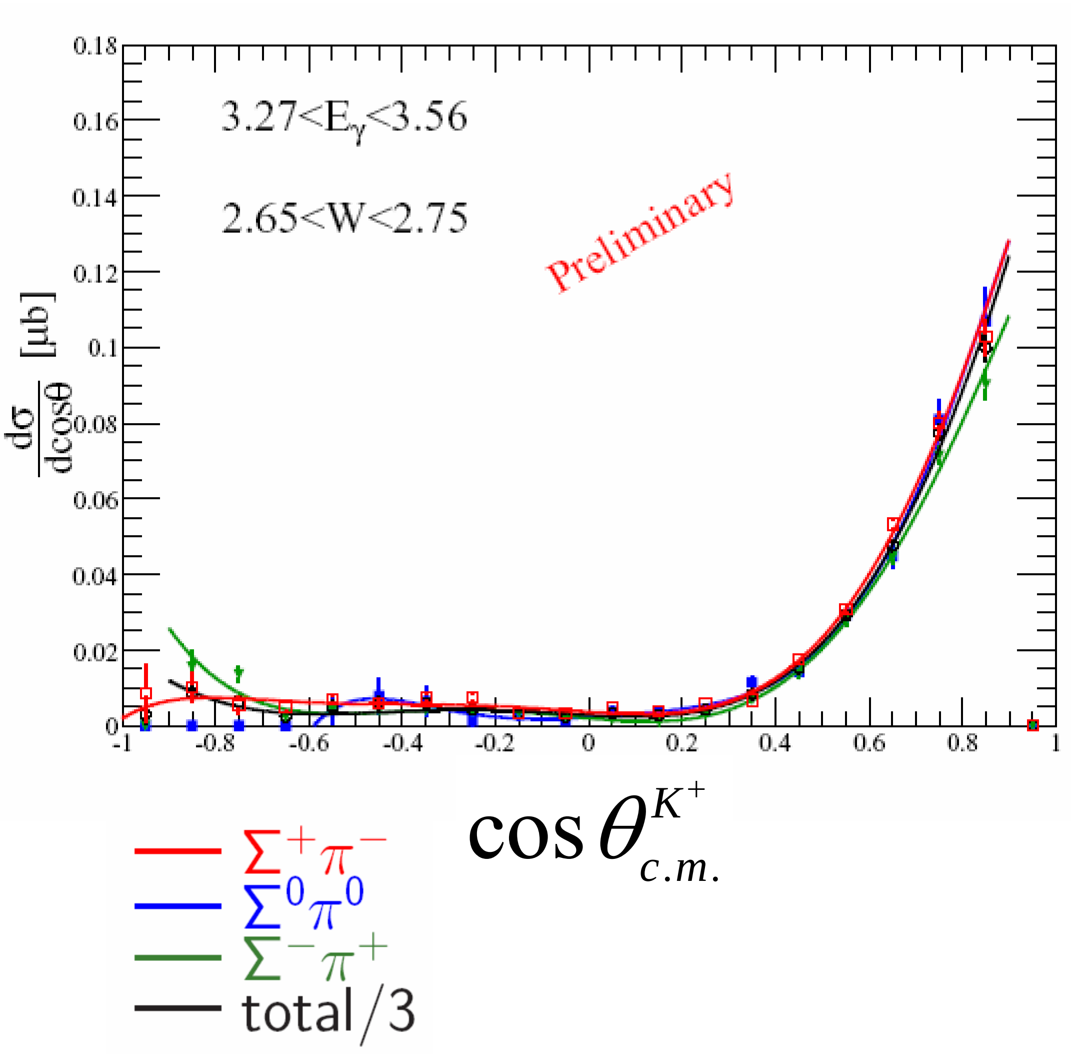

- The charge channels "merge" at higher W
- Theory: contact term only, no angular dependence, no energy dependence
- Experiment: see strong angular dependence and energy dependence

$\Lambda(1405)$ Remaining tasks:

- Internal consistency checks, e.g. equality of
  - $\Sigma^+ \rightarrow p\pi^0$
  - $\Sigma^+ \rightarrow n\pi^+$
- Tests for coherence of K^{*0} background
- Compare $\Lambda(1520)$ and $\Sigma^0(1385)$ cross sections
- CLAS analysis reviews

$\Lambda(1520)\ J^{\pi}=3/2^{+}$ Electro-Production

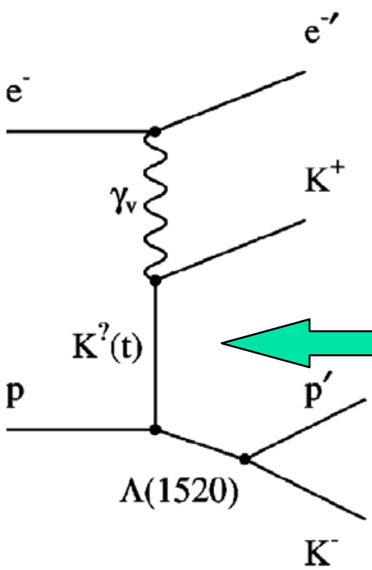

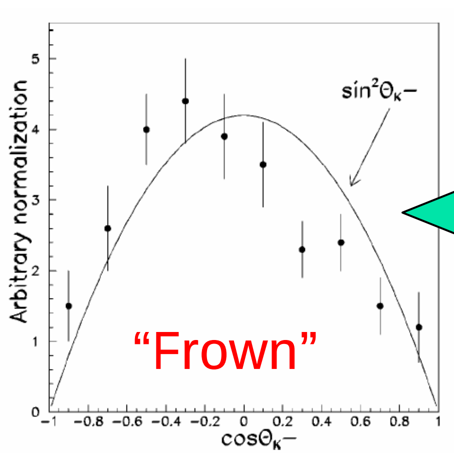

- t-channel dominates the production
- Is the exchange of K^+ $J^{\pi} = 0^-$ or the exchange of K^* $J > 0$ dominant?
- Examine $\Lambda(1520)$ decays in the t-channel helicity frame
- 0^- exchange leads to $|m_z|=1/2$
- $J>0$ exchange leads to $|m_z|=3/2$
  - Dominant at $Q^2=0$: photoproduction
  - D.Barber *et al.* Z. Physik **C7**, 17(1980).

S.P. Barrow *et al.* (CLAS) Phys. Rev. **C64** 044601 (2001)

Λ(1520) Decay Result

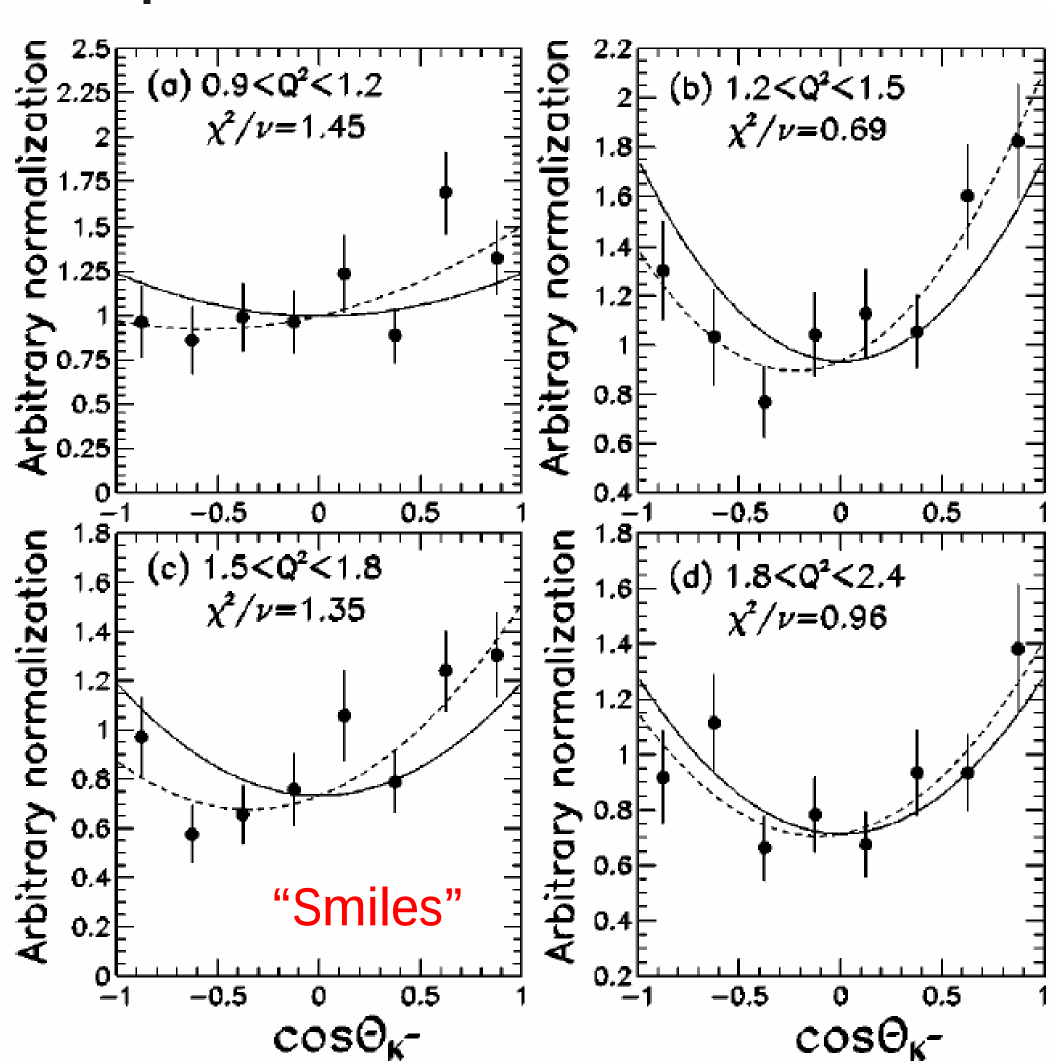

- For $Q^2 > 0.9$ $(GeV/c)^2$, contributions from $|m_z|=1/2$ become big
  - ~60% $|m_z|=1/2$ parentage seen
  - More K (J=0) exchange than in photoproduction
  - *A caveat*: W and t ranges differ from photoproduction result

S.P. Barrow *et al.* (CLAS) Phys. Rev. **C64** 044601 (2001)

$\Xi^{0,-(*)}$ Production: S=-2 physics

- Cascade physics under-explored
  - Only 6 states with 3 or 4 stars in PDG, most without spin-parity
  - Cross sections very small (few nb)
  - Narrower than S=-1 hyperons and N*
- Measured mass differences of Ξ's
- Model: effective Lagrangian approach:
  - K. Nakayama, Y. Oh, H. Haberzettl, PRC74 (2006) 035205
  - H. Lee GlueX Workshop http://conferences.jlab.org/php2008

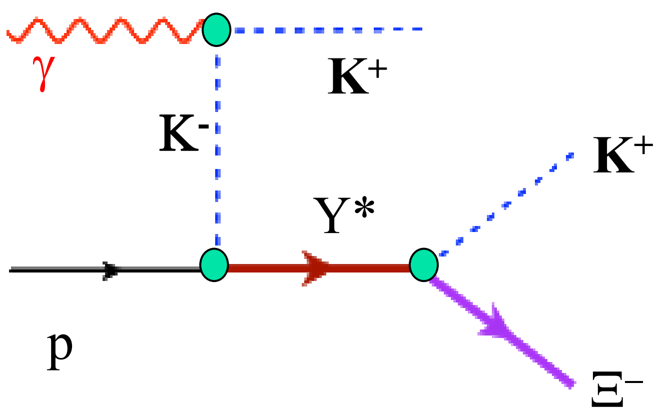

$\Xi^{-(*)}$ Production: S=-2 physics

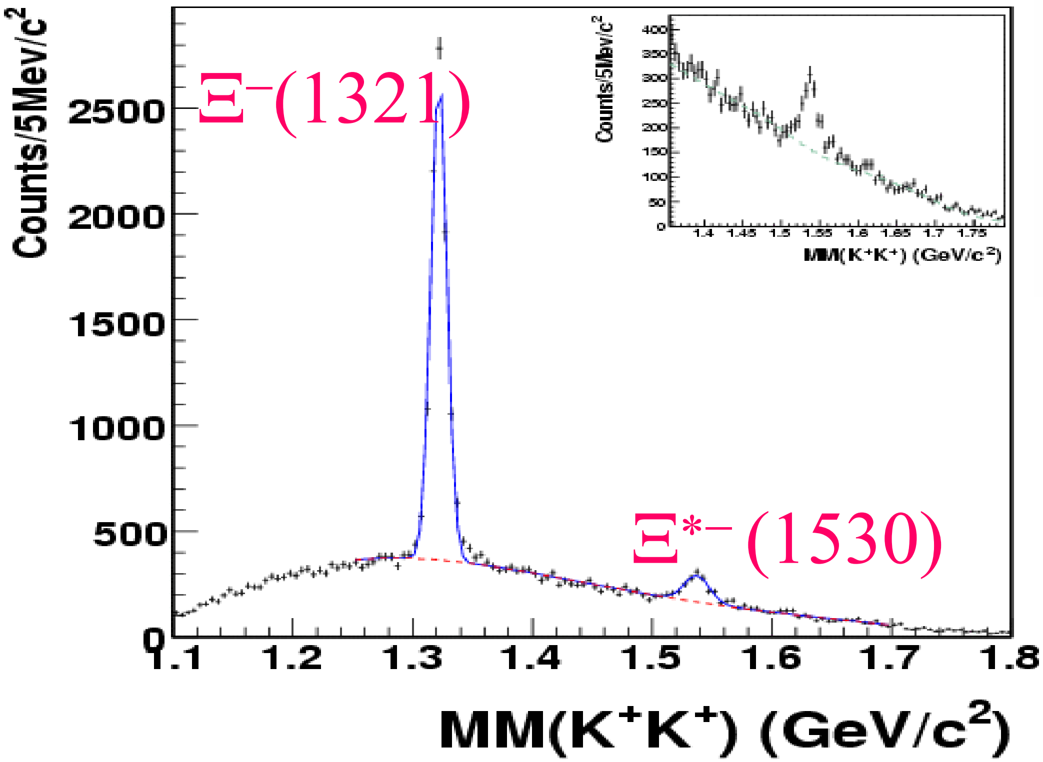

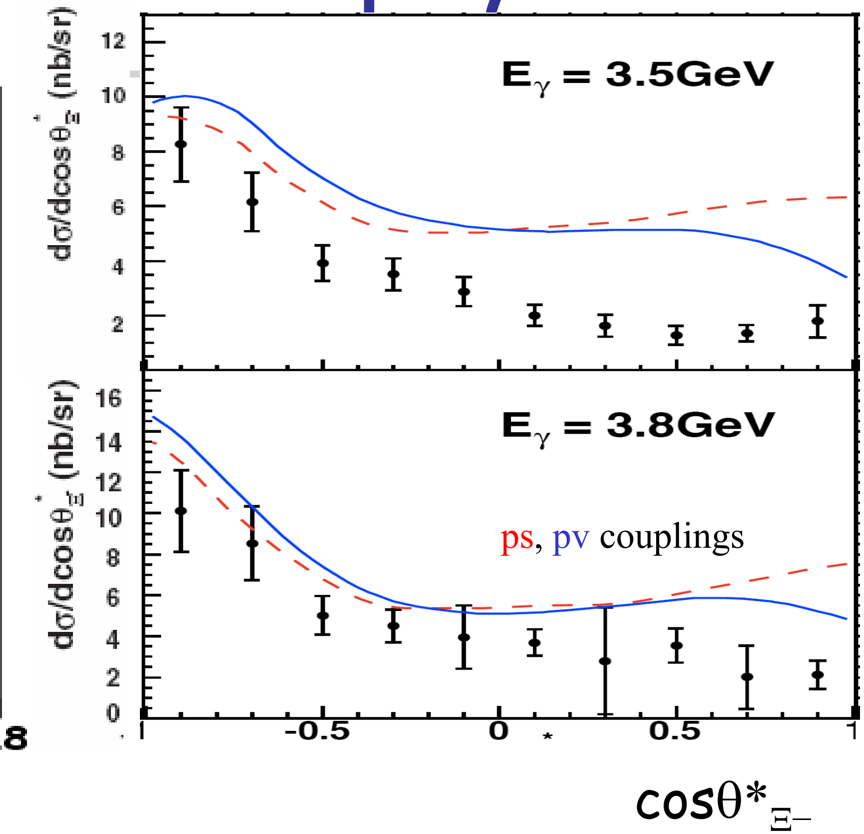

- Detect via $\gamma p \rightarrow K^+K^+(X^-)$
- Possible production through decay of excited hyperons
- High spin hyperon resonances needed ($J \geq 3/2$)

L. Guo *et al.* Phys Rev C **76** 025208 (2007)

Ξ^0 Production: S=-2 physics

Λ^0

Ξ^0

(M=1316.6± 0.6MeV)

Isospin Multiplet	ΔM (MeV) (PDG)
π^+/π^0	4.5936
D^+/D^0	4.79
p/n	1.293318
Σ^-/Σ^0	4.807
Ξ^-/Ξ^0	6.48±0.24

CLAS: $M(\Xi^-)-M(\Xi^0)=5.5\pm1.8$MeV

- Detect via $\gamma p \rightarrow K^+K^+\pi^-(X^0)$; Λ is from $\Xi^-\rightarrow\Lambda\pi^-$ decay
- *Mass splitting consistent with PDG value*

L. Guo et al. Phys Rev C **76** 025208 (2007)

$\pi^-\Xi^0$ Search for excited Ξ states

PDG

Excited cascades	Mass (GeV)	Width (MeV)	BR to $\Xi\pi$
$\Xi^{-0}(1530)$	1.535	9.1	100%
$\Xi^{0}(1620)$ (*)	1.6-1.63	~22	$\Xi\pi$
$\Xi^{-0}(1690)$ (***)	1.69	<30	seen

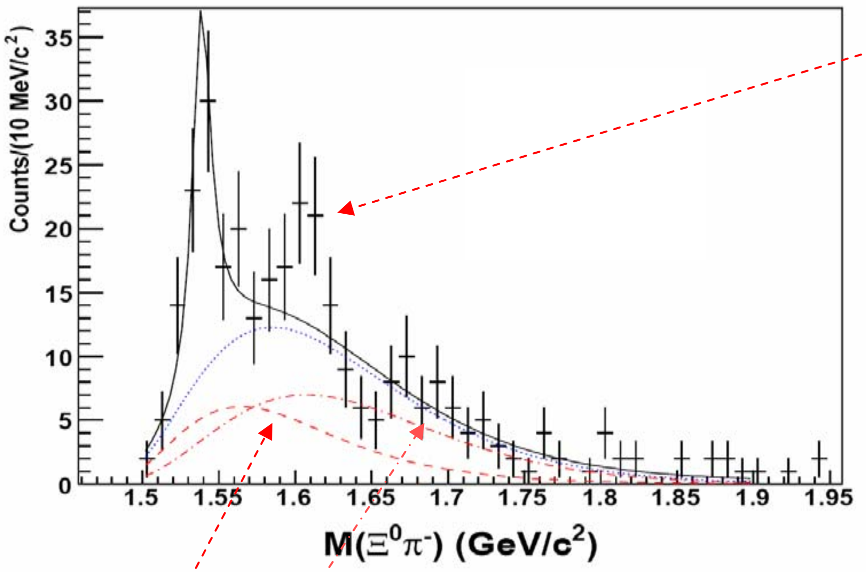

K* background

Non-Ξ events background

$\Xi^-(1620)$ plausible, but not significant
Interest: Dynamical generation of $J^\pi=1/2^-$ meson-baryon resonances à la
Ramos, Oset, Bennhold: PRL **89** 252001 (2002).

Further study of excited Ξ states:
- Higher energy/statistics CLAS 'g12' data under analysis now
- CLAS12 and Hall D in the 12 GeV era

Summary

- Hypernuclear electroproduction is now an established and essential tool in strange-particle physics
- Elementary Y* photo- and electro-production are probing the structure of excited hyperon formation
- $\Lambda(1405) \rightarrow \Sigma\pi$ shows non-Breit-Wigner shape & I=0, 1 interference structure
- Known Ξ hyperons measured in photoproduction – new ones sought…

End of Day 2 Talk

Supplemental Slides